AEROSPACE REPORT NO.
ATR-72(7316-01)-1, VOL. III-1

Advanced Missions Safety

Volume III: Appendices

Part 1, Space Shuttle Rescue Capability

Prepared by
SYSTEMS PLANNING DIVISION

15 October 1972

Prepared for
OFFICE OF MANNED SPACE FLIGHT
NATIONAL AERONAUTICS AND SPACE ADMINISTRATION
Washington, D. C.

Contract No. NASw-2301

Systems Engineering Operations
THE AEROSPACE CORPORATION

Aerospace Report No.
ATR-72(7316-01)-1 Vol. III-1

ADVANCED MISSIONS SAFETY

VOLUME III – APPENDICES

Part 1 – Space Shuttle Rescue Capability

Prepared by
Systems Planning Division

15 October 1972

Systems Engineering Operations
THE AEROSPACE CORPORATION
El Segundo, California

Prepared for

OFFICE OF MANNED SPACE FLIGHT
NATIONAL AERONAUTICS AND SPACE ADMINISTRATION
Washington, D.C.

Contract No. NASw-2301

Aerospace Report No.
ATR-72(7316-01)-1 Vol III-1

ADVANCED MISSIONS SAFETY

Volume III: Appendices

Part 1 – Space Shuttle Rescue Capability

Prepared by
Systems Planning Division

Approved by

E. Perchonok
Study Manager

Approved by

S. M. Tennant
Associate General Manager
Systems Planning Division
Systems Engineering Operations

PREFACE

This study on Advanced Missions Safety has been performed as Task 2.6 of Contract NASw-2301, entitled Advanced Space Program Analysis and Planning. The task consists of three subtasks:

Subtask 1 — Space Shuttle Rescue Capability (Vol. II-1 and Vol. III-1)
Subtask 2 — Experiment Safety (Vol. II-2 and Vol. III-2)
Subtask 3 — Emergency Crew Transfer (Vol. II-3)

Each subtask is an entity not related to or dependent upon any activity under either of the other two subtasks.

The results of Task 2.6 are presented in three volumes.

Volume I: Executive Summary Report presents a brief, concise review of results and summarizes the principal conclusions and recommendations for all three subtasks.

Volume II: Technical Discussion is in three parts, each providing a comprehensive discussion of a single subtask.

Part 1 provides an assessment of Earth Orbit Shuttle (EOS) capability to perform a rescue mission. It treats several concepts for augmenting this capability and increasing EOS rescue mission utility.

Part 2 presents an analysis of potential hazards introduced when experimental equipment is carried aboard the EOS. It identifies safety guidelines and requirements for eliminating or reducing these hazards.

Part 3 discusses the applicability and utility of various means of emergency crew transfer between a disabled and a rescuing vehicle.

Volume III: Appendices is in two parts, each devoted to an individual subtask. Part 1 contains supporting analysis and backup material for Subtask 1, and Part 2 contains similar material for Subtask 2. Volume III is of interest primarily to the technical specialist.

Since the reader is not necessarily interested in all three subtasks, each part of Volumes II and III is a separate document.

All calculations were made using the customary system of units, and the data are presented on that basis. Values in the International System of Units (SI) are also indicated.

Subtask 1 was completed prior to the interest in a parallel-burn Space Shuttle configuration with a solid motor Booster and an expendable Orbiter propellant tank. Moreover, the reports were completed before the Space Shuttle RFP was issued and the Shuttle development contract was awarded. Publication of the Subtask 1 reports was, however, delayed until appropriate information on the parallel-burn Space Shuttle configuration could be developed and added to the Subtask 1 reports.

The Advanced Missions Safety Task was sponsored by NASA Headquarters and managed by the Advanced Missions Office of the Office of Manned Space Flight. Mr. Herbert Schaefer, the study monitor, provided guidance and counsel that significantly aided the effort.

ACKNOWLEDGEMENT

The principal participants in Part 1 of the Advanced Missions Safety Task were:

A. E. Blanciak	Vehicle Definition
K. N. Easley	Multipass Reentry Analysis
W. A. Fey	Vehicle Performance
A. E. Goldstein	Vehicle Definition
Y. S. Hong	Reentry Heating Analysis
E. Perchonok	Study Director
W. J. Portenier	Mission Definition
R. G. Pruett	Trapped Radiation Effects
L. Raphael	Cost
J. Vasiliu	Reentry Heating Analysis

Contributions were also made by:

O. G. Kramer
I. B. Madison
F. J. Meyer
L. L. Schilb
R. E. Thompson

VOLUME III, PART 1

CONTENTS

APPENDIX A

MISSION EVALUATION

APPENDIX A

CONTENTS

APPENDIX A

TABLES

FIGURES

APPENDIX A

MISSION EVALUATION

A.1 REFERENCE MISSION CHARACTERISTICS *

A.1.1 General

The NASA mission model used in current space transportation studies is given in Reference A-1. Pertinent summary charts from that reference are included here in Tables A-1 through A-5.

The missions in this model can be grouped into general categories according to orbital characteristics as follows:

a. Synchronous equatorial orbit
b. Low and medium altitude polar orbits
c. Sun synchronous orbits
d. Heliocentric orbits
e. Low-altitude east orbits
f. Space station orbit
g. Sortie mission flights
h. Planetary missions

The planetary, high, and medium earth orbit missions utilize the manned Orbiter only to deliver/retrieve an upper stage-payload combination to an appropriately inclined parking orbit. This mission model therefore leads to an initial definition of potential rescue missions in low earth orbit only.

A.1.2 Low Earth Orbit

The parking orbit requirement identified in A.1.1 leads to the possibility of a rescue mission to a nominal orbit altitude of 100 nmi (185 km)** and inclinations from 28.5 to 99.17 degrees.

---

* Based on material provided by W. Portenier

** SI units in parenthesis are approximate

Low altitude missions, <500 nmi (925 km), where the Orbiter is the primary delivery vehicle and no upper stage is used, present more challenging requirements. Included in this category are RAM sortie missions, laboratory support missions, and space station support missions. These missions vary from 28.5 to 90 degree inclination and from 100 to 400 nmi (185 to 740 km) circular orbit altitude. Such orbits are within the ascent and direct reentry capability of the Orbiter.

A representative set of missions that covers the range of low orbit parameters are tabulated below:

Mission	Launch Site	Altitude		ΔV	
		nmi/55°	km/55°	kft/s	m/s
Space Station	ETR	270	500	1.5	460
Laboratories	ETR	350	650	2.0	610
Earth Physics Satellites	WTR	400	740	2.4	730
Earth Observation Module	WTR	100	185	0.25	76

The laboratories and satellites are unmanned but involve manned servicing or retrieval operations. The space station and the module are manned. All of these missions involve the manned Orbiter and obviously are within reach of a rescue mission flown by another Orbiter.

A.1.3 Geosynchronous Orbit

A geosynchronous earth orbit space station is a logical extension to the unmanned synchronous equatorial orbit mission and represents the only high-energy earth orbit mission included in advanced manned space planning. Its altitude and round trip ΔV characteristics are as follows:

Synchronous Space Station	19,323 nmi/0°	ETR 28.5 kft/s
	(35,802 km)	(8.7 km/s)

The round trip ΔV is referenced to 100 nmi (185 km) and 28.4° inclination.

A.1.4 Lunar Orbit

It is anticipated that future manned lunar operations will be based on an orbiting lunar space station from which excursions to the lunar surface will be made. Its altitude and round trip ΔV characteristics are:

Orbiting Lunar Station	60 nmi/90°	28.8 kft/s
	(110 km)	(8.8 km/s)

In this case, the round trip ΔV is referenced to 100 nmi (185 km) and 31.5°. inclination.

A.1.5 ΔV Requirements

A.1.5.1 Low Earth Orbit Missions

The ΔV requirements for low earth orbit missions generally fall within the capability of the basic Earth Orbit Shuttle. The round trip ΔV from a reference orbit for the missions listed in A.1.2 are given in Table A-6. If direct ascent to the final altitude is used, a small reduction occurs in the total ΔV given in Table A-6.

A.1.5.2 Geosynchronous Orbit

Geosynchronous orbit is well beyond the reach of the conventionally flown Earth Orbit Shuttle. Moreover, the round-trip ΔV required for such a mission will vary somewhat, depending upon whether or not enroute phasing is required in either or both directions. Phasing orbits are used to reach longitudinal locations that cannot be reached by direct transfer. (The total ideal ascent and descent ΔVs are essentially the same whether a phasing orbit is used or a single Hohmann transfer is made.)

For a rescue mission to geosynchronous orbit, phasing and rendezvous with the distressed vehicle are clearly required. Unless direct reentry from synchronous orbit is feasible, phasing and rendezvous on the return to a low earth parking orbit is also probable. The sequence, in both cases, is to apply a ΔV to leave the initial orbit and enter the phasing orbit, apply a further ΔV to leave the phasing orbit and enter the transfer orbit, and finally apply the third ΔV increment to circularize in the target orbit.

The round trip ΔV for a typical mission, referenced to initial and final conditions of 100 nmi (185 km) and 28.4° inclination, is given in Table A-7. Except for the small additional ΔV needed to separate a refueled Orbiter from the fuel donor, the values in Table A-7 apply to both a refueled Orbiter and an Orbiter-launched third stage (Tug).

A.1.5.3 Lunar Orbit

Missions to lunar orbit are also well beyond the reach of the conventionally flown Earth Orbit Shuttle. Some form of staging, such as orbital refueling of the Orbiter or an Orbiter-launched third stage, must be used. The round trip ΔV to lunar orbit for a refueled Orbiter is given in Table A-8. Except for the small ΔV required to separate the Orbiter from the fuel donor, the same total ΔV would be required for the Orbiter-launched third stage case.

A.2 RESCUE MISSION REQUIREMENTS

A.2.1 Introduction

Rescue missions performed with the Earth Orbit Shuttle initially originate at the launch pad. Ascent to low earth orbit is consistent with conventional EOS operation and capability and is well defined and documented. The energy requirements for Orbiter ascent beyond a basic mission are not so well known and publicized.

Generalized parametric studies of plane change and altitude change ΔV requirements have long been available in the literature. It is appropriate to summarize some of the results herein. These results were obtained from Reference A-2.

A.2.2 Assumptions

The Orbiter may be called upon to perform a rescue mission which requires either or both a plane change and ascent from a low earth parking orbit. Propulsive maneuvers in which the velocity increase occurs in approximately zero time and for which there are no propulsive losses are assumed. This assumption is valid when the thrusting times are small relative to the orbital period.

A two-impulse Hohmann transfer is assumed in all cases. When a simultaneous altitude and plane change are desired, it was assumed that the plane change maneuver is optimally divided between the two velocity impulses.

A.2.3 Transfer ΔV Requirements

The velocity requirements for a Hohmann transfer, with or without plane change, from 100 nmi (185 km) to a higher circular orbit altitude, are plotted in Figure A-1.

A.2.4 Transit Time

The corresponding orbit-to-orbit transfer times are plotted in Figure A-2. The time added by introducing a plane change is considered negligible and a single curve describes all altitude-plane-change combinations. It should be noted that any phasing delays must be added to these transit time values.

A.2.5 High-Energy Mission Summary

Typical ΔV requirements and one-way trip durations from low earth orbit for lunar and geosynchronous orbit missions which were used as reference values in this study are given below:

Mission	ΔV, kft/s (km/s)			One-Way Trip Duration
	Round Trip	Transearth Injection	Earth Orbit Injection	
Lunar Orbit	28.8 (8.8)	~3.3 (1.0)	~11 (3.4)	~3 days
Geosynchronous Orbit	28.6 (8.7)	~6 (1.8)	~8 (2.4)	~5.3 hr

In general, the lunar rescue mission will represent a more difficult requirement than the geosynchronous orbit rescue mission. The ΔV needed for lunar orbit departure is less than that required for transearth injection from geosynchronous orbit. The earth orbit injection ΔV, however, is greater. The net result is that approximately the same total ΔV is required for either

mission. Both mission duration and earth return velocity are greater for the lunar mission. If a lunar capability is available, then a geosynchronous mission should also be possible. Shuttle capability, therefore, was compared only to the lunar rescue mission requirement.

A.3 REFERENCES

A-1. Integrated Operations/Payloads/Fleet Analysis Final Report: Volume V, Mission, Capture, and Operations Analysis; Aerospace Corporation; ATR-72(7231)-1; August 1971 (Contract No. NASw-2129).

A-2. Space Planners Guide; United States Air Force, Air Force Systems Command; 1 July 1965.

Table A-1. NASA Physics and Astronomy Payloads
(Reference A-1)

Payload	$h_p^*/h_a^*/i$	Wt, lb
Astronomy Explorers - A	270/260/28.5°	860
Astronomy Explorers - B	S.E.	860
Magnetosphere Expl. Low	180/1800/28.5 & 90[(a)]	1,160
Magnetosphere Expl. Middle	1000/20000/28.5 & 90°	965
Magnetosphere Expl. High	1 A.U./1 A.U./Ecliptic	580
Orbiting Solar Observatory	350/350/Any	1,900
Gravity/Relativity Expl. A, C, E	300/300/85-95°	1,450
Gravity/Relativity Expl. B, D	1 A.U./1 A.U./28.5°	485
Radio Interferometer, Sync.	40000/40000/28.5°	10,000
Solar Orbit Pair, Sync	19300/19300/30°	1,820
Solar Orbit Pair, 1 A.U.	1 A.U./1 A.U./28.5°	2,440
Optical Interferometer, Pair	19300/19300/30°	3,010
HEAO-C	230/230/30°	19,750
High Energy Stellar Astron. (Alternative)	230/230/30°	21,000

(a) Two sets of NASA data, the (a) set is the more realistic

* The apogee (h_a) and perigee (h_p) altitudes are in nmi

Table A-1. NASA Physics and Astronomy Payloads (Cont)
(Reference A-1)

Payload	$h_p^*/h_a^*/i$	Wt, lb
Revisits	230/230/30°	6,000
LST (Star) } Alternative	350/350/28.5°	21,300
LST (RAM) } Alternative	350/350/28.5°	30,000
Revisits	350/350/28.5°	4,500
Large Solar Observatory	350/350/30°	27,000
Revisits	350/350/30°	4,500
Large Radio Observatory	350/350/30°	19,300
Revisits	350/350/30°	4,500
Retrieval Equipment		2,000
Teleoperator & Strongback		6,700

* The apogee (h_a) and perigee (h_p) altitudes are in nmi

Table A-2. NASA Earth Observatory, Communication, Systems Demonstration Payloads (Reference A-1)

Payload	$h_p^*/h_a^*/i$	Wt, lb
Earth Observations R & D		
Polar Earth Obs. Satellite	500/500/99.17°	2,500
Sync. Earth Obs. Satellite	Synchronous Equatorial	1,000
Earth Physics Satellite	400/400/90°	580
Systems Demonstration		
Sync. Meteorological Sat.	Synchronous Equatorial	1,000
Tiros	700/700/100.92°	1,000
Polar Earth Res. Sat.	500/500/99.17°	2,500
Sync. Earth Res. Sat.	Synchronous Equatorial	1,000
Communication & Nav., R & D		
Applications Tech. Sat.	Synchronous Equatorial	7,950
Small Appl. Sat. Sync.	Synchronous Equatorial	600
Small Appl. Sat. Polar	300/3000/90°	600

* The apogee (h_a) and perigee (h_p) altitudes are in nmi

Table A-2. NASA Earth Observatory, Communication, Systems Demonstration Payloads (Reference A-1) (Cont)

Payload	$h_p^*/h_a^*/i$	Wt, lb
Communication & Nav., R & D (Contd)		
Cooperative Appl. Sync.	Synchronous Equatorial	820
Cooperative Appl. Polar	300/3000/90°	820
Systems Demonstration		
Medical Network Satellite	Synchronous Equatorial	2,000
Education Broadcast Sat.	Synchronous Equatorial	3,400
Follow-on Sys. Demo.	Synchronous Equatorial	2,000
Operational		
Tracking & Data Relay	Synchronous Equatorial	2,300

* The apogee (h_a) and perigee (h_p) altitudes are in nmi

Table A-3. NASA Model, Non-NASA and Planetary Payloads
(Reference A-1)

Payload	$h_p^*/h_a^*/i$	Wt, lb
Non-NASA		
Comsat Satellites	Synchronous Equatorial	1,420
U.S. Domestic Comm.	Synchronous Equatorial	3,525
Foreign Domestic Comm.	19300/19300/28.5-0°	1,000
Nav. & Traffic Control (3 ea.)	16000/30000/29°	700
Nav. & Traffic Control (1 ea.)	19300/19300/28.5°	700
TOS Met.	700/700/100.92°	1,000
Synchronous Met.	Synchronous Equatorial	1,000
Polar Earth Resources	500/500/99.17°	2,500
Sync. Earth Resources	Synchronous Equatorial	1,000
Planetary		
Viking		7,570
Mars Sample Return		11,055 **10,290
Venus Explorer		970

*The apogee (h_a) and perigee (h_p) altitudes are in nmi)

**Two Sections, Mate On-Orbit

Table A-3. NASA Model, Non-NASA and Planetary Payloads (Reference A-1) (Cont)

Payload	$h_p^*/h_a^*/i$	Wt, lb
Planetary (Contd)		
Venus Radar Mapping		7,636
Venus Explorer Lander		7,260
Jupiter Pioneer Orbiter		900
Grand Tour		1,480
Jupiter TOPS Orbiter/Probe		3,180
Uranus TOPS Orbiter/Probe		3,580
Asteroid Survey		1,840
Comet Rendezvous		2,000

* The apogee (h_a) and perigee (h_p) altitudes are in nmi)

Table A-4. NASA RAM Sortie
(Reference A-1)

Payload	$h_p^*/h_a^*/i$	Wt, lb
General Science Research Module	200/200/55°	27,500
General Applications Module Dedicated Science	100/100/65°	30,000
Research Module Astron. Dedicated Applications	200/200/55°	29,500
Earth Observation Module	100/100/75°	22,500
Pallet-Type Module		
Earth Observation	125/125/90°	6,000
Bio Research	200/200/28.5°	4,300
Astronomy	200/200/28.5°	5,700
Fluid Management	200/200/28.5°	7,100
Teleoperator	200/200/28.5°	5,000
Manned Work Platform	200/200/28.5°	6,700
Large Telescope Mirror Test	200/200/28.5°	13,000
Astronaut Maneuvering Unit (AMU)	200/200/28.5°	3,800

* The apogee (h_a) and perigee (h_p) altitudes are in nmi

Table A-5. Space Station and Laboratories
(Reference A-1)

Payload	$h_p^*/h_a^*/i$	Wt, lb
Station Module, Crew	270/270/55°	20,000
Station Module, Others	270/270/55°	20,000
Crew Cargo	270/270/55°	20,000
Physics Lab	270/270/55°	22,000
Cosmic Ray Lab	270/270/55°	30,000
Life Science Lab	270/270/55°	33,000
Earth Obs. Lab	270/270/55°	25,000
Comm/Nav Lab	270/270/55°	19,000
Space Manufacturing Lab	270/270/55°	25,000
Possible Expendable Components		
Station Module	270/270/55°	58,525
Min-Mod Big G		35,030

* The apogee (h_a) and perigee (h_p) altitudes are in nmi

Table A-6. Low Earth Orbit Mission Round-Trip ΔV Requirements

Mission	Space Station	Laboratories	Earth Physics Satellites	Earth Observation Module
Initial Altitude, nmi (km)	100 (185)	100 (185)	100 (185)	100 (185)
Initial Inclination, degrees	55	30	90	75
Final Circular Altitude, nmi (km)	270 (500)	350 (650)	400 (740)	100 (185)
Final Inclination, degrees	55	30	90	75
ΔV_1, enter transfer orbit, ft/s (m/s)	298 (91)	431 (132)	514 (157)	--
ΔV_2, circularize in mission orbit, ft/s (m/s)	294 (90)	425 (130)	504 (154)	--
ΔV_r, rendezvous, ft/s (m/s)	150 (46)	150 (46)	150 (46)	150 (46)
ΔV_3, enter return transfer orbit, ft/s (m/s)	294 (90)	425 (130)	504 (154)	--
ΔV_4, circularize parking orbit, ft/s (m/s)	298 (91)	431 (132)	514 (157)	--
ΔV_p, 2% performance dispersion, ft/s (m/s)	30 (9)	40 (12)	45 (14)	3 (0.9)
ΔV_D, guidance, navigation dispersion, ft/s (m/s)	100 (30)	100 (30)	100 (30)	100 (30)
Total ΔV, ft/s (m/s)	1464 (446)	2002 (611)	2331 (711)	253 (77)

Table A-7. Geosynchronous Orbit Mission
Round-Trip ΔV Requirement

Initial/Final Earth Orbit		
Altitude, nmi (km)	100	(185)
Inclination, degrees	28.4	
ΔV, ft/s (m/s)	28,555	(8704)
Phasing orbit insertion	7,897	(2407)
Transfer orbit insertion	252	(77)
Midcourse correction	10	(3)
Synchronous orbit circularization	5,859	(1786)
Rendezvous with distressed vehicle	437	(133)
Phasing orbit insertion	5,845	(1782)
Transfer orbit insertion	5,397	(1645)
Midcourse correction	10	(3)
Low earth orbit circularization	2,728	(831)
Rendezvous	120	(37)

Table A-8. Lunar Orbit Mission Round-Trip ΔV Requirement

Initial Earth Orbit		
Altitude, nmi (km)	100	(185)
Inclination, deg	31.5	
Lunar Orbit		
Altitude, nmi (km)	60	(110)
Inclination, deg	90	
Final Earth Orbit		
Altitude, nmi (km)	100	(185)
Inclination, deg	31.5	
ΔV, ft/s (m/s)	28,794	(8776)
Separation from fuel donor	35	(11)
Translunar injection	11,292	(3442)
Midcourse correction	100	(30)
Lunar Orbit Insertion	3,200	(975)
Rendezvous	150	(46)
Separation	25	(8)
Transearth injection	2,900	(884)
Midcourse correction	100	(30)
Earth Orbit Insertion	10,792	(3289)
Rendezvous	200	(61)

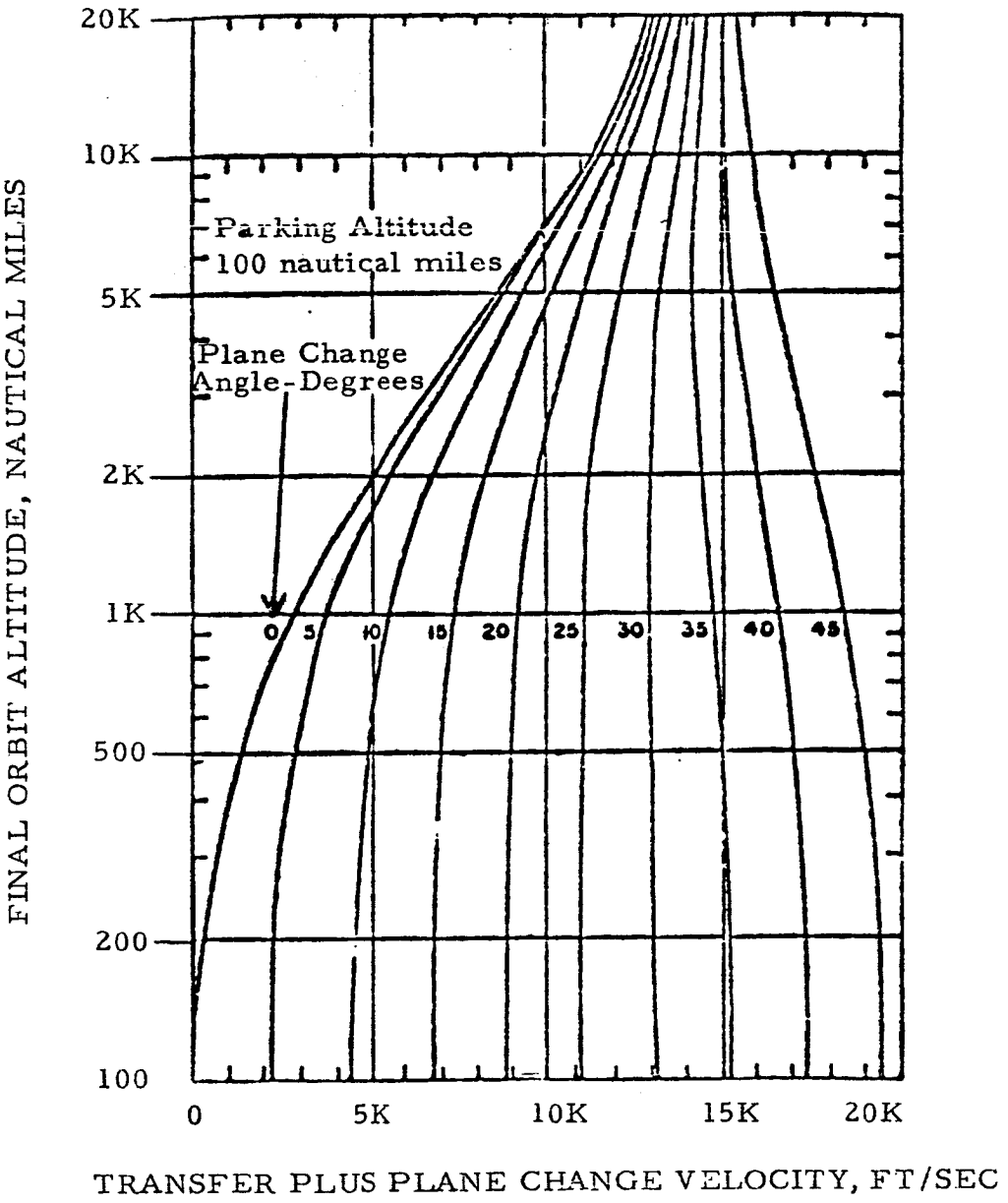

Figure A-1. ΔV Requirements for Hohmann Transfer Between Orbits (Reference A-2)

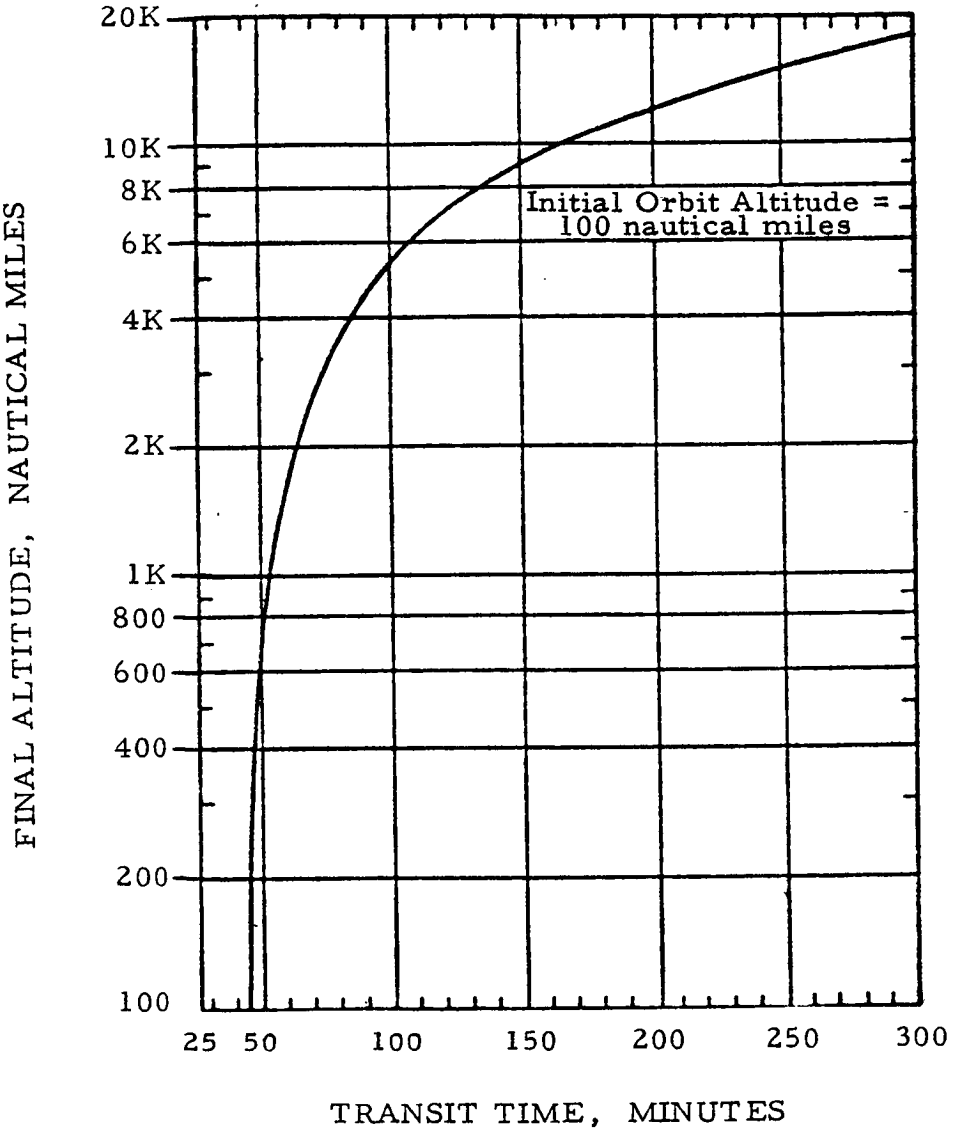

Figure A-2. Transit Time for Hohmann Transfer Between Orbits (Reference A-2)

APPENDIX B

SHUTTLE CONFIGURATIONS AND PERFORMANCE

APPENDIX B

CONTENTS

APPENDIX B

TABLES

FIGURES

APPENDIX B

SHUTTLE CONFIGURATIONS AND PERFORMANCE

B.1 DESCRIPTION*

In general, only the Orbiter characteristics are of interest to this study. The Booster can be expendable or reusable so long as it is sized to accommodate an Orbiter with the specified characteristics. Naturally, the gross lift-off weight as well as the versatility of the system will be influenced by Booster design. However, these issues were beyond the scope of this study.

Descriptions of the four basic Shuttle configurations initially assessed are given in this appendix. See Section J.1 in Appendix J for the system description and operating characteristics of the solid rocket boosted parallel-burn Space Shuttle.

B.1.1 Fully Reusable Shuttle - Configuration A

A representative Phase B design from Reference B-1 was used as a typical fully reusable Shuttle configuration. A line drawing of the configuration is reproduced in Figure B-1.

The system consists of two stages, a Booster and an Orbiter, both fully recoverable and reusable. Gross lift-off weight is approximately 4.6×10^6 lb (20.4×10^6 N). Twelve hydrogen/oxygen engines in the Booster generate a lift-off thrust of 6.6×10^6 lb (29.3×10^6 N). The Booster configuration is characterized by a jet canard and a swept wing mounted near the base of the body. After first-stage thrusting is terminated, the Orbiter is separated from the Booster. The Booster is protected by a heat shield of

*The material discussed in this section was provided by A. E. Blanciak.

hardened compacted fibers (HFC), and after reentering the atmosphere and decelerating to subsonic speeds, cruises back to the launch site using ten JP-fueled turbojet engines.

The delta-wing planform of the Orbiter was selected to provide a desired 1100 nmi (2040 km) crossrange after reentry. Heat protection is provided by metallic heat shields using titanium, nickel, and columbium materials and a carbon-carbon nose cap. Ascent thrust is provided by two H_2/O_2 rocket engines. Four turbojet engines similar to those of the Booster provide cruise-back thrust. These engines are optional and their use depends upon specific mission requirements.

At launch, the Booster and Orbiter are mated in "piggyback" fashion. The Orbiter location is governed by available booster hardpoints and the desirability of having the separation load pass through the Orbiter center of gravity. Booster and Orbiter main propulsion burn in series, with Orbiter ignition occurring as the Booster thrust terminates.

The Orbiter planform facilitates both hypersonic and supersonic longitudinal stability. A single vertical fin with a flared rudder provides dynamic directional stability. A large cargo bay door provides access to a 15 ft (4.6 m) diameter and 60 ft (18.3 m) long cargo bay. On-orbit payload deployment and retrieval capability are provided.

The two Orbiter propulsion engines are mounted in the fuselage base. A capability for an Orbiter abort to orbit with one engine out is provided. Two RL-10 rocket engines are mounted in the upper aft fuselage and provide orbital maneuvering and deorbit thrust.

Pertinent vehicle features and engine performance specifications of interest to this study are listed in Table B-1.

B.1.2 Drop-Tank Orbiter - Configurations B, C, D

A representative Mark II design from Reference B-2 was used as a typical drop-tank-Orbiter Shuttle configuration. Three sizes of this design,

each having different cargo bay dimensions, were considered. A line drawing of Configuration B, which has the largest cargo bay, is given in Figure B-2.

The Booster is a fully recoverable delta-wing configuration employing a center vertical fin and powered with five F-1, H_2/O_2 engines. The Booster is configured around S-IC tanks modified to carry loads and to resist reentry temperatures. The S-IC main propulsion feed system has been modified for larger intertank spacing and higher mounting and canting of the F-1 engines. The cruise propulsion system for return to the launch site after separation and reentry consists of nine turbojet engines mounted in deployable pods, one under each wing and seven in a single pod under the intertank section.

The Orbiter and its external H_2/O_2 tank are mounted in a tank-end-loaded arrangement on the Booster. Orbiter and tank loads are transmitted to the Booster through a folding petal structure. This metal structure closes after Booster-Orbiter separation to form a faired aerodynamic nose for Booster reentry.

The Orbiter fuel tank is centered under the fuselage and is separated and expended after being emptied. Main propulsion consists of four high-pressure rocket engines. A delta-wing planform is also employed in this design in order to achieve the desired 1100 nmi (2040 km) crossrange after reentry.

Pertinent Configuration B features of interest to this study are included in Table B-1. Also included in Table B-1 are the pertinent characteristics of Configurations C and D. Both are conceptually similar to Configuration B but with smaller cargo bays. The characteristics of C were scaled down from Configuration B, whereas the characteristics of D are based on an IDA mini-shuttle design, Reference B-3.

B.2 BASIC VEHICLE PERFORMANCE*

B.2.1 General

The performance data required to analyze rescue missions differs in some respects from that found in the usual presentation of vehicle performance capabilities. If all the desired additional data were determined by trajectory simulations, the number required would become unfeasibly large. Therefore, the basic technique adopted was to employ the data that were available and extend data by means of ideal velocity calculations.

The standard procedure for Shuttle vehicles is to shape the ascent trajectory so that burnout of the Orbiter at depletion of the main tank propellant occurs at an altitude of 50 nmi (90 km). The main engines have no restart capability; no further use can be made of the main engines during a mission. The nominal orbit established at burnout is 50 x 100 nmi (90 x 185 km). However, if a final orbit above 100 nmi (185 km) is desired, it is normally advantageous to burn-out at a higher velocity so that an orbit is established with apogee at the desired altitude. The effect of this is to use the main engines for ascent to orbit altitude. In many situations, the altitude capability is limited by OMS tank capacity. Using the main engines for direct ascent to the desired orbit altitude allows the Shuttle system to reach a higher altitude for the same OMS tank capacity.

Burnout velocity at 50 nmi (90 km) is a function of the Orbiter burnout weight assuming that main propellant tanks are fully loaded. The two variable items in the burnout weight are the payload and OMS propellant loading. Therefore, in order to obtain the required velocity for a particular altitude, payload and OMS propellant are reduced appropriately. The relative size of the two items must be adjusted so that the OMS propellant can provide sufficient ΔV with the corresponding payload. ΔV requirements on the OMS system consist of circularizing the vehicle at final altitude after arrival there at

*The material discussed in this section was provided by W. A. Fey.

apogee of the transfer ellipse, and providing the impulse for deboost from final altitude. Direct reentry as discussed in Appendix F was assumed for all cases.

Weight and specific impulse data employed for the various vehicles are shown in Table B-1. As indicated in Table B-1, there is neither a design specification consistency nor a main propellant or OMS capability consistency between the four configurations being examined. Consequently, each represents a unique performance capability even for the same payload requirement (Configurations A and B, for example).

Comparison of the performance data contained in References B-4 and B-2 with ideal velocity calculations for Configurations A and B indicated that the determination of payload as a function of altitude can be done satisfactorily by means of the ideal velocity computations. This was found to be true also of the OMS velocity increments. Correlation of ideal velocity requirements with orbital inclination was also possible.

Reference B-3 contained performance data for Configuration D for several orbit inclinations. These data were extended to include altitude effects by means of the ideal velocity calculations. Configuration C weight data were the result of an in-house design effort which has not been documented formally. No Configuration C performance data were available. Estimates made for this study used as a basis for ideal velocity calculations the ideal velocity requirements as a function of inclination determined for the other configurations.

Basic performance data for the parallel-burn Space Shuttle configuration are given in Appendix J.

B.2.2 Rescue Mission Performance

The results of these analyses in terms of payload as a function of orbital altitude and inclination are presented in Figure B-3 for the four configurations. In Figure B-3(a) for Configuration A, it can be seen that

payload is constant up to an altitude of about 235 nmi (435 km). This results from a specification on this vehicle that in the event of failure of one of the two orbiter engines at staging, the vehicle will be able to proceed to orbit and then deboost. OMS propellant sufficient for a ΔV of approximately 1 kft/s (305 m/s) is necessary for this purpose since the OMS engines are employed to assist in attaining orbit in this situation. This sets a minimum on the amount of OMS propellant required. Otherwise, the OMS propellant requirement would continue to decrease with attendant payload increase as orbital altitude decreases below 235 nmi (435 km). Another feature of the curve to be noted is that for the lower inclinations the maximum altitude capability is limited by the capacity of the OMS tanks to contain sufficient propellant to perform the circularization and deboost maneuvers. Otherwise, the payload capability shown is limited by the weight lifting capability of the configuration.

Data for Configuration B is shown in Figure B-3(b). No abort requirement was specified for this vehicle, so the payload limit shown before does not appear. The nominal configuration has an OMS tank capacity for only 1 kft/s (305 m/s) which significantly limits altitude capability of the vehicle. However, there is provision for an auxiliary OMS tank to be carried in the cargo bay. Data for this case are also presented. The data for Configurations C and D given in Figures B-3(c) and B-3(d) illustrate the decreasing payload capabilities associated with the smaller design payloads specified and also the decreased altitude capability as a result of the limited OMS tank capacities available.

The rescue mission does not necessarily impose the maximum shuttle payload requirement. Rescue payloads fall into two general categories, special rescue equipment and Rescue Module. Study results on each suggest that 10 klb (4.5 t) is a representative weight for either, References B-5 and B-6.

At low orbit altitudes, all four Orbiter configurations have a satisfactory rescue payload capability over the entire inclination range. The available maneuvering capability at target altitude increases with OMS capacity and payload margin.

A crossplot of the Figure B-3 data as a function of orbit inclination is given in Figure B-4 for an orbit altitude of 100 nmi (185 km). The payload drop-tank configuration (B) is somewhat superior to the integral-tank design (A).

B.2.3 Rescue Mission ΔV

As discussed previously, the Shuttle weight lifting capability can be utilized to carry a combination of payload and OMS propellant weights. When the rescue mission payload is lighter than the maximum payload capability of the vehicle, then the amount of OMS propellant carried can be increased over the basic amount necessary to circularize the vehicle in final orbit and deboost. This added propellant can be used to perform maneuvers and to expedite rendezvous with a distressed spacecraft. The velocity capabilities corresponding to this added OMS propellant for the four EOS configurations are shown in Figure B-5. Similar data for the parallel-burn Shuttle configuration are given in Figure J-6 of Appendix J.

The variation of available ΔV with orbit altitude and inclination is presented for payload weights of 0 and 10 klb (0 and 4.5 t). The decreasing performance at altitude for the vehicles with the smaller OMS tank capacities is evident again in these figures. No abort constraint occurs for Configuration A in this case because sufficient OMS propellant for abort is on board in all situations.

Two sets of curves are plotted for Configuration B in Figure B-5(b). The lower set corresponds to the basic configuration having a 1 kft/s (305 m/s) OMS tank capacity. The upper set represents Configuration B capability with a 2 kft/s (610 m/s) OMS tank capacity.

Initially, the Shuttle can lift both the specified payload and a full OMS propellant tank to the apogee of the desired initial elliptic orbit. The ΔV remaining, after circularization at the apogee altitude and allowing a reserve for direct deorbit, is set by the OMS tank capacity. A single curve describes the ΔV variation with orbit altitude at all inclinations for each EOS configuration. However, if a condition is reached, when the altitude/inclination

combination exceeds the Shuttle capability with the payload weight specified, OMS propellant is off-loaded. The total weight delivered to the target orbit is reduced and the available on-orbit ΔV is also lowered. Thus, a break in the curve occurs at the point where off-loading is initiated and the available ΔV decreases more rapidly as the altitude increases. As expected, this situation is initially encountered at the high orbit inclinations.

A modest increase in vehicle capability may be possible for the situations in which performance is limited by the load lifting ability and the OMS tanks are not filled. This is achieved by filling the OMS tanks to capacity and burning the additionally loaded propellant to augment the main engine propulsion during ascent to the initial orbit. This procedure produces increased velocity losses during ascent and hence its efficacy must be evaluated by means of detailed trajectory simulations.

B.3 REFERENCES

B-1. Impact Study Shuttle System: Two Stage Fully Reusable Shuttle Assessment; McDonnell Douglas Astronautics Company - East; No. S-87347; 24 November 1971

B-3. Impact Study Shuttle System: Mark II/RF1B Shuttle Assessment; McDonnell Douglas Astronautics Company - East; No. S-87346; 24 November 1971

B-3. IDA Presentation to PSAC Space Shuttle Panel on 15 October 1971

B-4. Memorandum FM8(71-76) "Space Shuttle Performance Capabilities"; Director of Flight Operations, Mission Planning and Analysis Division, NASA Manned Spacecraft Center; July 15, 1971

B-5. Space Rescue Operations; Aerospace Corporation; ATR-71(7212-05)-1; 12 May 1971 (Contract No. NASw-2078)

B-6. Technical Study For The Use Of The Saturn V, Int-21, And Other Saturn V Derivatives To Determine An Optimum Fourth Stage - Space Tug; The Boeing Company - Southeast Division; CR 103004(D5-15811); 26 February 1971 (Contract NAS 8-5608)

Table B-1. Reference Shuttles

Design Specifications	A Fully Reusable	B Drop Tank	C Drop Tank	D Drop Tank
*Payload, klb (t)	40 (18.2)	40 (18.2)	25 (11)	10 (4.5)
Orbit, nmi (km)	polar 50 × 100 (90 × 185)	polar 50 × 100 (90 × 185)	polar 50 × 100 (90 × 185)	Polar 100 × 100 (185 × 185)
ΔV, ft/s (m/s)	once around abort 1000 (305)	650 (200)	650 (200)	850 (260)
Cargo Bay, ft (m) D × L	15 × 60 (4.6 × 18.3)	15 × 60 (4.6 × 18.3)	12 × 40 (3.7 × 12)	10 × 20 (3 × 6)
Staging Velocity (actual), kft/s (km/s)	11 (3.3)	7 (2.1)	7 (2.1)	7 (2.1)
Orbiter Dry Weight, klb (t)	228 (104)	130 (59)	108 (49)	46 (21)
Drop Tank Weight	--	35 (16)	31 (14)	23.4 (11)
Propellant Weight	518 (235)	704 (320)	603 (274)	237 (108)
Orbiter Propulsion - Main Propellants	H_2/O_2 Hi Pc	H_2/O_2 Hi Pc	H_2/O_2 Hi Pc	H_2/O_2 Hi Pc
Thrust, klb (10^3 N)	2 @ 632(2820)	4 @ 306(1360)	3 @ 306(1360)	2 @ 242(1080)
Orbiter Propulsion - OMS Propellants	H_2/O_2	Storable	Storable	H_2/O_2
Thrust, klb (10^3 N)	2 @ 15 (67)	2 @ 3.5 (16)	2 @ 3.5 (16)	1 @ 12 (53)
ΔV capacity kft/s(m/s)	2 (610)	1 (305)	1 (305)	0.85 (260)

*no airbreather

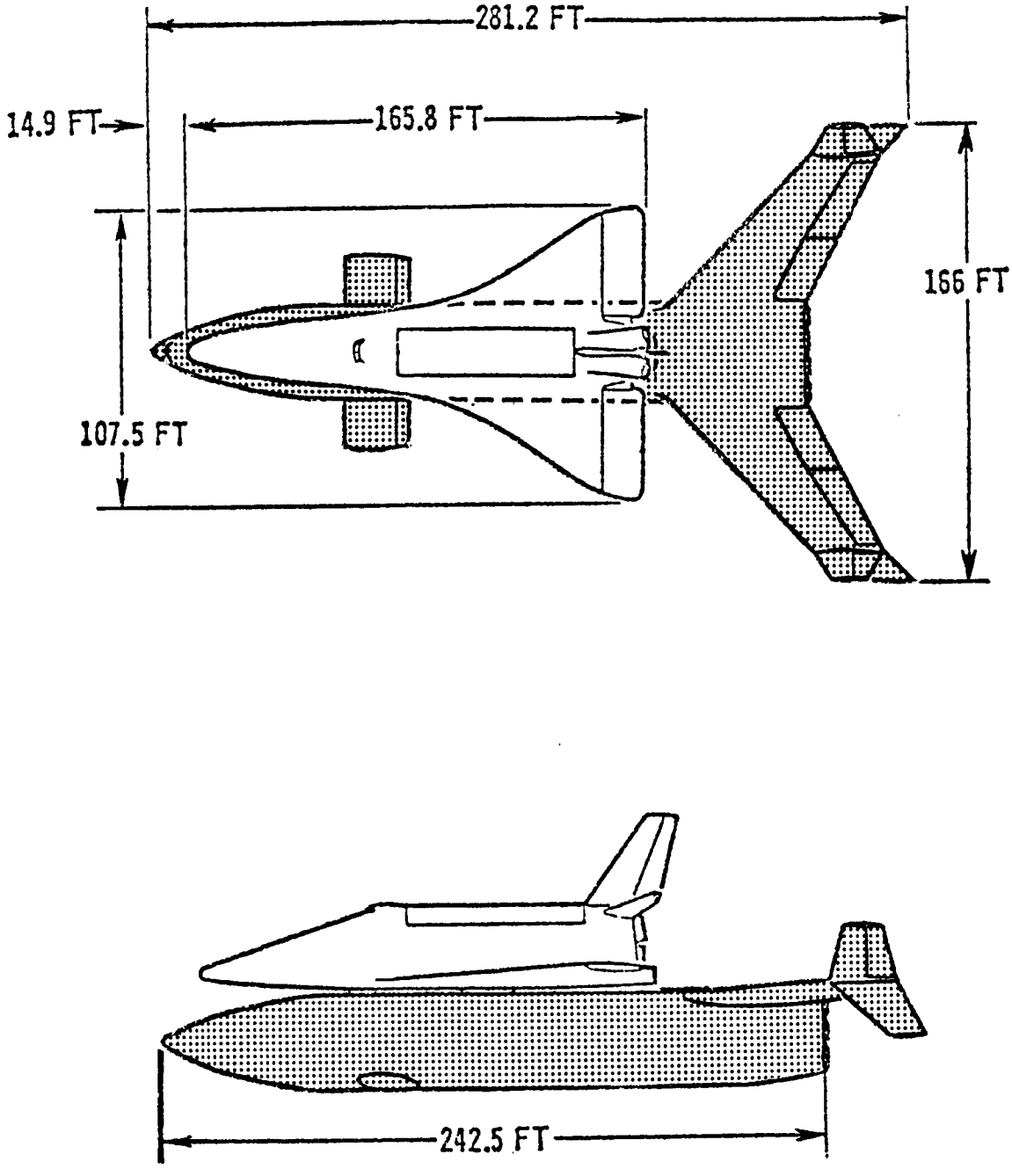

Figure B-1. Typical Fully Reusable Earth Orbit Shuttle (Reference B-1)

(Configuration A)

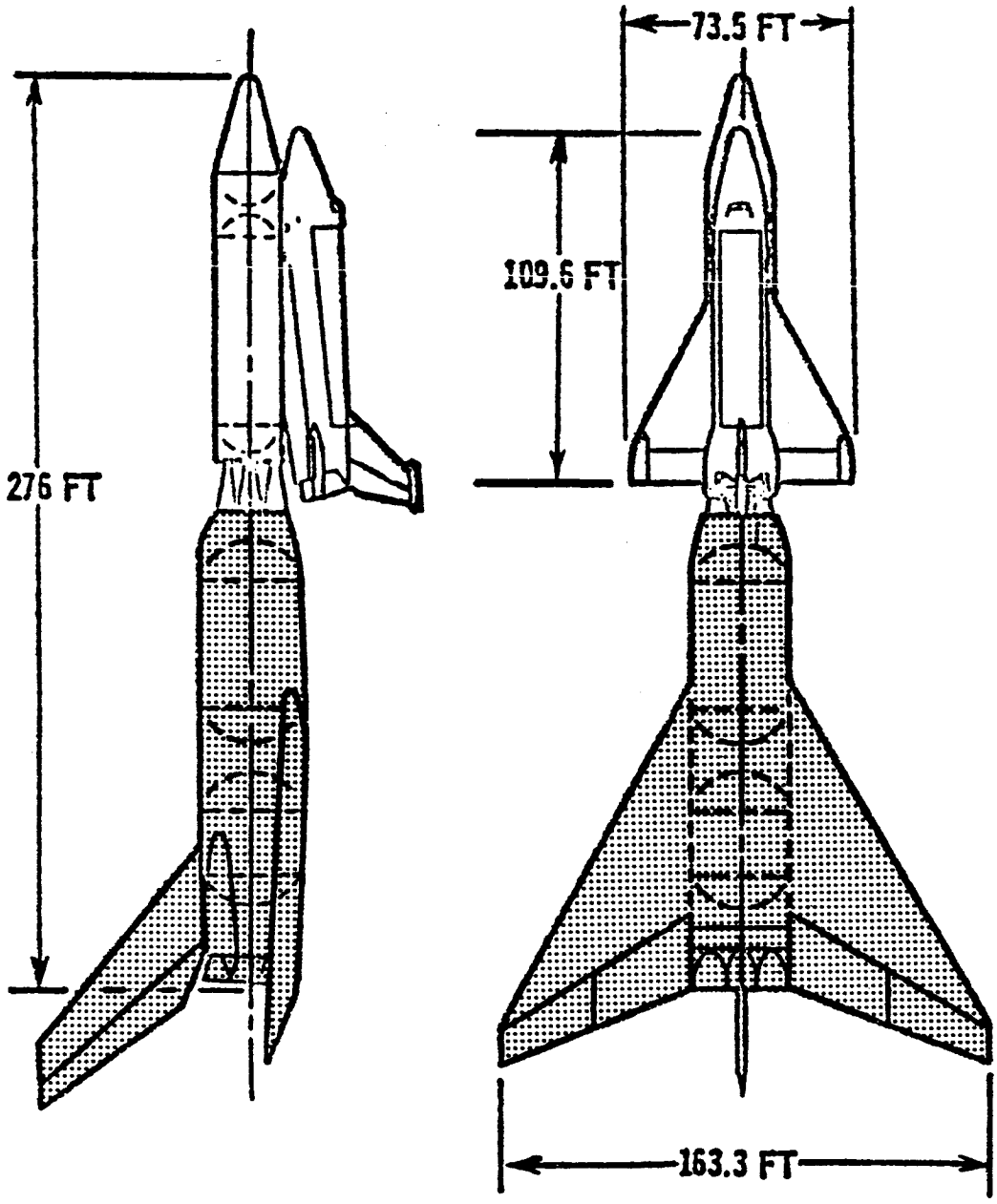

Figure B-2. Typical Mark II Earth Orbit Shuttle With Drop-Tank Orbiter (Reference B-2)

(Configuration B)

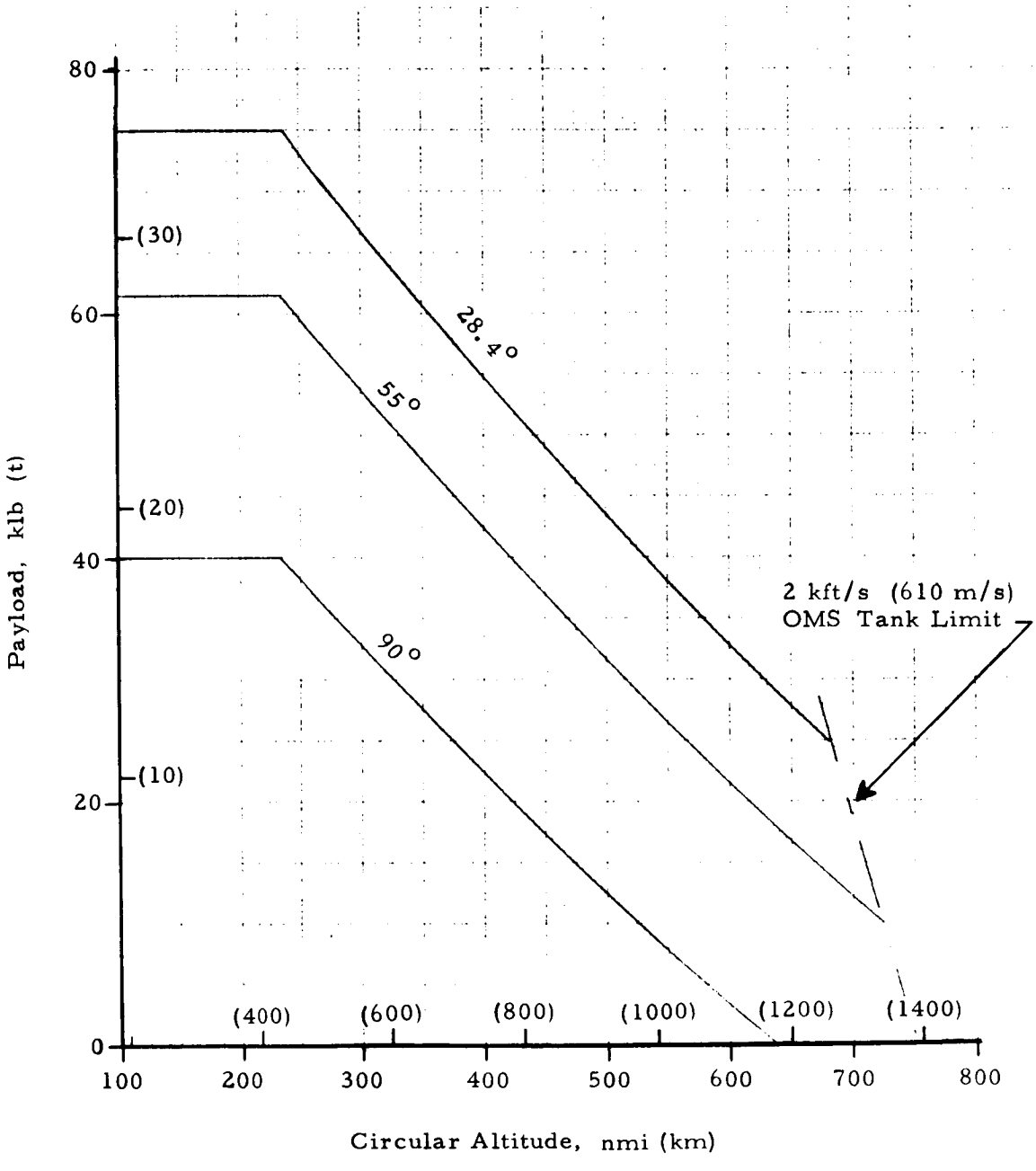

Figure B-3a. Configuration A – Shuttle Performance

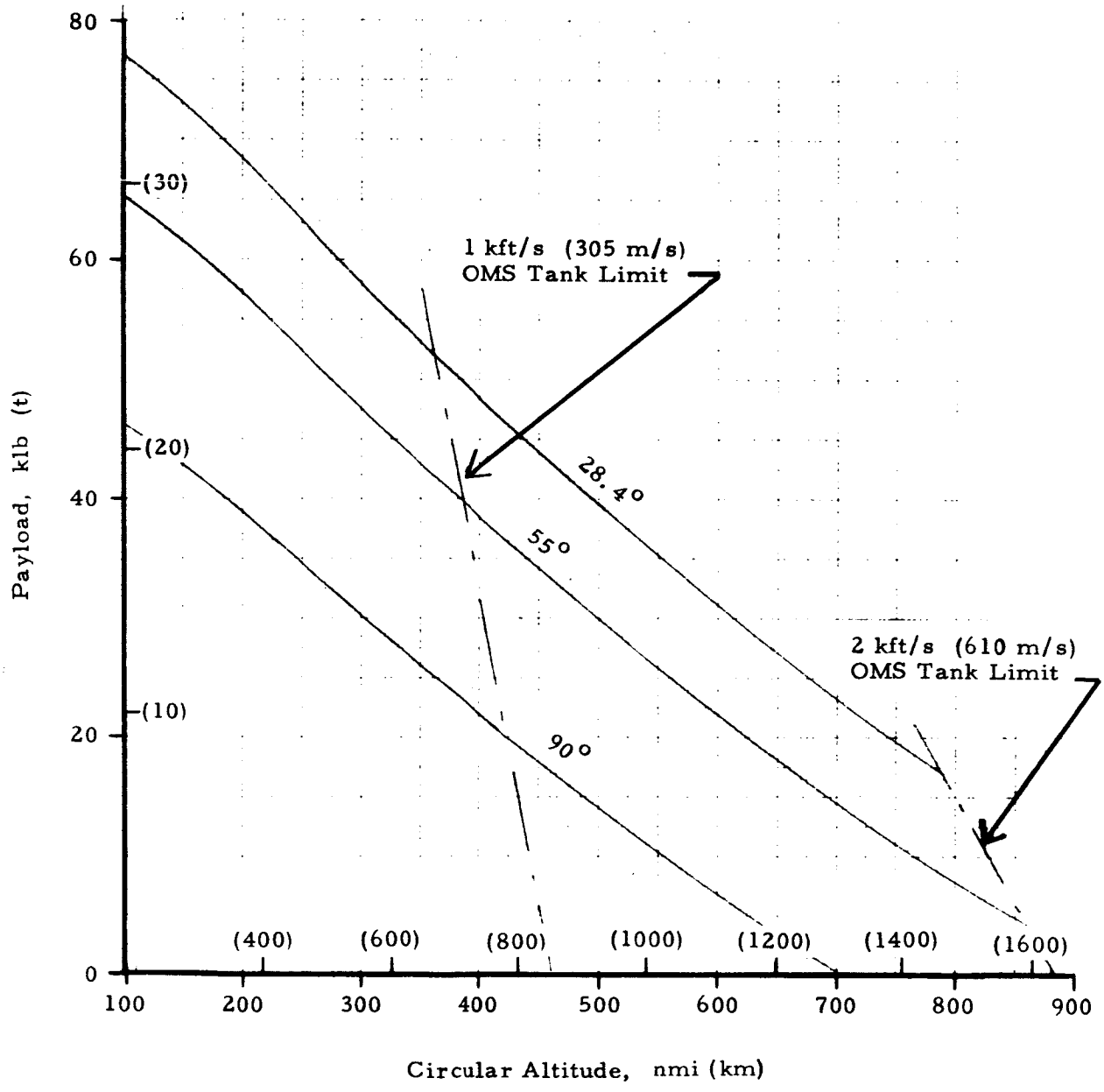

Figure B-3b. Configuration B — Shuttle Performance

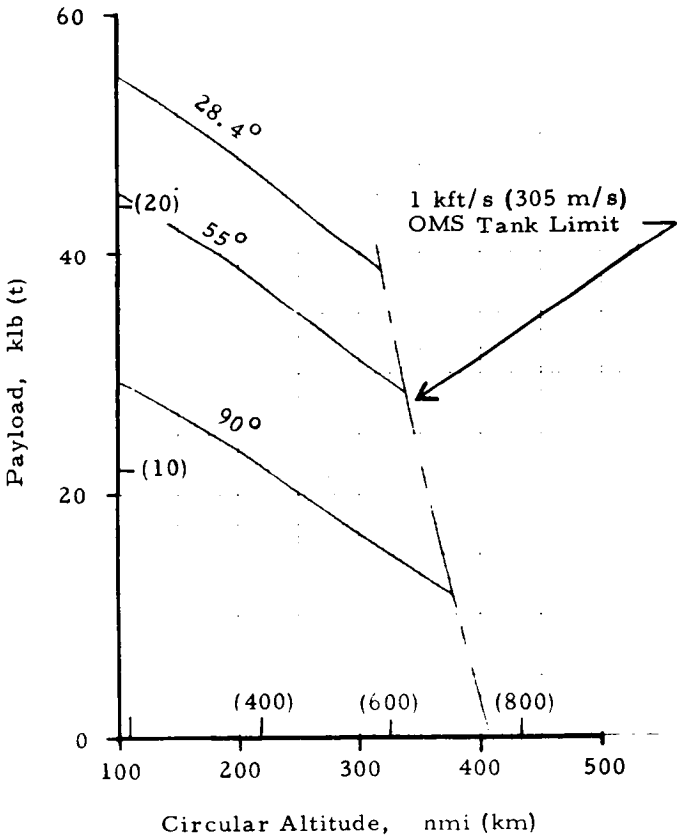

Figure B-3c. Configuration C — Shuttle Performance

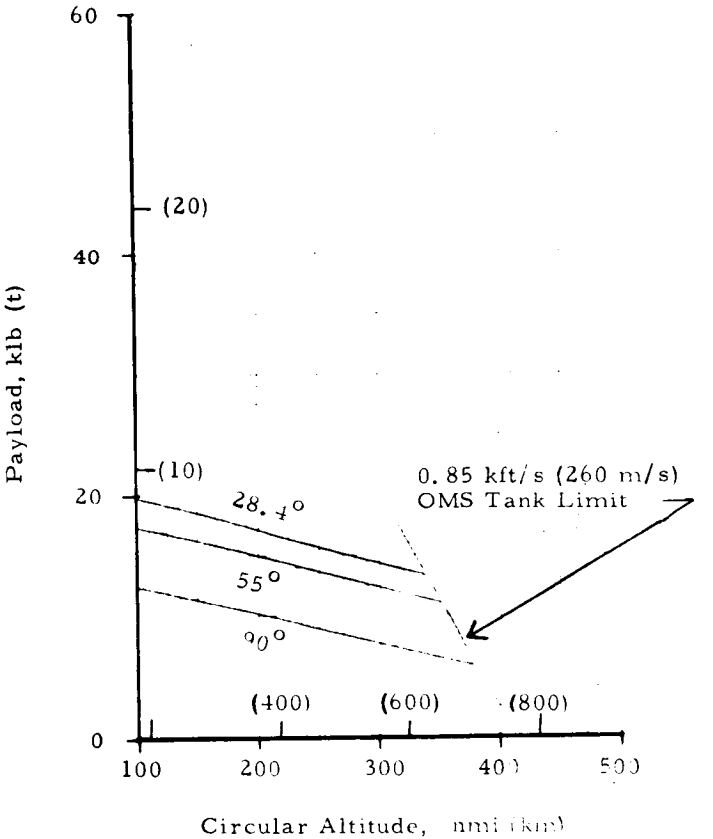

Figure B-3d. Configuration D — Shuttle Performance

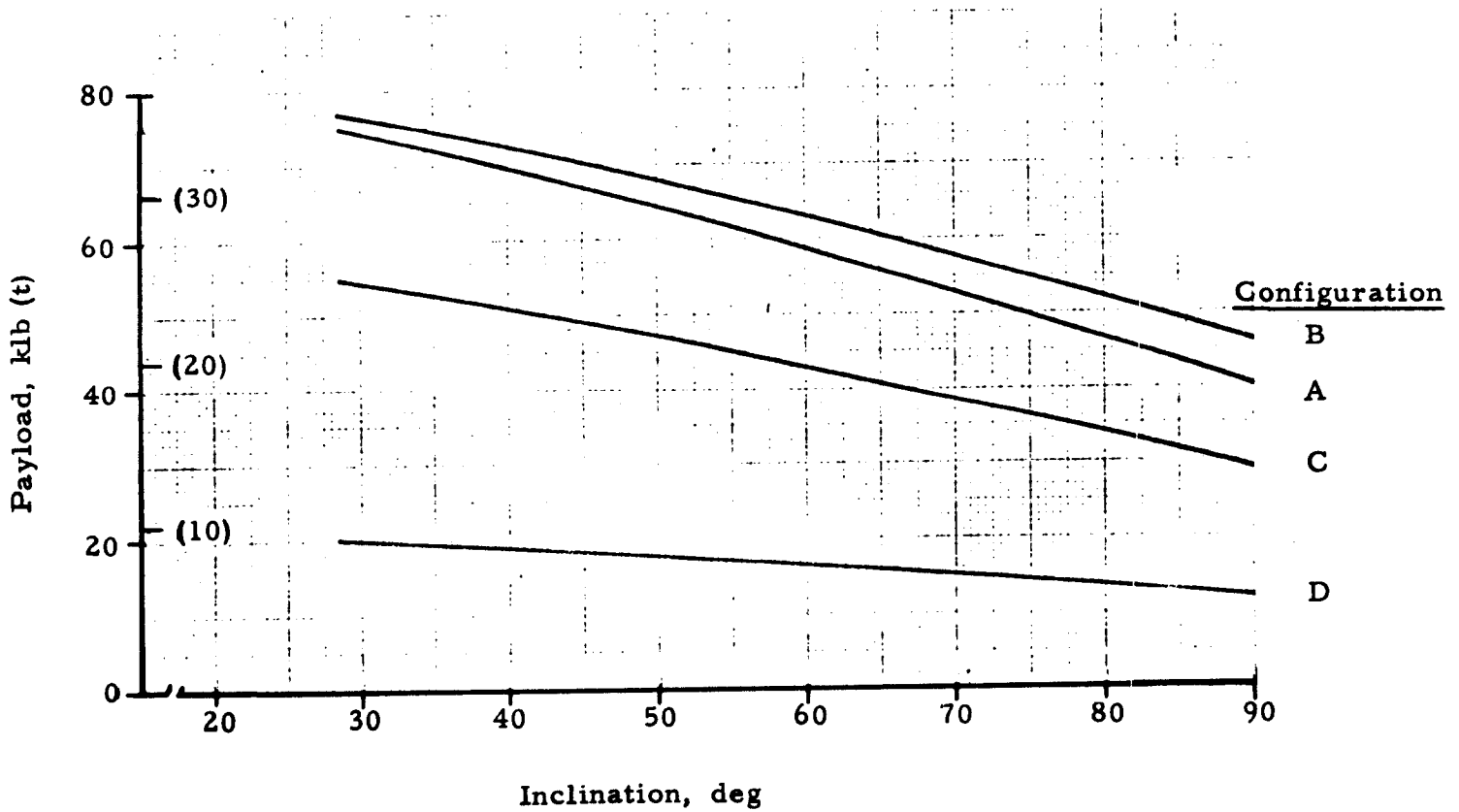

Figure B-4. Shuttle Payload Capability, 100 nmi (185 km) Circular Altitude

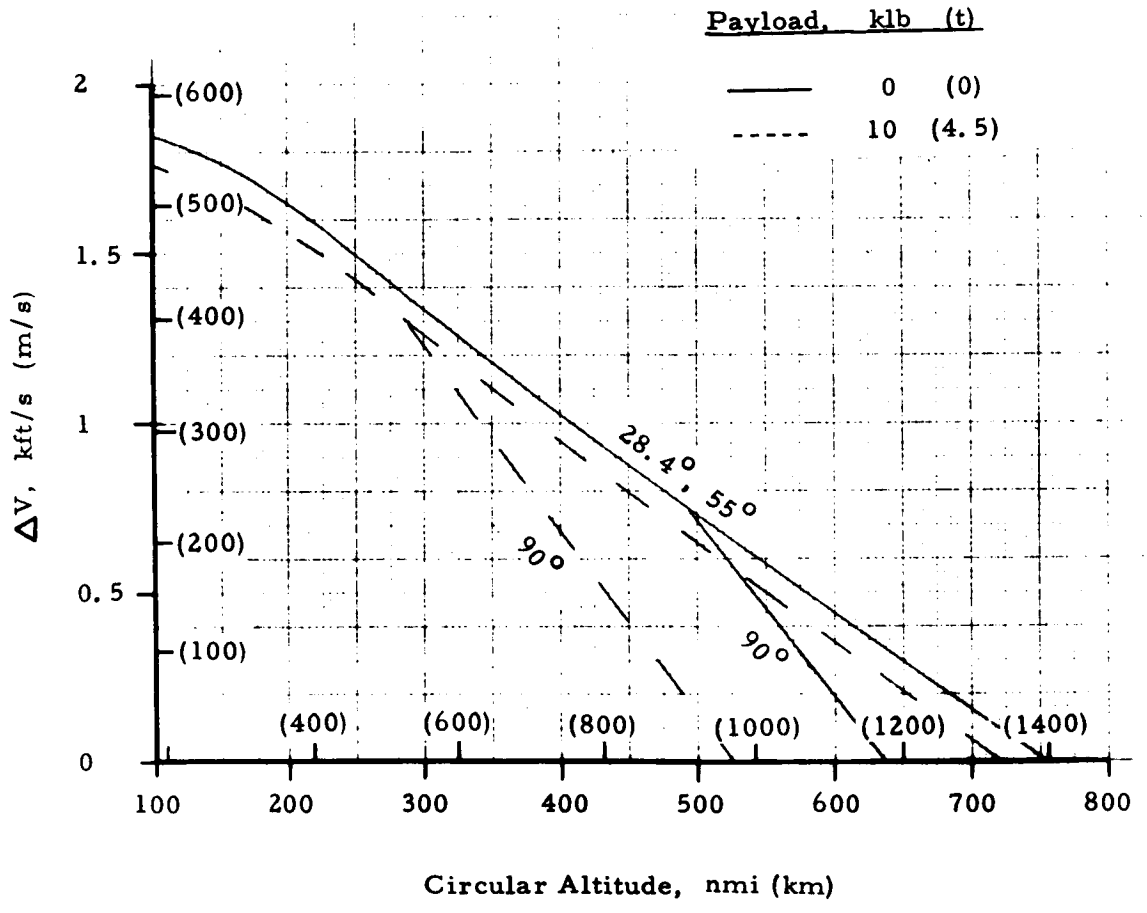

Figure B-5a. Configuration A — Basic Shuttle Rescue Mission Δ V

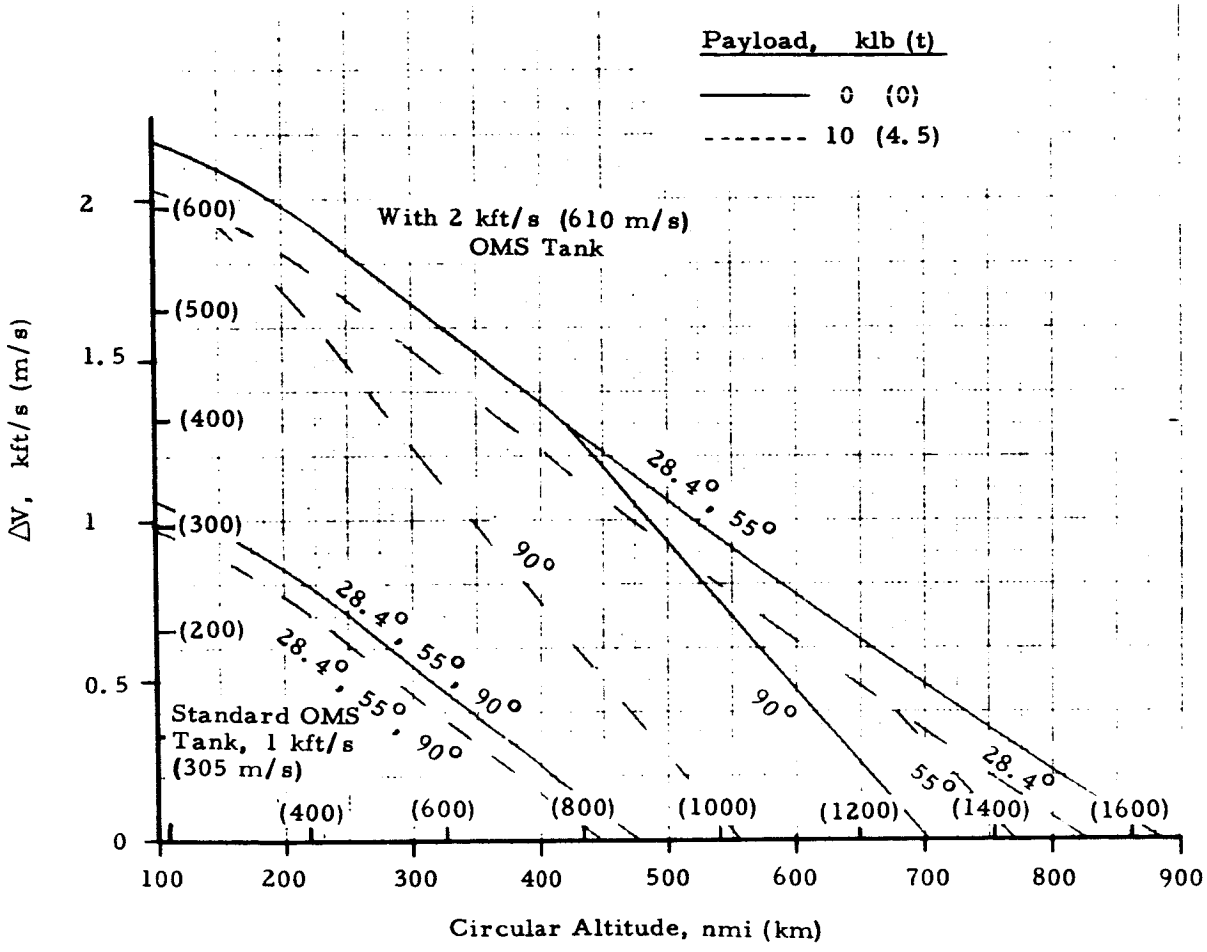

Figure B-5b. Configuration B — Basic Shuttle Rescue Mission ΔV

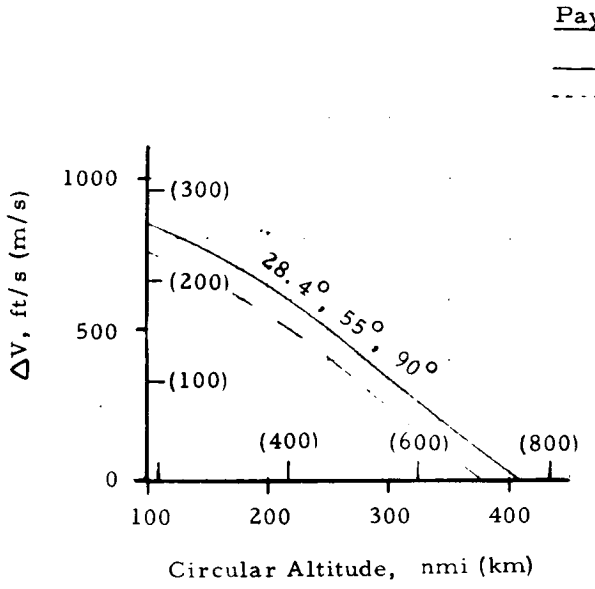

Figure B-5c. Configuration C – Basic Shuttle Rescue Mission ΔV

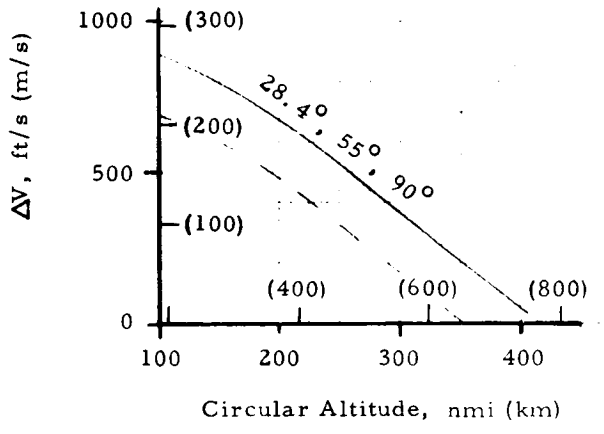

Figure B-5d. Configuration D – Basic Shuttle Rescue Mission ΔV

APPENDIX C

PERFORMANCE WITH INCREASED PROPELLANT LOADING

APPENDIX C

CONTENTS

APPENDIX C

TABLES

FIGURES

APPENDIX C

PERFORMANCE WITH INCREASED PROPELLANT LOADING

C.1 CARGO BAY TANK DESCRIPTION

Increased Orbiter propellant loading is an obvious method for improving EOS performance. All additional propellant is carried in removable tanks installed in the cargo bay. The manner in which the tank plumbing is connected to the Orbiter propellant lines and the specific propellant carried depend upon whether main or OMS propellant is being augmented. If the propellant loading is increased at launch only, then this propellant is burned by the OMS engines. Also, the amount of added propellant is limited by the EOS payload capability.

On the other hand, if a cargo bay tank is refueled in orbit by a propellant donor (see Appendix D), then it can be filled to its volume limit. In this latter case, a very large amount of propellant is involved and must be burned by the main engines. Otherwise, acceleration is extremely low and the burning time excessively long.

It was assumed that the same cargo bay tank design would be used in both cases. It was also assumed that the tank would be sized to fill all available cargo bay space after allowance is made for the rescue payload volume. A cylindrical configuration with elliptic domes having a 2:1 ratio was used.

The various tank sizes used with the four shuttle configurations being examined are given in Table C-1 for 0 and 10 klb (4.5 t) payloads. The tanks are designed to store cryogenic propellants for at least 7 days. The quoted tank weight includes lines and the pumps which give the tank propellant transfer/pressurization capability.

C.2 SHUTTLE PERFORMANCE*

The Shuttle payload capability presented in Figure B-3 of Appendix B includes an OMS propellant budget for circularization and direct reentry from the target orbit. This same payload capability remains valid for the increased propellant loading case, and all payload capacity in excess of the rescue mission payload weight is converted into cargo bay tank plus added propellant weight. The additional propellant load was thus specified for any situation, and the resulting ΔV available by burning this propellant through the OMS engines was determined.

It was assumed that all the loaded OMS propellant is consumed in the basic mission and no excess OMS propellant is available for on-orbit maneuvering. Only the cargo bay propellants are available for this purpose.

A tabulation of the performance capability with increased propellant loading at launch is given in Table C-2 for the four Shuttle configurations examined. Both the maximum circular orbit altitude and the ΔV available in a 100 nmi (185 km) circular orbit are listed for three inclinations (28.4°, 55°, 90°) and two rescue payload weights, 0 and 10 klb (0 and 4.5 t).

Data are shown for two versions of Configuration B (see Appendix B). The "standard" version includes the basic 1 kft/s (305 m/s) OMS capacity, whereas the "auxiliary OMS" version has a 2 kft/s (610 m/s) OMS capacity. If the "auxiliary OMS" capacity is located within the cargo bay, only the basic Shuttle performance will differ from the performance of the "standard" version Shuttle. Shuttle performance with increased propellant loading will be similar for both cases since the "auxiliary OMS" propellant is included in the total weight of the added cargo bay propellant.

The 10 x 20 ft (3 x 6 m) cargo bay of Configuration D is too small to accommodate both a rescue payload (for which a 20 ft (6 m) length allowance was

*The material discussed in this section was provided by W.A. Fey.

assumed) and an added propellant tank. Thus, increased propellant loading can be achieved with Configuration D only when no rescue payload is carried.

The performance available with increased propellant loading is more readily displayed in Figure C-1. The on-orbit ΔV is presented as a function of orbit altitude for each of the four Shuttle configurations. Only payloads of 0 and 10 klb (0 and 4.5 t) are considered and curves are plotted for inclinations of 28.4, 55, and 90°. The curve intercept with the abscissa at $\Delta V = 0$ and with the ordinate of 10 nmi (185 km) are the values tabulated in Table C-2 for the augmented performance case.

In comparing the available ΔV with those shown for the baseline configurations in Figure B-5, it can be seen that the increases are often substantial. The regions of increased performance occur where baseline configuration performance is limited by OMS tank capacity. Where the baseline performance is limited by the load carrying ability (at high altitude and at the larger values of inclination), some decrease in performance is incurred due to the weight penalty of the cargo tank. There is one instance where the performance is limited by capacity of the cargo bay tank, as can be seen on Figure C-1c for an inclination of 28.4° (east launch) and a 10 klb (4.5 t) payload at orbit altitudes from 100 to 225 nmi (185 to 416 km).

C.3 PERFORMANCE COMPARISON

By crossplotting data from Figure C-1 and Figure B-5 of Appendix B, comparisons can be made between the basic and augmented Shuttle on-orbit ΔV capability. Such comparisons are given in Figure C-2 for a 100 nmi (185 km) circular orbit. Results are shown for both the "standard" and "auxiliary" Configuration B versions. A corresponding comparison between the basic and maximum augmented on-orbit ΔV capability of the parallel-burn Space Shuttle is given in Figure J-7 (Appendix J).

The altitude at which the on-orbit ΔV becomes zero is the maximum altitude which can be attained with a rescue mission payload. A maximum altitude

comparison between the reference and augmented EOS configuration is also included in Figure C-2.

The effectiveness of increased propellant loading depends on both the Shuttle configuration and the specific rescue mission. If the mission imposes a requirement approaching the limit of the basic EOS capability, little can be gained. In fact, when allowance is made for the weight of the cargo bay tank and related plumbing, the augmented Shuttle performance may actually be less than previously available with the basic EOS. This occurs because the cargo bay tank was oversized to occupy all available cargo bay space and not sized to the propellant weight that can be carried from launch. The 10 klb (4.5 t), 90° cases for Configurations A and B_{aux} fall into this category. With the tank sized to match the added fuel load at launch, the augmented performance should always be equal to or greater than the basic Shuttle capability to the same inclination. However, even at lower inclinations, increased propellant loading does little to improve the maximum altitude capability of these two configurations.

The primary benefit of increased propellant loading occurs at low orbit altitudes and inclinations. An increase in available ΔV between 1 and 2 kft/s (305 and 610 m/s) is observed at 100 nmi (185 km) and 28.4° with a 10 klb (4.5 t) payload for all configurations except D. The 20 ft (6 m) length assumed for the 10 klb (4.5 t) rescue payload fills the entire cargo bay of Configuration D leaving no volume for a cargo bay propellant tank.

Table C-1. Cargo Bay Propellant Tank Characteristics

Shuttle Config.	Cargo Bay Size, ft (m)	Rescue P/L Weight, klb (t)	Tank Size ft (m)	Tank Weight klb (t)	H_2/O_2 *Capacity klb (t)
A	15 x 60	0	15 x 60	11	214
		(0)	(4.6 x 18.3)	(5)	(97)
	(4.6 x 18.3)	10	15 x 40	7.5	149
		(4.5)	(4.6 x 12)	(3.4)	(68)
B	15 x 60	0	15 x 60	11	214
		(0)	(4.6 x 18.3)	(5)	(97)
	(4.6 x 18.3)	10	15 x 40	7.5	149
		(4.5)	(4.6 x 12)	(3.4)	(68)
C	12 x 40	0	12 x 40	4.8	97
		(0)	(3.7 x 12)	(2.2)	(44)
	(3.7 x 12)	10	12 x 20	2.3	46
		(4.5)	(3.7 x 6)	(1.0)	(21)
D	10 x 20	0	10 x 20	1.6	32
	(3 x 6)	(0)	(3 x 6)	(0.7)	(15)

*6:1 Mixture Ratio

Table C-2. Performance Comparison Between Basic and Increased Propellant Loading Shuttle Configurations

Configuration	Rescue P/L, klb (t)	*Augmented Propellant Wt, klb (t)	Maximum Altitude, nmi (km)						ΔV, ft/s (m/s) @ 100 nmi (185 km)					
			28.4°		55°		90°		28.4°		55°		90°	
			Basic	Aug.	Basic	Aug.	Basic	Aug.	Basic	Aug.	Basic	Aug.	Basic	Aug.
A	0 (0) 10 (4.5)	** 75/40 (34/18) 65/30 (30/14)	755 (1400) 725 (1340)	835 (1540) 760 (1410)	755 (1400) 725 (1340)	710 (1310) 640 (1180)	640 (1180) 525 (970)	515 (950) 450 (830)	1850 (565) 1760 (536)	3900 (1190) 3540 (1080)	1850 (565) 1760 (536)	3270 (1000) 2910 (886)	1850 (565) 1760 (536)	2220 (676) 1840 (560)
B (Std.)	0 (0) 10 (4.5)	77/46 (35/21) 67/36 (30/16)	470 (870) 445 (820)	885 (1640) 785 (1450)	470 (870) 445 (820)	755 (1400) 655 (1210)	470 (870) 445 (820)	540 (1000) 455 (840)	1060 (323) 970 (296)	3540 (1080) 3130 (955)	1060 (323) 970 (296)	3000 (915) 2580 (786)	1060 (323) 970 (296)	2040 (622) 1640 (500)
B (Aux. OMS)	0 (0) 10 (4.5)	77/46 (35/21) 67/36 (30/16)	885 (1640) 825 (1530)	885 (1640) 785 (1450)	885 (1640) 765 (1410)	755 (1400) 655 (1210)	705 (1300) 555 (1030)	540 (1000) 455 (840)	2180 (664) 2030 (619)	3540 (1080) 3130 (955)	2180 (664) 2030 (619)	3000 (915) 2580 (786)	2180 (664) 2030 (619)	2040 (622) 1640 (500)
C	0 (0) 10 (4.5)	55/29 (25/13) 45/19 (20/ 9)	405 (750) 380 (700)	830 (1540) 695 (1290)	405 (750) 380 (700)	700 (1300) 575 (1060)	405 (750) 380 (700)	485 (900) 365 (680)	850 (259) 760 (232)	3400 (1040) 2280 (695)	850 (259) 760 (232)	2830 (863) 2250 (686)	850 (259) 760 (232)	1820 (555) 1230 (375)
D	0 (0) 10 (4.5)	20/12 (9/5) N/A —	415 (770) 355 (660)	880 (1630) N/A —	415 (770) 355 (660)	785 (1450) N/A —	415 (770) 205 (380)	575 (1060) N/A —	890 (271) 690 (210)	4550 (1390) N/A —	890 (271) 690 (210)	4050 (1240) N/A —	890 (271) 690 (210)	2880 (880) N/A —

*Includes Tank Weight

**DUE EAST/POLAR

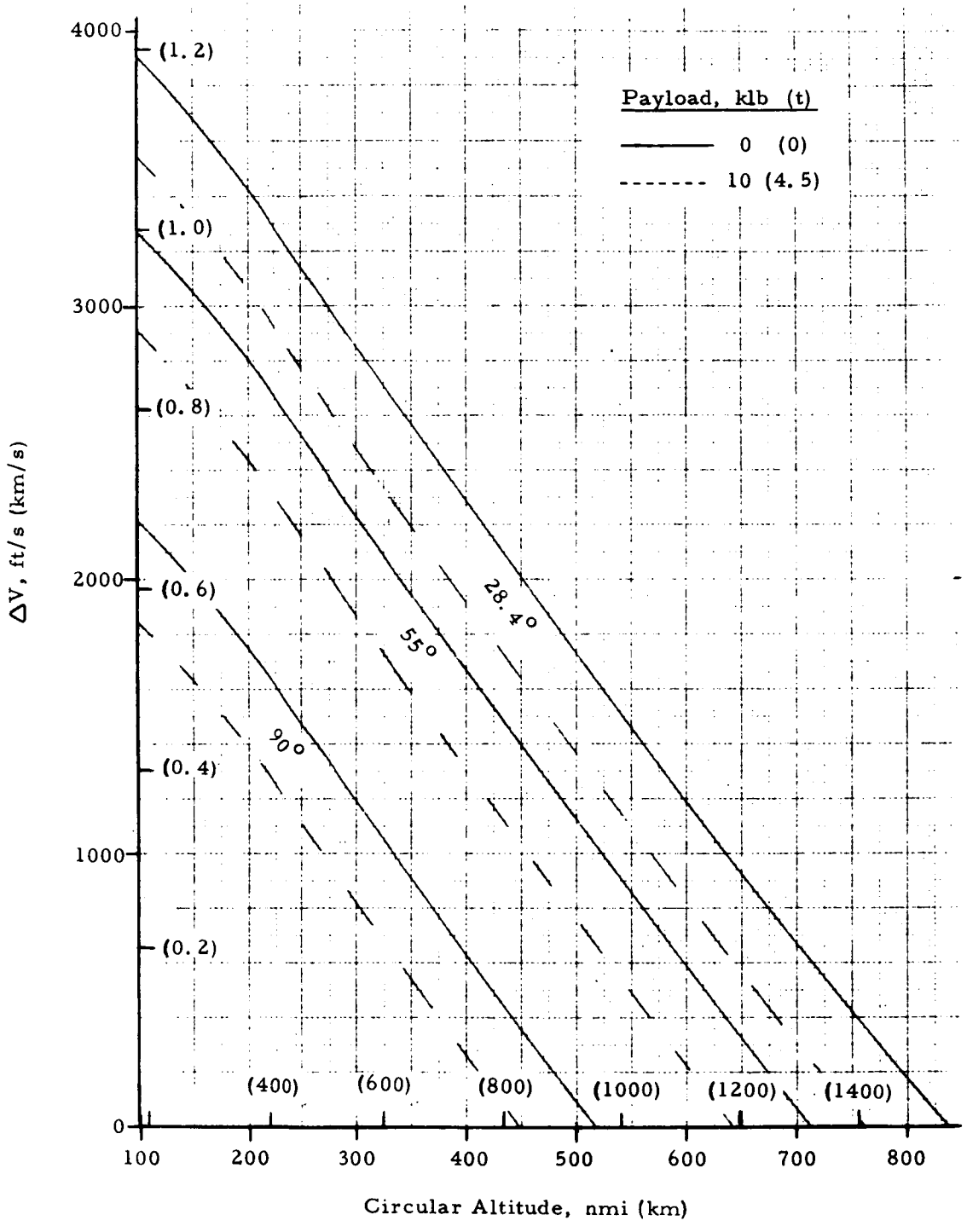

Figure C-1a. Configuration A - Available On-Orbit ΔV with Increased Propellant Loading (Direct Reentry)

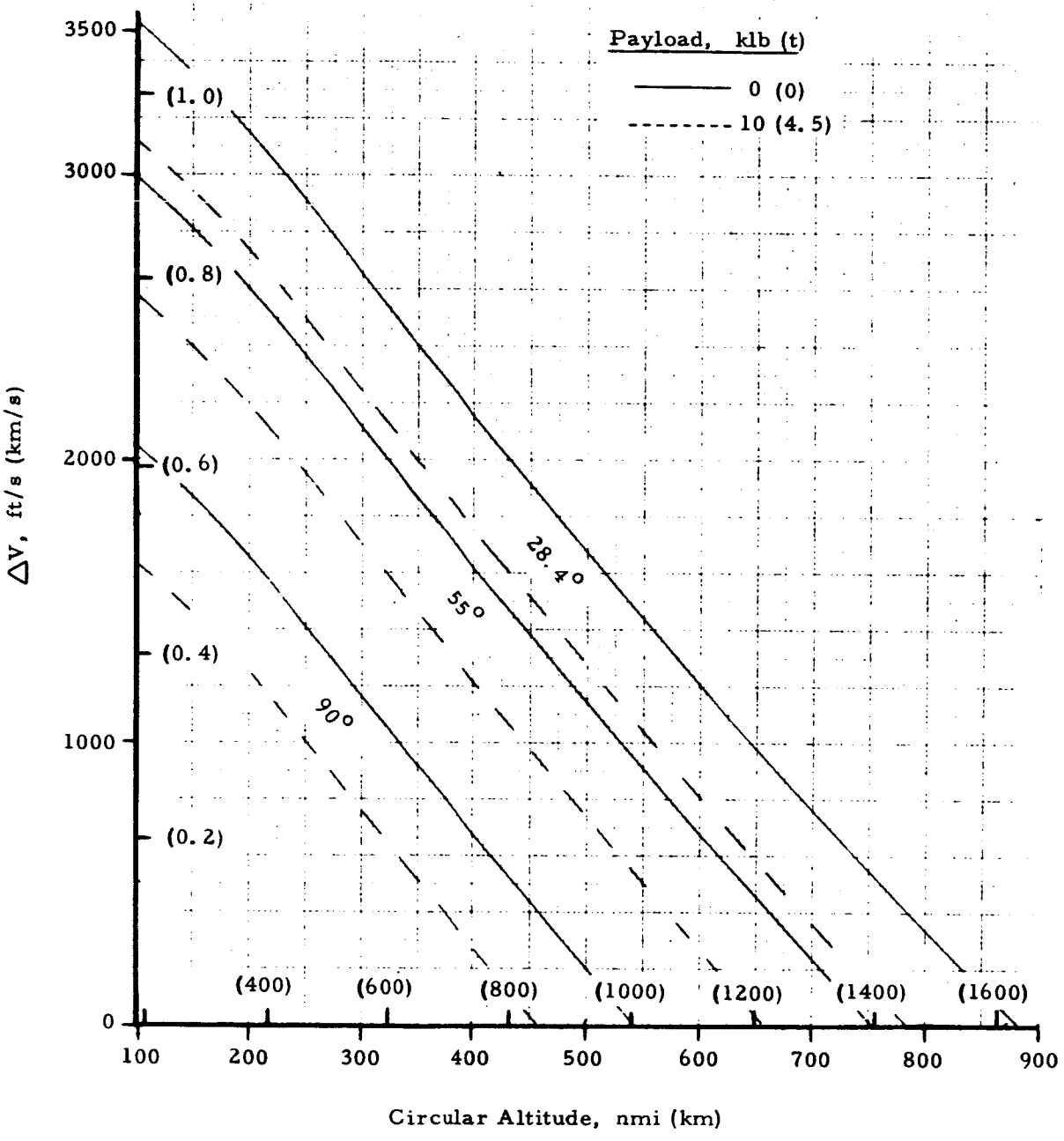

Figure C-1b. Configuration B - Available On-Orbit ΔV with Increased Propellant Loading (Direct Reentry)

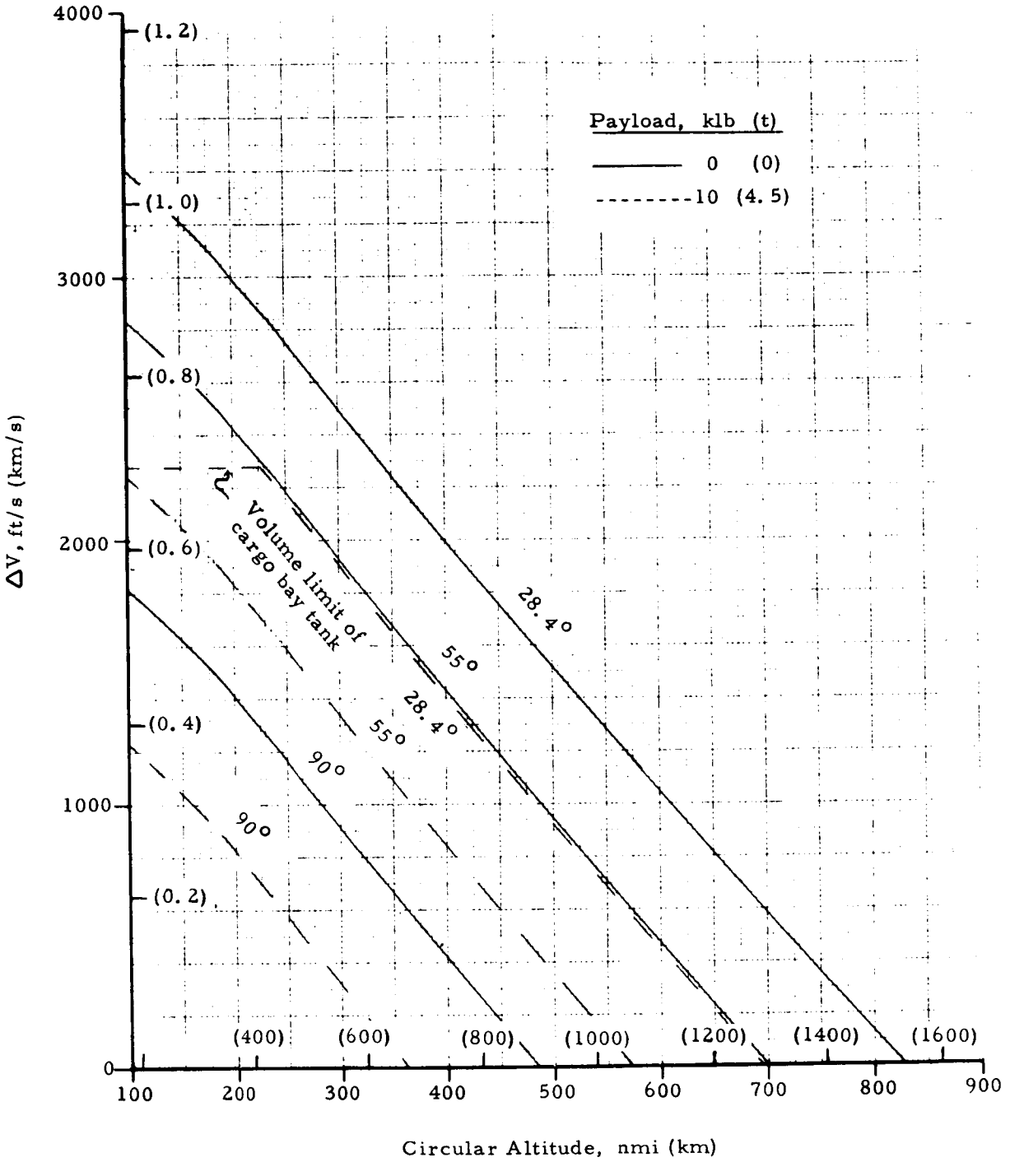

Figure C-1c. Configuration C - Available On-Orbit ΔV With Increased Propellant Loading (Direct Reentry)

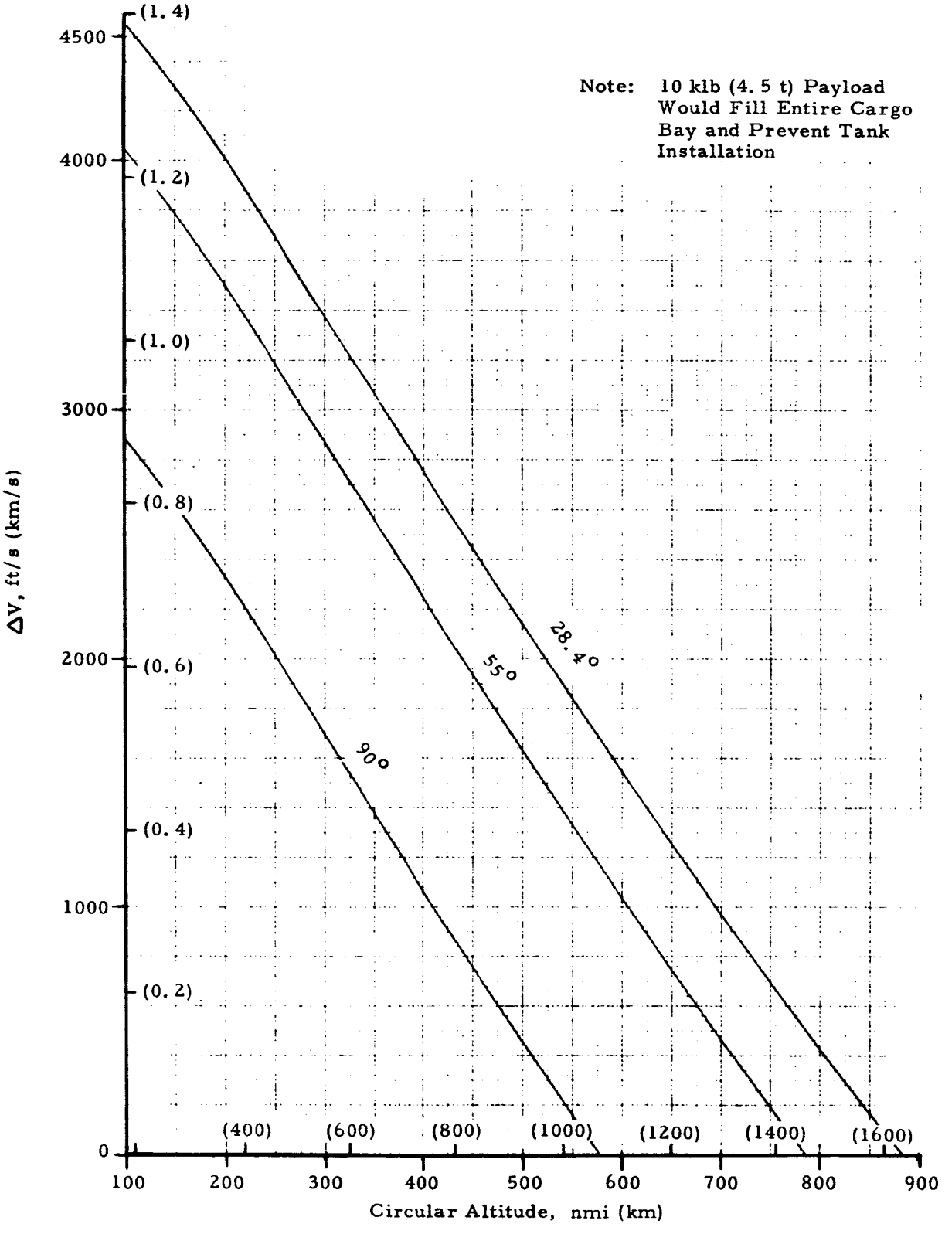

Figure C-1d. Configuration D; Zero Payload Case - Available On-Orbit ΔV with Increased Propellant Loading (Direct Reentry)

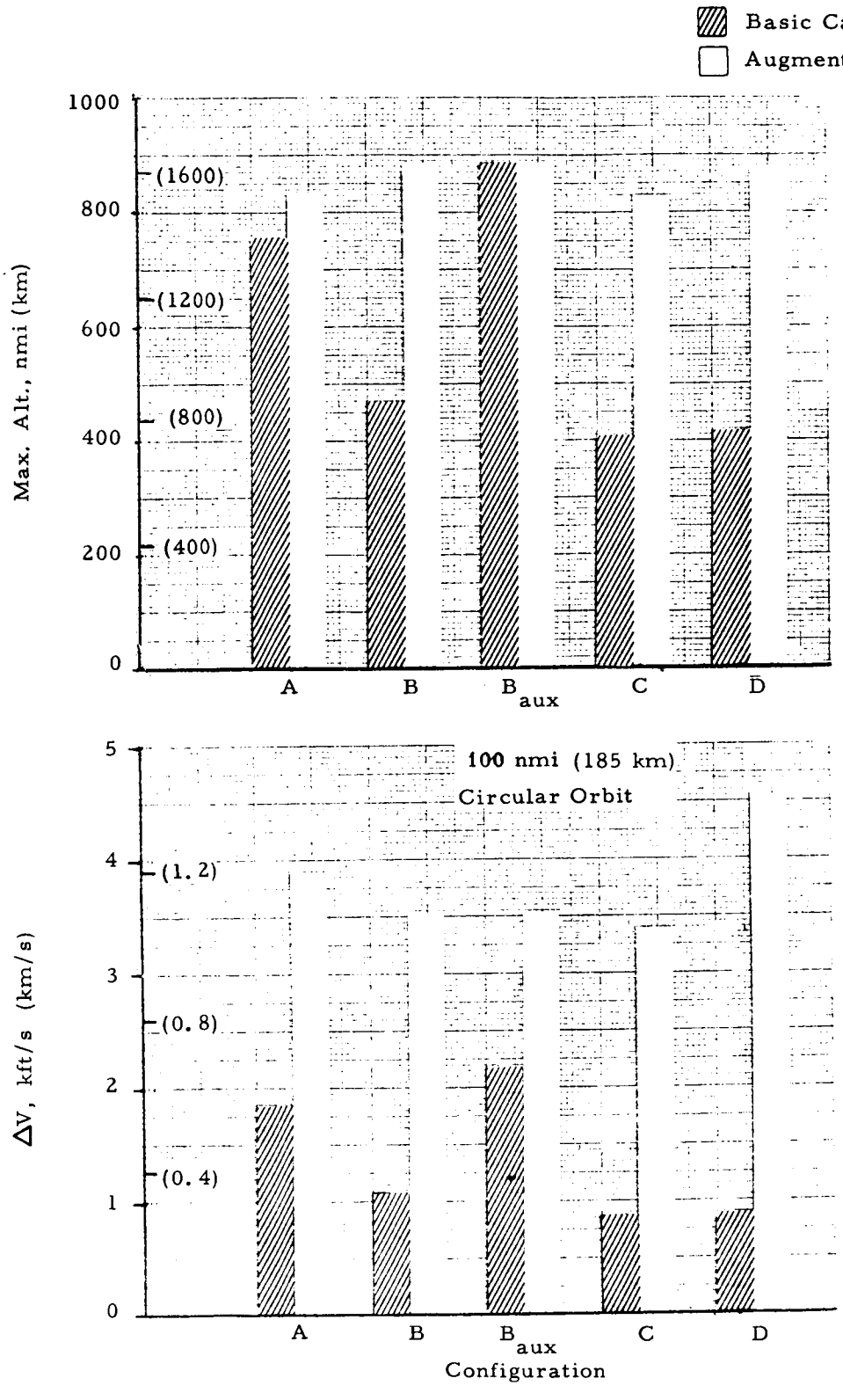

Figure C-2a. "0" Payload; 28.4° Inclination - Shuttle Performance Comparison with Increased Propellant Loading (Direct Reentry)

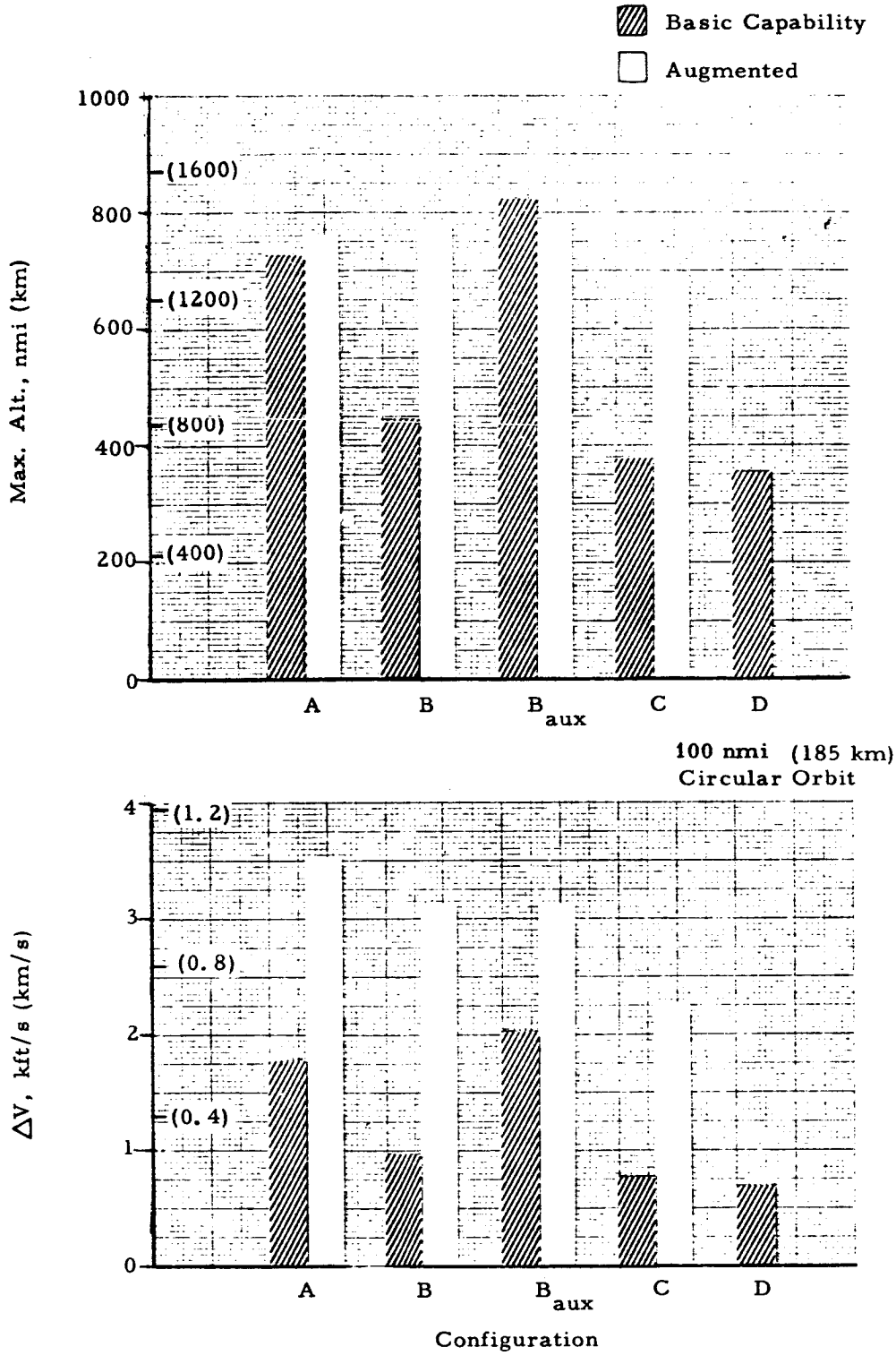

Figure C-2b. 10 klb (4.5 t) Payload; 28.4° Inclination - Shuttle Performance Comparison with Increased Propellant Loading (Direct Reentry)

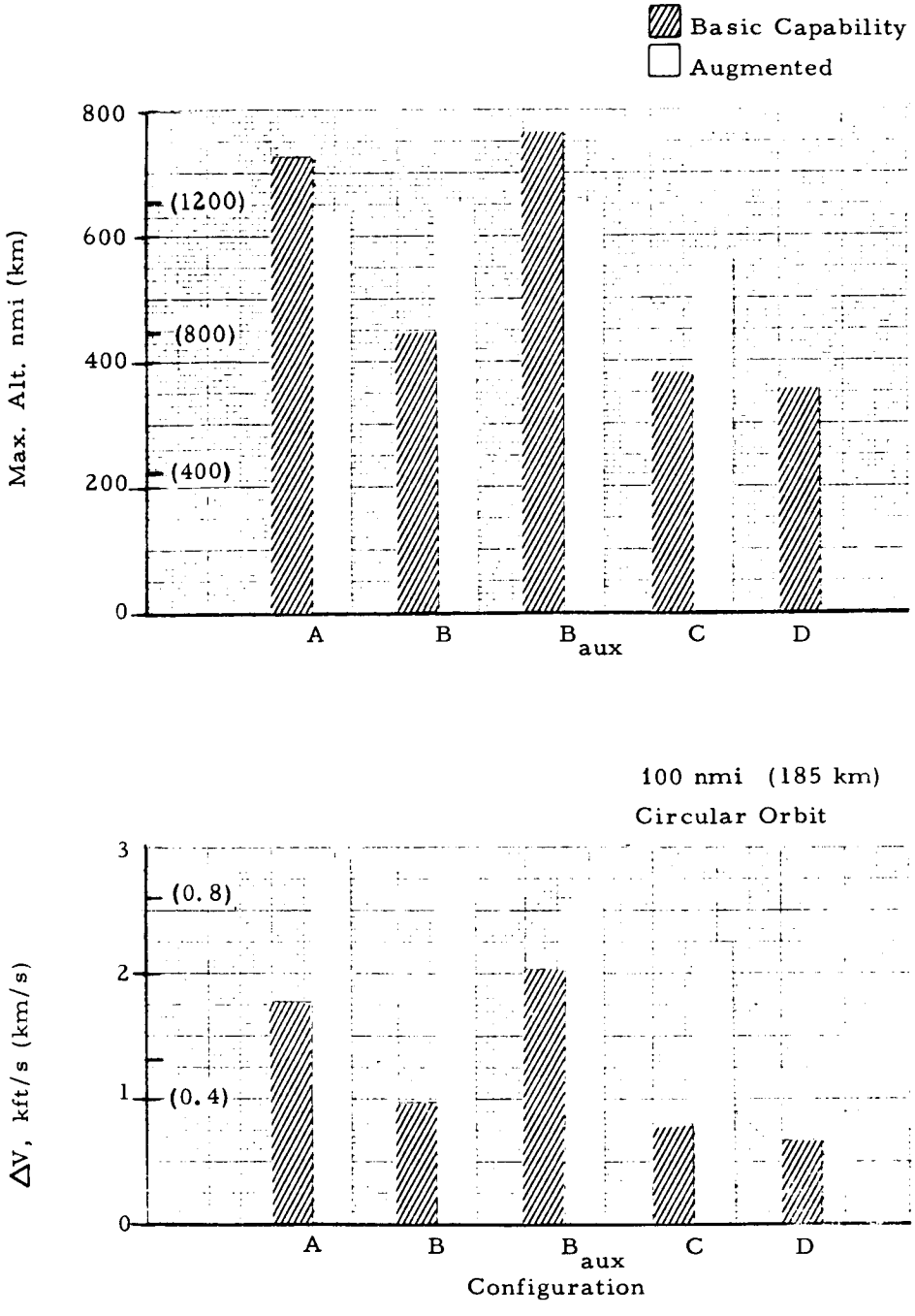

Figure C-2c. 10 klb (4.5 t) Payload; 55° Inclination - Shuttle Performance Comparison with Increased Propellant Loading (Direct Reentry)

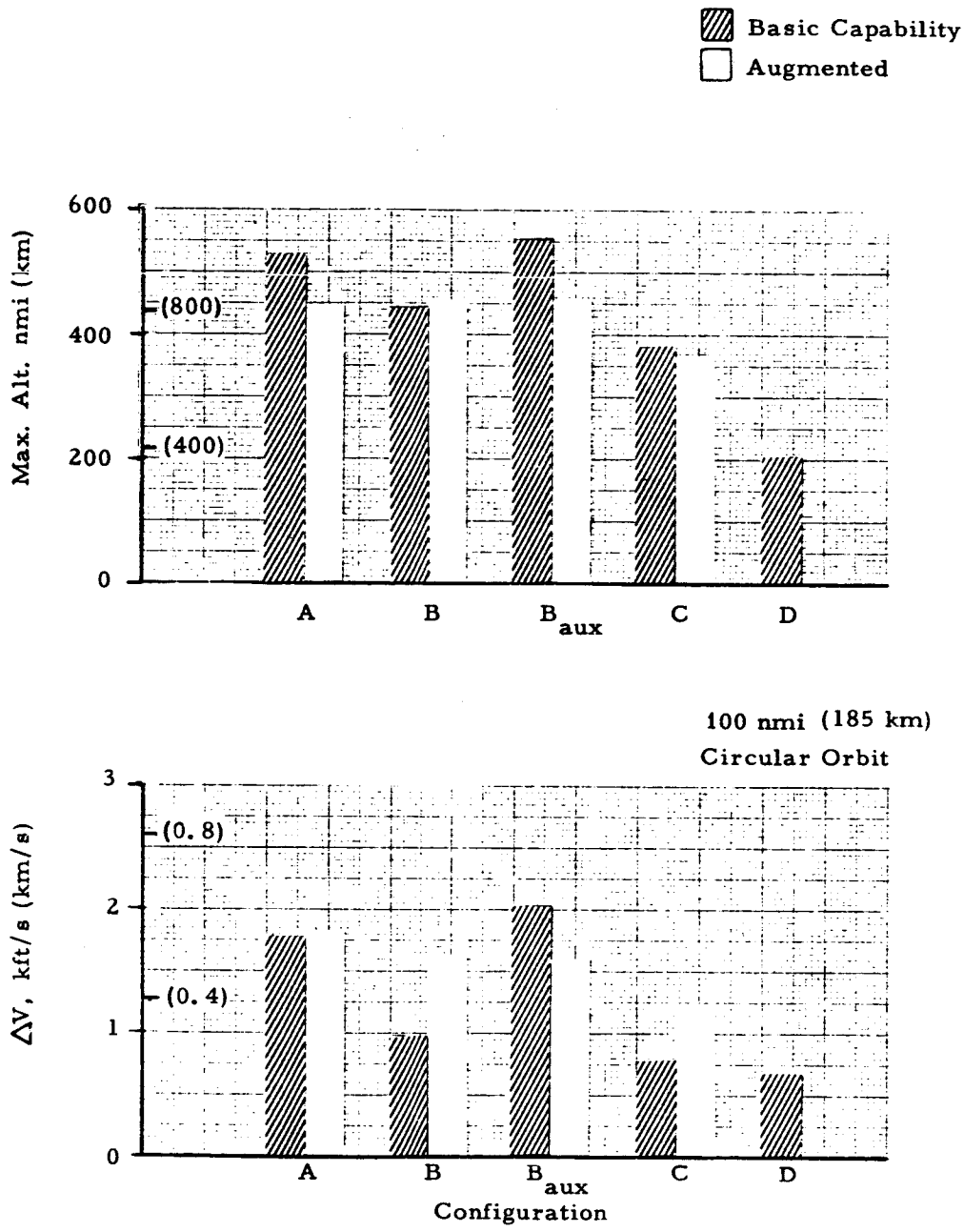

Figure C-2d. 10 klb (4.5 t) Payload; 90° Inclination - Shuttle Performance Comparison with Increased Propellant Loading (Direct Reentry)

APPENDIX D

PERFORMANCE WITH ORBITAL REFUELING

APPENDIX D

CONTENTS

APPENDIX D

TABLES

FIGURES

APPENDIX D

PERFORMANCE WITH ORBITAL REFUELING

D.1 INTRODUCTION

Numerous techniques have been considered for providing large quantities of propellant in low earth orbit. The intended use of this propellant was the Reusable Nuclear Shuttle and/or the Chemical Interorbital Shuttle. Although current interest in these vehicles has waned, the results of orbital refueling studies made when interest was high remain valid and are useful in assessing the feasibility of refueling the Earth Orbit Shuttle (EOS) Orbiter stage in low earth orbit.

Several methods have been proposed for donating propellant to a vehicle in space. They include an orbiting propellant depot; a propellant-filled, expendable second stage; and a caravan of propellant carrying, EOS logistic flights. This study did not require specific identification of the propellant donor method employed.

Significant time and effort have been devoted to assessing the feasibility and technical details of an Orbiting Propellant Depot (OPD). Refueling the Orbiter at an OPD is not necessarily recommended as the preferred technique in this Space Shuttle Rescue Capability study. However, many of the problems to be faced in donating propellant to the Orbiter were examined in past OPD studies and the results are directly applicable. Orbital propellant storage need not be involved, and yet the problems remain of propellant delivery to orbit and the transfer of propellant from the donor to the user.

D.2 PROPELLANT TRANSFER

D.2.1 General

Completed OPD studies included detailed analyses of the procedures involved in transferring propellant from a donor (an OPD in this case) to a user. Also included were analyses of the procedures involved in transferring propellant from a logistics delivery vehicle to an OPD.

D.2.2 Transfer Timelines

Typical timelines for propellant transfer from an OPD to a Tug and to a Reusable Nuclear Shuttle were presented in Reference D-1 and are reproduced as Figures D-1 and D-2, respectively. The propellant quantities and the total time for the refueling operation, as established by liquid hydrogen (LH_2) transfer requirements, are summarized in Table D-1. The LH_2 flow rates upon which these times are based are as follows:

30 klb/hr (13.6 t/hr) – fast fill
3 klb/hr (1.4 t/hr) – low flow chill; throttled flow

Based upon these timelines, estimates were made for the total time to refuel Orbiter Configurations A, B, C and D; the Tug; and a cargo bay tank sized for Configurations A and B. The refueling times so determined are listed in Table D-2.

It should be noted that docking, tank preparation, post transfer and undocking activities occupy over half the total time for the refueling operation. As a consequence, the estimated total time varies by just a few hours between Orbiter, Tug, and cargo bay tank.

A liquid hydrogen flow rate approximately 50% greater was suggested in Reference D-2 and 5 times greater in Reference D-3. As a consequence, a Tug refueling timeline of 12 hours (as compared to 20 hours in Table D-2) is projected in Reference D-3. The extrapolated value for Orbiter refueling would be an additional 1 – 2 hours.

Clearly, one-half to a full day will be occupied with refueling the Orbiter from an OPD. Other propellant donors which also involve propellant transfer (i.e., an expendable second stage or a caravan of propellant carrying EOS logistic flights) introduce even longer refueling timelines.

The timeline for transferring propellant in orbit from a Space Shuttle propellant-carrying logistic vehicle to a propellant user was also presented in Reference D-1 and is reproduced as Figure D-3. A single Shuttle flight will deliver about 65 klb (29.5t) of propellant into low earth orbit (less for Configurations C and D). Following rendezvous between donor and user, the estimated time to transfer this small amount of propellant is 26 hours. Thus, even if all logistic Shuttles needed to completely refuel an Orbiter were sequentially available, the propellant transfer operation would require more than one week (see Table B-1).

More propellant could be delivered per flight with an expendable second-stage Shuttle configuration. But even this approach involves a propellant transfer total time in excess of 3 days (see Table 5, Volume IIA).

D.2.3 Tank Exchange

For a rescue mission where time can be critical, a less time consuming approach to orbital refueling is desirable. Tank exchange represents an interesting possibility. An empty propellant tank is exhanged for a fully fueled tank previously placed in orbit as part of an OPD or refueled from an OPD.

This approach is applicable to Orbiter configurations such as B, C, and D which have separable main propellant tanks. It can also be used with removable cargo bay tanks. Although rendezvous and docking are involved, the procedures are similar to those for payload deployment and retrieval. Based on the applicable procedures from Figure 3, the total time for tank exchange is estimated to be under 2 hours.

D.3 SHUTTLE PERFORMANCE *

D.3.1 Refueling Altitude

The concept of refueling the Orbiter after it attains orbit provides an interesting method of increasing Orbiter performance capability. Refueling would occur in low earth orbit. The exact altitude selected depends on a compromise between tanker vehicle payload and avoiding substantial Orbiter and fuel donor orbit decay. Orbit sustaining techniques may be advantageous, and an altitude providing frequent rendezvous opportunities for the Orbiter, fuel donor, and tanker vehicles is desirable. A discussion of these factors is given in Reference D-4.

Orbiter velocity requirements for various rescue maneuvers are dependent upon the refueling altitude but only to a minor degree, considering the large velocity capability available after full refueling. Therefore, no precise definition of an optimum refueling altitude is required.

D.3.2 Assumptions and Operating Procedure

It was assumed that main and OMS propellant tanks of the baseline vehicle can be fully refueled. It was further assumed that the main tanks are burned to propellant depletion, the drop tanks (if any) are then jettisoned, and finally the OMS propellant is used. The basic weight and propulsion data used are given in Table B-1 of Appendix B.

If the vehicle is provided with an additional cargo bay propellant tank, it can also be filled during on-orbit refueling. Moreover, it can be filled to capacity, since there is no load-lifting capability limit imposed on a vehicle already in orbit. The cargo bay tank weights used in these calculations are given in Table C-1 of Appendix C.

In determining the velocity capabilities of an Orbiter with a cargo bay tank, it was assumed that the main tank propellant is used first, the drop tanks (if any)

*The material discussed in this section was provided by W.A. Fey.

are jettisoned, and then the cargo bay tank propellant is also burned by the main engines. Finally, the OMS propellant is used. This procedure differs from that employed when the cargo bay tanks are fueled on the pad in that the main engines use the cargo bay propellant rather than the OMS engines. This is advantageous because the amount of available propellant is generally larger, and a higher thrust level is desirable to prevent the burning time from becoming excessive. The procedure also takes advantage of the higher specific impulse available with the main engines. Unless restart capability is provided for the main engines, the propellant in the main tanks and cargo bay tanks must be used sequentially with no engine shutdown.

D.3.3 ΔV Capability

A summary of the Orbiter ΔV available after refueling in low earth orbit, 100 nmi (185 km), 28.4° is given in Table D-3. Values are given for rescue payloads of 0 and 10 klb (0 and 4.5 t). The former represents the system maximum capability and is not meant to suggest that a rescue payload would not be carried.

Values are also given with and without a refueled cargo bay tank. With no rescue payload, the tank is assumed to fill the entire cargo bay. With a 10 klb (4.5 t) payload, the tank is shortened by 20 ft (6 m). Thus with Configuration D which only has a 20 ft (6 m) long cargo bay, no cargo bay tank can be carried for the 10 klb (4.5 t) case.

An additional calculation was made for Configuration A with two external drop tanks and zero payload. These tanks were identically sized with the cargo bay tank and appear to offer some performance benefit.

The results in Table D-3 have been plotted in Figure D-4. Corresponding results for the parallel-burn Space Shuttle are given in Figure J-8. Included in the figure are dashed lines representing the nominal ΔV requirements for one-way and round-trip lunar missions from low earth orbit. Also

included is a line representing the nominal ΔV requirement for the one-way trip plus transearth injection. This latter requirement is of interest to a multiple-pass grazing earth reentry.

The data have been plotted as a function of rescue payload weight. The 70 klb (31.8 t) point for Configurations A and B represents a fully fueled Tug plus a rescue module.

The drop-tank Orbiters are all superior to the integral tank design. The configuration with the largest drop-tank provides the greatest refueled capability. However, even the smallest drop-tank configuration (D) can deliver a 10 klb (4.5 t) rescue payload to lunar orbit and return to earth via multiple-pass grazing reentry.

D.4 RENDEZVOUS REQUIREMENTS

When using orbital refueling on a rescue mission, the Orbiter must rendezvous with both the propellant donor(s) as well as the distressed vehicle. For low earth orbit rescue, orbital refueling offers no advantage because of the time delays and the ΔVs associated with rendezvous. However, this mode of Shuttle performance augmentation is of interest on lunar and geosynchronous orbit rescue missions. With ETR as the launch site, both of these missions originate with approximately due east launch azimuths. The rescue vehicle is similarly launched and its initial orbit inclination is between approximately 28.4 and 31.5°. A refueling rendezvous in this range of inclination imposes no significant plane change requirement between the Orbiter and a fuel donor placed in a 28.4° inclined orbit. If the fuel donor is an Orbiting Propellant Depot, a subsynchronous orbit may be selected to encourage Orbiter rendezvous without lengthy phasing maneuvers, Reference D-4. Similarly, if direct refueling by ground-launched tankers is used, then the Orbiter can be placed in such an orbit.

The phasing adjustment required after refueling for travel to the distressed vehicle in lunar or geosynchronous orbit can be made in approximately one low earth orbit period wait.

D.5. REFERENCES

D-1. S-II Stage Orbital Propellant Storage System Feasibility Study; North American Rockwell Corporation – Space Division; Report No. SD 70-554-1; 31 March 1971; NASA Contract NAS 7-200, Change Order 1980

D-2. Orbital Refueling and Checkout Study; Lockheed Missiles and Space Company; Report T 1-51-67-21; 12 February 1968; NASA Contract NAS-10-4606

D-3. Orbit-To-Orbit Shuttle (Chemical) Feasibility Study, Volume III; McDonnell Douglas Astronautics Company; September 1971; SAMSO Contract No. F04701-71-C-0173

D-4. Alternate Operational Techniques Which Increase The Useful Payload of the Earth-to-Orbit Shuttle; Stewart F. McAdoo, Jr. and Jack Funk, NASA Manned Spacecraft Center. Paper No. AAS 71-302 Presented at AAS/AIAA Astrodynamics Specialists Conference 1971

Table D-1. Donor-to-User Propellant Transfer Time
(Ref. D-1)

Vehicle	Propellant, klb		Time, hr		
	LH_2	LO_2	Propellant Transfer Cycle	Fill Operation	Total
Tug	9	51	9	8	20
Reusable Nuclear Shuttle	362	69	17	14	28

Table D-2. Estimated Propellant Transfer Total Time
(Simultaneous Propellant Transfer)

Configuration	LH_2		LO_2		Total Time hr
	klb	t	klb	t	
A	74	33.6	444	202	22
B	100	45.4	604	274	23
C	86	39.1	517	235	23
D	34	15.5	203	92.2	21
Tug Only	7.8	3.5	47	21.4	20
P/L Bay Tank Only	30.6	13.9	184	83.6	21

Table D-3. Orbiter ΔV With Refueling At 100 nmi (185 km), 28.4°

Config.	P/L Wt.		*Cargo Bay Propellant		Available ΔV in LEO							
					Main Tank		Cargo Tank		OMS		Total	
	klb	t	klb	t	kft/s	km/s	kft/s	km/s	kft/s	km/s	kft/s	km/s
A	0	0	—	—	15.4	4.7	—	—	2.2	0.7	17.6	5.4
	0	0	214	97	10.4	3.2	8.1	2.5	2.1	0.6	20.6	6.3
	10	4.5	—	—	15.1	4.6	—	—	2.1	0.6	17.2	5.2
	10	4.5	149	68	11.4	3.5	6.0	1.8	2.0	0.6	19.4	5.9
**A plus two drop tanks	0	0	642	292	15.5	4.7	8.1	2.5	2.1	0.6	25.7	7.8
B	0	0	—	—	21.6	6.6	—	—	1.5	0.5	23.1	7.1
	0	0	214	97	14.1	4.3	11.4	3.5	1.4	0.4	26.9	8.2
	10	4.5	—	—	21.1	6.4	—	—	1.4	0.4	22.5	6.9
	10	4.5	149	68	15.4	4.7	8.5	2.6	1.4	0.4	25.3	7.7
C	0	0	—	—	21.7	6.6	—	—	1.2	0.4	22.9	7.0
	0	0	97	44	16.8	5.1	8.1	2.5	1.2	0.4	26.1	8.0
	10	4.5	—	—	21.1	6.4	—	—	1.1	0.3	22.2	6.8
	10	4.5	46	21	18.5	5.6	4.0	1.2	1.1	0.3	23.6	7.2
D	0	0	—	—	20.6	6.3	—	—	1.0	0.3	21.6	6.6
	0	0	32	15	16.8	5.1	7.0	2.2	1.0	0.3	24.8	7.6
	10***	4.5	—	—	19.2	5.8	—	—	0.85	0.3	20.1	6.1

*Added main engine propellant

**Two additional cargo bay tanks carried externally; propellant used and tanks jettisoned prior to using main tank propellants

***Rescue payload fills entire cargo bay

SEQ. NO.	MAJOR MISSION EVENTS	DURATION (HR:MIN)
1	INITIATE OPD/TUG PRETRANSFER CHECKOUT	1:20
2	PERFORM HARD DOCKING OF TUG TO OPD	:30
3	EXTEND RACK & ENGAGE INDEX PROBE	:15
4	ENGAGE ELECTRICAL CONNECTORS	:15
5	EXTEND PROPELLANT & SYSTEM LINES	:15
6	TRANSFER PREPARATION & CHECKOUT	3:00
7	PROPELLANT TANK PURGE	:30
8	PROPELLANT SETTLING ROTATION	:30
	PROPELLANT TRANSFER CYCLE	10:00
9	PRESSURIZATION AND CHILLING	:30
	PROPELLANT FILL OPERATION	8:00
10	FAST FILL	3:50
11	THROTTLED FILL	4:10
12	LIQUID DRAIN: TRANSFER LINES	:30
13	DEPRESSURIZATION	1:00
14	ROTATION DECELERATION	:30
15	POST TRANSFER CHECKOUT & SECURING	2:00
16	RETRACT PROPELLANT & SYSTEM LINES	:15
17	DISENGAGE ELECTRICAL CONNECTORS	:15
18	PERFORM UNDOCKING OF TUG & OPD	:15

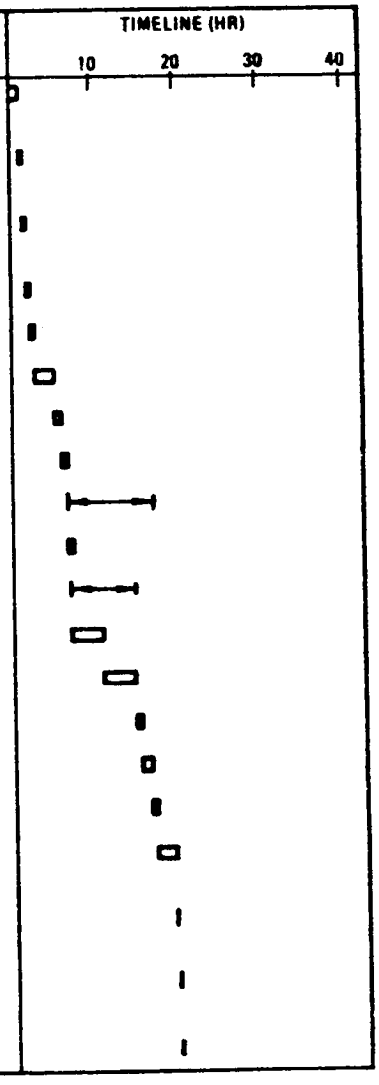

Figure D-1. Propellant Transfer Timeline From Orbiting Propellant Depot to Tug (Ref. D-1)

SEQ. NO.	MAJOR MISSION EVENTS	DURATION (HR:MIN)
1	INITIATE OPD/RNS PRETRANSFER CHECKOUT	1:20
2	PERFORM HARD DOCKING OF RNS TO OPD	:38
3	EXTEND RACK & ENGAGE INDEX PROBE	:15
4	ENGAGE ELECTRICAL CONNECTORS	:15
5	EXTEND PROPELLANT & SYSTEM LINES	:15
6	TRANSFER PREPARATION & CHECKOUT	3:00
7	PROPELLANT TANK PURGE	1:00
8	PROPELLANT SETTLING ROTATION	:30
	PROPELLANT TRANSFER CYCLE	18:30
9	PRESSURIZATION AND CHILLING	3:00
	PROPELLANT FILL OPERATION	
10	FAST FILL	11:24
11	THROTTLED FILL	2:36
12	LIQUID DRAIN: TRANSFER LINES	:30
13	DEPRESSURIZATION	1:00
14	ROTATION DECELERATION	:30
15	POST TRANSFER CHECKOUT & SECURING	2:00
16	RETRACT PROPELLANT AND SYSTEM LINES	:15
17	DISENGAGE ELECTRICAL CONNECTORS	:15
18	PERFORM UNDOCKING OF RNS & OPD	:15

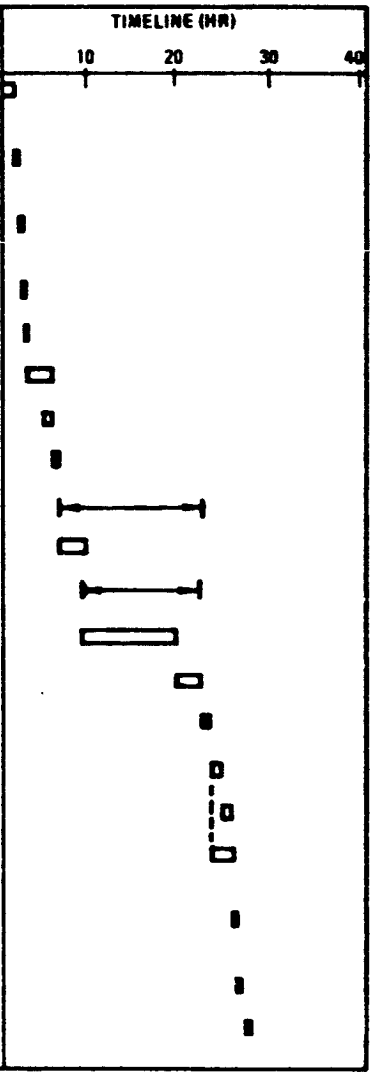

Figure D-2. Propellant Transfer Timeline From Orbiting Propellant Depot to Reusable Nuclear Shuttle (Ref. D-1)

SEQ. NO.	MAJOR MISSION EVENTS	DURATION (HR:MIN)
1	INITIATE OPD/SHUTTLE PRETRANSFER CHECKOUT	1:20
2	PERFORM HARD DOCKING OF SHUTTLE TO OPD	:30
3	EXTEND RACK & ENGAGE INDEX PROBE	:15
4	ENGAGE ELECTRICAL CONNECTORS	:15
5	EXTEND PROPELLANT & SYSTEM LINES	:15
6	TRANSFER PREPARATION & CHECKOUT	3:00
7	PROPELLANT TANK PURGE	:30
8	PROPELLANT SETTLING ROTATION	:30
	PROPELLANT TRANSFER CYCLE	17:30
9	PRESSURIZATION AND CHILLING	1:00
	PROPELLANT FILL OPERATION	15:00
10	FAST FILL	12:00
11	THROTTLED FILL	3:00
12	LIQUID DRAIN: TRANSFER LINES	:30
13	DEPRESSURIZATION	1:00
14	ROTATION DECELERATION	:30
15	POST TRANSFER CHECKOUT & SECURING	2:00
16	RETRACT PROPELLANT AND SYSTEM LINES	:15
17	DISENGAGE ELECTRICAL CONNECTOR	:15
18	PERFORM UNDOCKING OF SHUTTLE & OPD	:15

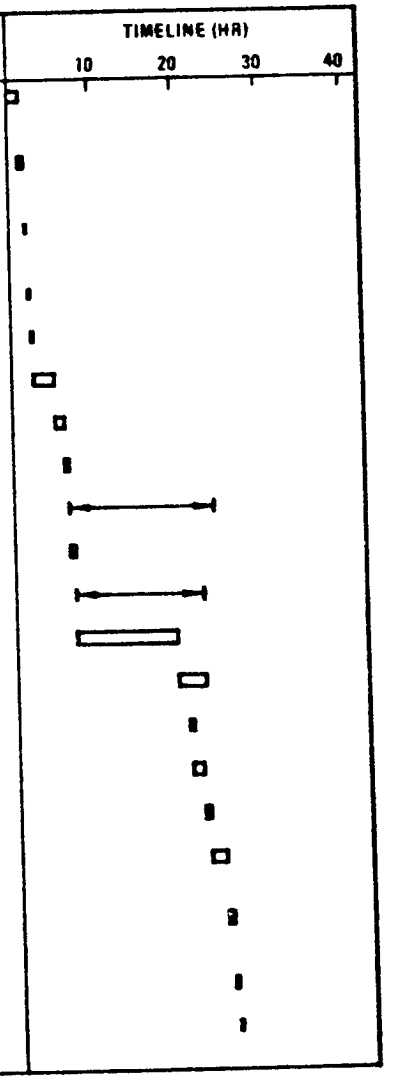

Figure D-3. Propellant Transfer Timeline From Space Shuttle Logistic Vehicle to Orbiting Propellant Depot (Ref. D-1)

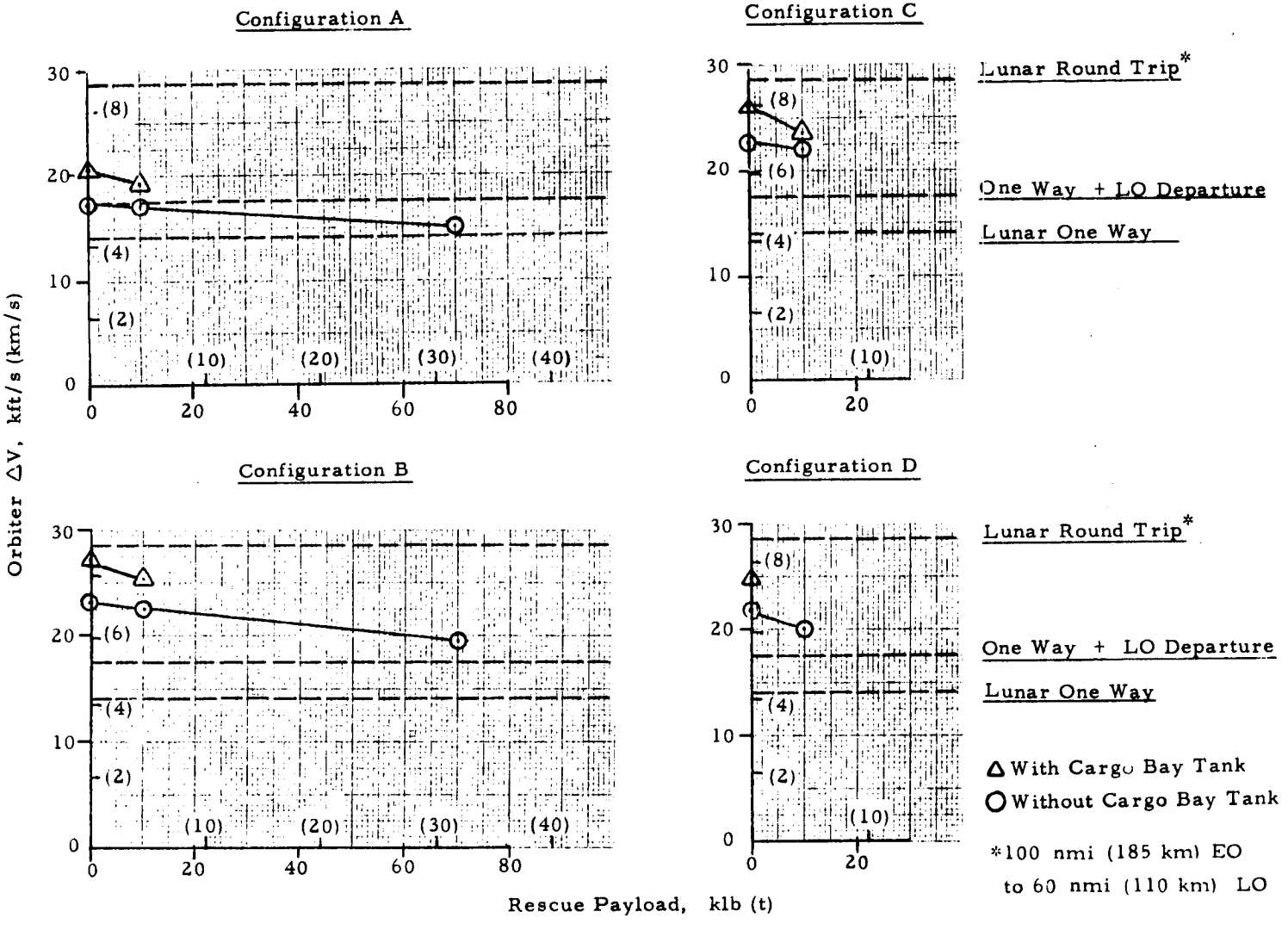

Figure D-4. On-Orbit ΔV with Orbital Refueling

APPENDIX E

PERFORMANCE OF SHUTTLE-LAUNCHED TUG SYSTEM (THREE-STAGE EOS)

APPENDIX E

CONTENTS

APPENDIX E

TABLES

FIGURES

APPENDIX E

PERFORMANCE OF SHUTTLE-LAUNCHED TUG SYSTEM (THREE-STAGE EOS)

E.1 INTRODUCTION

It is recognized that the Earth Orbit Shuttle rescue mission utility can be significantly improved by adding a third stage. Since the rescue mission payload fills only a small part of the Shuttle total weight and volume payload capacity, a third stage could be simultaneously carried into and launched from low earth orbit.

It is unlikely that a special stage would be developed for rescue mission use. Instead, a Tug developed for a broader application spectrum would also be used for the rescue application. For this reason, the performance estimates for a three-stage EOS were based on an available Tug design.

E.2 ASSUMPTIONS

Both the third stage and the emergency payload are to be carried within the cargo bay and into low earth orbit simultaneously. Neither has reentry capability and each depends on the Orbiter for return to earth. The Tug is reusable, but this feature is not a rescue mission requirement.

The rescue payload is a 10 klb (4.5 t) manned rescue module based on a design treated in Reference E-1. The module is 14 ft (4.3 m) in diameter and approximately 10 ft (3 m) long.

E.3 THIRD STAGE SELECTION

E.3.1 Existing Stages

Presently, there are available only two upper stages which may be considered candidates for the three-stage EOS. They are the Agena and the Centaur.

E.3.1.1 Ascent Agena

The Ascent Agena is a standardized upper-stage vehicle that has been flown on the Titan IIIB Booster. Its characteristics are summarized in Table E-1. Additional details may be found in Reference E-2. Payload capability is given in Figure E-1.

The one-way synchronous equatorial orbit payload (from 100 nmi (185 km), 28.5°) is approximately 2.5 klb (1.1 t). With a 10 klb (4.5 t) rescue payload, a ΔV of only 7.3 kft/s (2.2 km/s) is available.

Because of a small payload delivery capability and because vehicle diameter [5 ft (1.5 m)] is undersized for the cargo bay diameter of all Orbiter configurations under consideration (see Appendix B), the Ascent Agena was eliminated from consideration.

E.3.1.2 Centaur D1-T

The Centaur D1-T is a version of the Centaur vehicle adapted for Orbiter compatability, Reference E-3. The characteristics of this vehicle are summarized in Table E-3 and payload versus ΔV capability is given in Figure E-2.

When staged at 100 nmi (185 km), 28.5° inclination, the one-way synchronous equatorial payload is 13 klb (5.9 t). With a 10 klb (4.5 t) rescue payload, a ΔV of 15.7 kft/s (4.8 km/s) is available. It should be noted that the structure is only stressed for a 12 klb (5.4 t) payload.

At present, the Centaur is not man-rated nor man-compatible for being carried by the Orbiter. In addition, the vehicle uses cryogenic propellants and the tanks are not insulated for long coast or storage periods. However, in lieu of a Tug, which requires a new development, a modification of the Centaur appears to be the best available alternate.

E.3.2 New Stage (Tug)

Recent studies offer a range of Tug designs from which to select an appropriate third stage compatible with the rescue mission and sized for the

Orbiter cargo bay. The characteristics of typical candidates are tabulated in Table E-3. Configuration No. 5 was chosen as the third stage and the performance of the Shuttle-launched Tug system presented in Volume II, Part 1 is based on that Tug design. Not only does Configuration No. 5 have the lightest gross weight and the lightest inert weight, but the design is supported by extensive industry analysis, Reference E-8, as well.

The Tug selected is an integral stage design with a restartable single LH_2/LO_2 engine. Its orbital stay time is 14 days. An inboard profile is shown in Figure E-3, and a weight summary is given in Table E-4.

In addition to reuse and cargo bay installation requirements, this Tug design also meets manned application requirements.

E.4 PERFORMANCE*

E.4.1 General

Only Configurations A and B (and the parallel-burn Space Shuttle of Appendix J) with 15 ft (4.6 m) diameter by 60 ft (18.3 m) length cargo bay can accommodate the Tug and be flown as a three-stage system. The cargo bay of Configuration D is too short for an Agena even with a zero rescue payload. Also, the Configuration C cargo bay, which could accommodate a Centaur, is too short to simultaneously accommodate a Rescue Module. A smaller Tug than that discussed in E.3.2 could be designed for compatibility with the smaller cargo bay dimensions of Configurations C and D. However, a study ground rule was to use an available Tug design and current Tug studies were all sized for a 15 x 60 ft (4.6 x 18.3 m) cargo bay.

E.4.2 Basic Tug

The performance capability of the basic Tug is reproduced from Reference E-8 as Figure E-4. Payload versus velocity curves are shown for four missions:

a. Payload delivery in an expendable mode

b. Payload delivery in a reusable mode

*The material discussed in this section was provided by W. A. Fey.

c. Payload retrieval in a reusable mode

d. Payload delivery/retrieval mode

The ΔV plotted as the abscissa is the one-way value. However, for missions b, c, and d the Tug has sufficient propellant to return to the launch site.

E.4.3 Three-Stage System

The Tug ΔV available at staging in a 100 nmi (185 km) circular earth orbit is given in Figure E-5 as a function of orbit inclination. Figure E-5(a) represents the capability with Configuration A, and E-5(b) with Configuration B. Curves are shown for both 0 and 10 klb (0 and 4.5 t) payloads. The latter represents the weight of a Rescue Module and the zero payload case represents the maximum ΔV capability of the launched Tug. The break in each curve occurs when it becomes necessary to off-load Tug propellants to avoid exceeding the EOS payload capability.

Lunar orbit rescue capability of the basic three-stage system is shown in Figure E-6. For a Tug mission initiated from and terminated at a circular orbit altitude of 100 nmi (185 km) and an inclination of ~28.4°, Configurations A and B have identical capabilities. The Tug ΔV available at launch is plotted as a function of payload weight. Superimposed are dashed lines at the ΔVs needed for a one way and a round trip to a 60 nmi (110 km) lunar polar orbit.

The variation between the two data points has been approximated by a straight line. On this basis, the lunar round trip capability from 100 nmi (185 km) and 28.4° is in the order of a 4 klb (1.8 t) payload. The 10 klb (4.5 t) Rescue Module can be delivered to lunar orbit, but insufficient ΔV remains for the Tug to return to low earth orbit.

If, as suggested in Reference E-9, two of these Tugs in a tandem configuration are sequentially staged from LEO, the round-trip payload increases to ~10 klb (4.5 t), allowing for return of both stages to LEO (see Figure E-6).

This latter approach introduces the added complexity of a second EOS flight plus rendezvous and assembly of the two Tugs.

E.4.4 Refueled Three-Stage System

If the Orbiter stage is refueled in low earth orbit, then the altitude at which the Tug is staged and retrieved can be significantly raised. Retrieval includes returning to rendezvous with the Orbiter at the staging altitude and taking the Tug aboard the Orbiter, followed by Orbiter return to a 100 nmi (185 km) orbit and then deorbit from 100 nmi (185 km).

The total Orbiter ΔV available after refueling for ascent to the staging/retrieval altitude is a function of the Shuttle configuration and the weight of the rescue payload. Similarly, the required and available Tug ΔV for going to and returning from the moon are also dependent upon the rescue payload weight and the staging/retrieval altitude.

A summary of Orbiter ΔV available and the maximum staging/retrieval altitude that can be achieved after orbital refueling is given in Table E-5. Results are given for lunar emergency payloads of 0 and 10 klb (0 and 4.5 t). Also listed in the table are the Tug ΔVs available and required at the staging/retrieval altitude for the lunar round trip.

With orbital refueling, both Configurations A and B appear capable of delivering and recovering the Tug plus a 10 klb (4.5 t) payload from lunar orbit. Since "B" stages at the higher altitude 6500 nmi (12,000 km), the excess ΔV available in lunar orbit is also greater than for Configuration A.

The performance data in Table E-5 are plotted in Figure E-7 for ease of comparison and analysis.

E.5. REFERENCES

E-1. Technical Study For The Use Of The Saturn V, Int-21, And Other Saturn V Derivatives To Determine An Optimum Fourth Stage – Space Tug; The Boeing Company – Southeast Division; CR 103004(D5-15811); 26 February 1971 (Contract NAS8-5608).

E-2. Annex E-2, SAMSO Tug Studies, November 1971

E-3. Annex E-3, SAMSO Tug Studies; April 1972

E-4. Integrated Operations/Payloads/Fleet Analysis Final Report: Volume IV, Launch Systems; Aerospace Corporation; ATR-72(7231)-1; August 1971 (Contract No. NASW-2129).

E-5. Annex E-1, SAMSO Tug Studies; 19 January 1972

E-6. Advanced Space Programs Studies: Monthly Progress Review, Study 2.4; Aerospace Corporation; 11 November 1971.

E-7. Orbit-To-Orbit Shuttle (Chemical) Feasibility Study; North American Rockwell Corporation – Space Division; SAMSO – TR-71-238; October 1971

E-8. Orbit-To-Orbit Shuttle (Chemical) Feasibility Study; McDonnell Douglas Astronautics Company; SAMSO – TR-71-221; October 1971

E-9. Application of the Orbit-Orbit Shuttle for Space Rescue Missions; Aerospace Corporation; TOR-0059(6758-07)-7, 14 August 1970.

Table E-1. Ascent Agena Characteristics
(Ref. E-2)

Gross Weight, lb	14,700	Diameter, ft.	5.0
Propellant Weight, lb	13,500	Length, ft.	20.7
Inert Weight, lb	1,169		
Propellants	UDMH/IRFNA		
Thrust, lb	16,100		
I_{sp}, sec	291		

Table E-2. Centaur D1-T Characteristics
(Ref. E-3)

Gross Weight, lb	35,143	Diameter, ft	10
Propellant Weight, lb	29,794	Length, ft.	31.5
Inert Weight, lb	4,160		
Burnout Weight, lb	4,632		
Propellants	LO_2/LH_2		
Thrust (each of 2 engines), lb	15,000		
Specific Impulse, sec	444		

Table E-3. Candidate Tug Characteristics

Tug Design		Config. 1 (Ref. E-4)	Config. 2 (Ref. E-5)	Config. 3 (Ref. E-6)	Config. 4 (Ref. E-7)	Config. 5 (Ref. E-8)
Stage Gross Weight,	lb	63,600	67,500	62,700	64,380	61,893
Propellant Weight,	lb	56,760	61,098	56,500	56,530	54,833
Stage Burn-Out Weight,	lb	6,840	7,183	6,900	7,090	6,441
Stage Inert Weight,	lb		6,402	6,190	6,080	5,786
Length	ft	34.5	33.2	32	38.9	35.1
Diameter,	ft	15	15	15	15	15
Thrust,	klb	1 @ 23.8	1 @ 20		1 @ 20	1 @ 20
Specific Impulse,	sec	460	470	470	471	471

Table E-4. Tug Weight Summary (lb)
(Ref. E-8)

Dry Weight		5,786
Structure	2,598	
Thermal Control	480	
Avionics	879	
Propulsion	1,303	
Contingencies (~10%)	526	
Residuals		655
Burnout Weight		6,441
Usable Main Propellants		54,833
Other Propellants and Losses		619
Stage Gross Weight		61,893
Stage Mass Fraction		0.886
EOS Interface Kits		2,000
Deployment/Retrieval Mechanism	500	
Structural Support Cradle	1,250	
Fluid/Electrical Interface Kit	250	

Table E-5. Lunar Mission Rescue Capability of Three-Stage EOS Refueled in Low Earth Orbit

Config.	Rescue P/L		Available Orbiter ΔV						*Max. Altitude Staging/Rendez.		Round Trip ΔV Max. Altitude to LO		Tug ΔV		Tug Excess ΔV	
			Main Tank		OMS		Total									
	klb	t	kft/s	km/s	kft/s	km/s	kft/s	km/s	nmi	km	kft/s	km/s	kft/s	km/s	kft/s	km/s
A	0	0	13.6	4.2	1.8	0.5	15.4	4.7	3900	7200	21.3	6.5	34.3	10.5	13.0	4.0
	10	4.5	13.3	4.1	1.7	0.5	15.0	4.6	3800	7000	21.5	6.5	22.4	6.8	0.9	0.3
B	0	0	18.7	5.7	1.1	0.3	19.8	6.0	6900	12,800	18.8	5.7	34.3	10.4	15.5	4.7
	10	4.5	18.3	5.6	1.0	0.3	19.3	5.9	6500	12,000	19.3	5.9	22.4	6.8	3.1	0.9

*Based on Orbiter initial and final altitude of 100 nmi (185 km); includes final deorbit capability from 100 nmi (185 km).

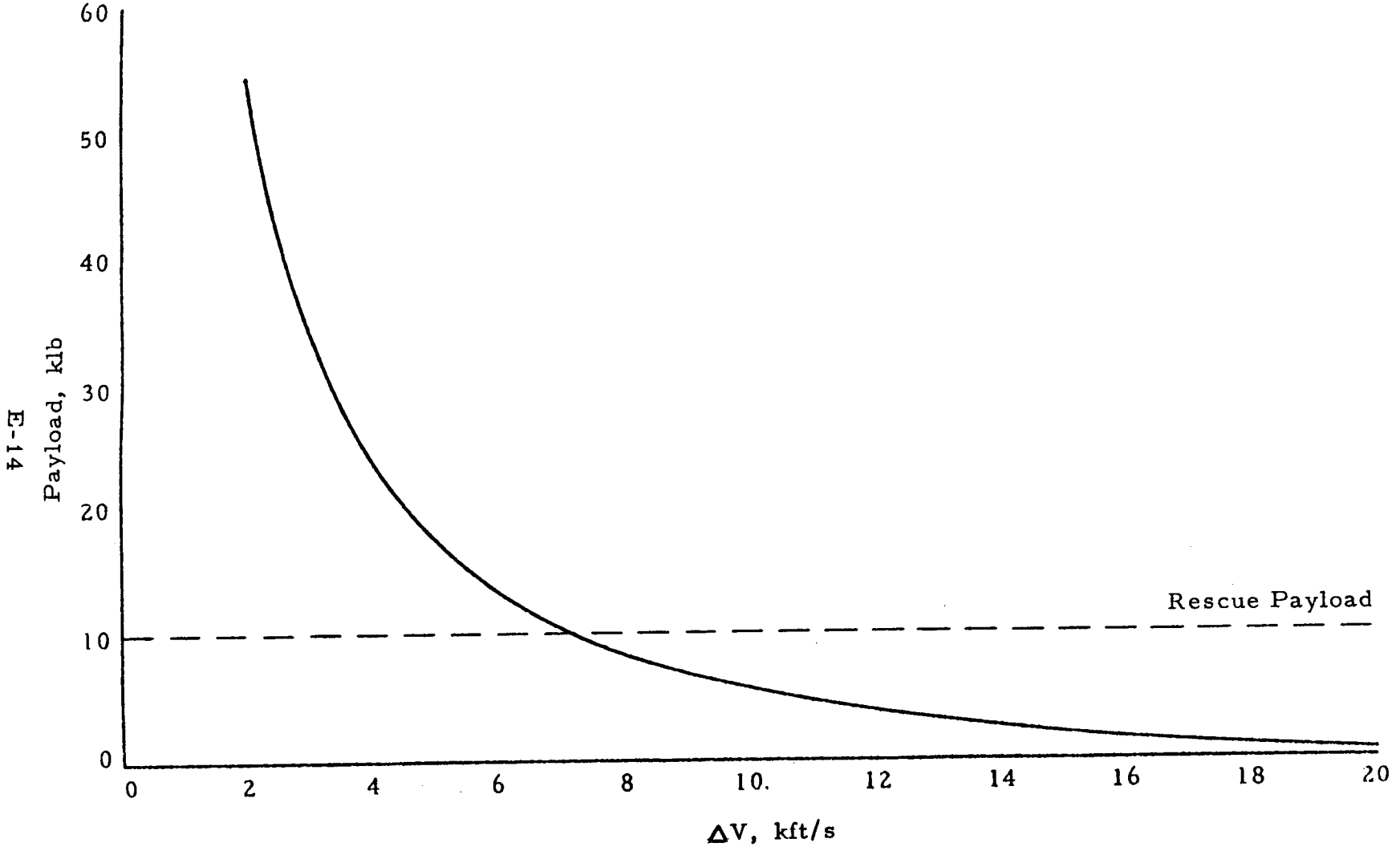

Figure E-1. Ascent Agena Performance Capability (Ref. E-2)

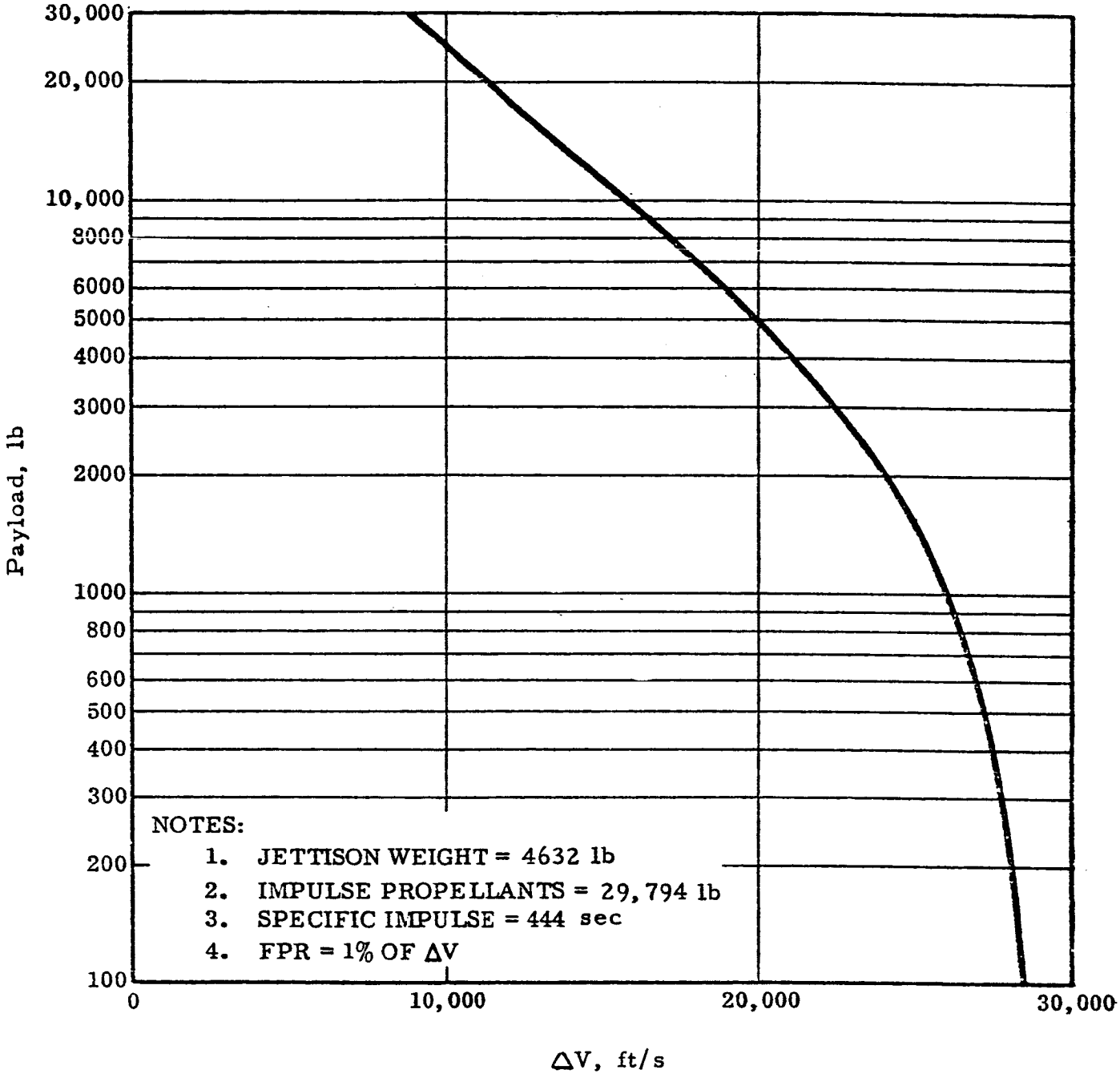

Figure E-2. Centaur D1-T Performance Capability (Ref. E-3)

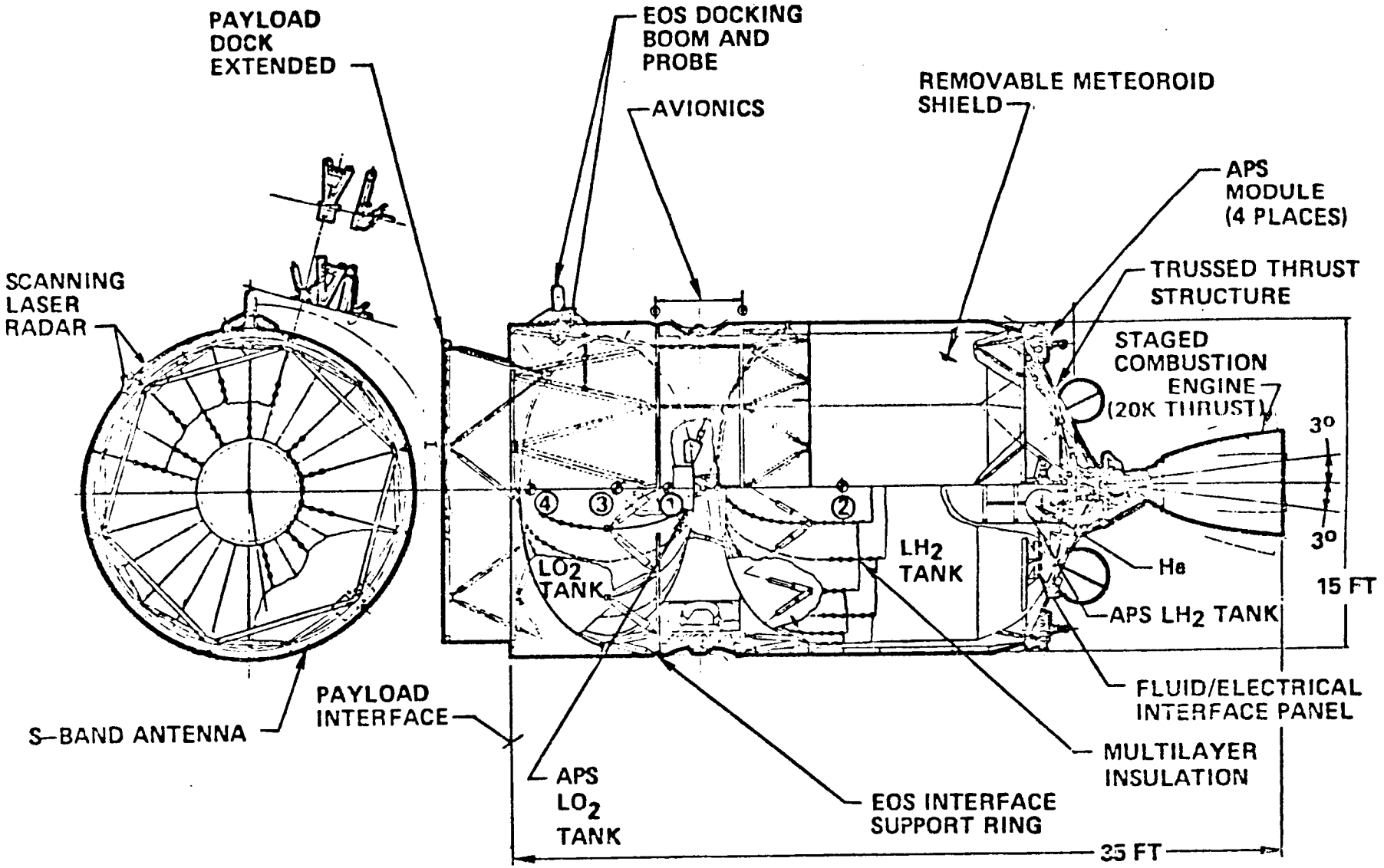

Figure E-3. Integral Stage Tug Inboard Profile (Ref. E-8)

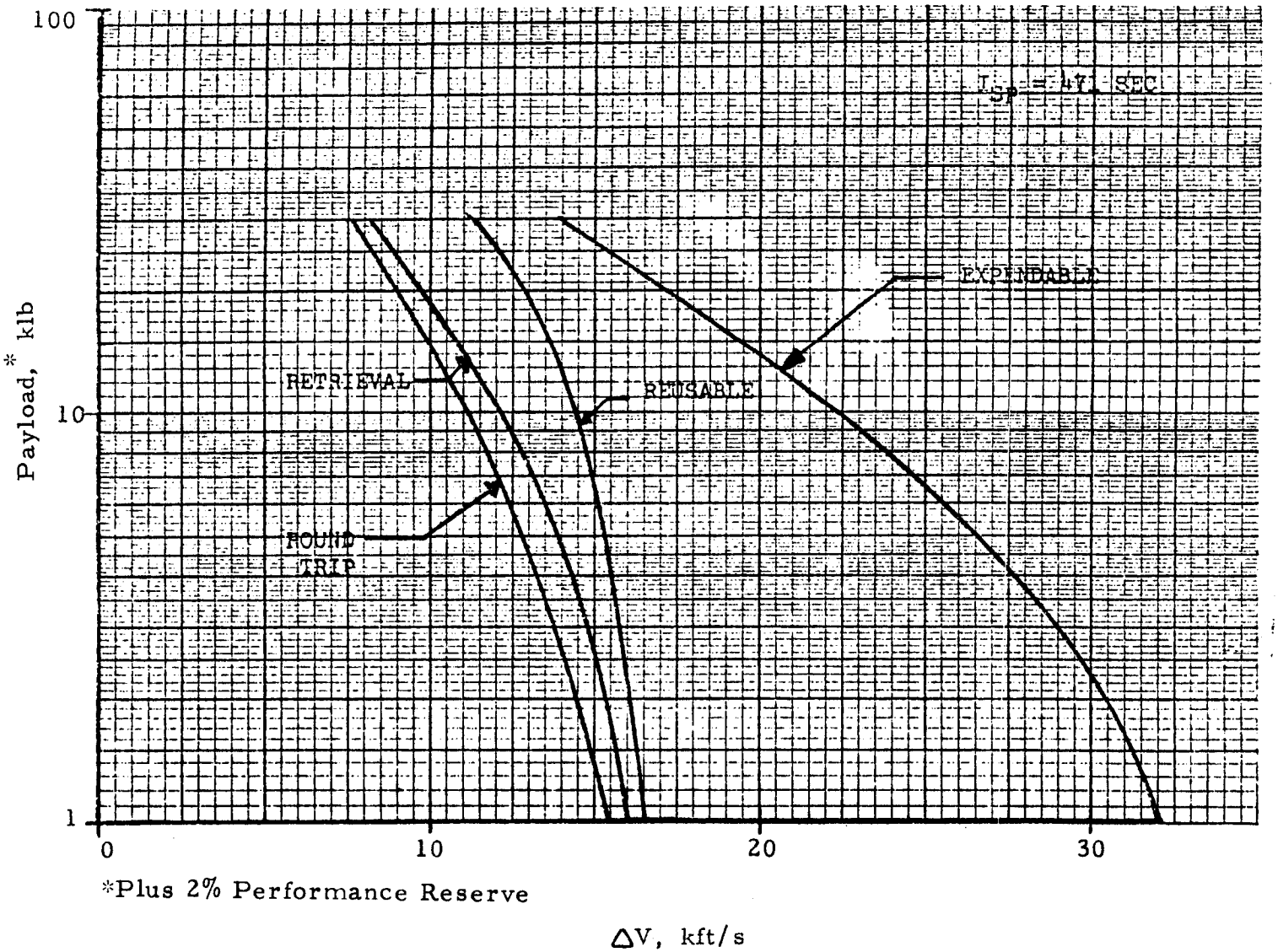

Figure E-4. Tug Performance Capability (Ref. E-8)

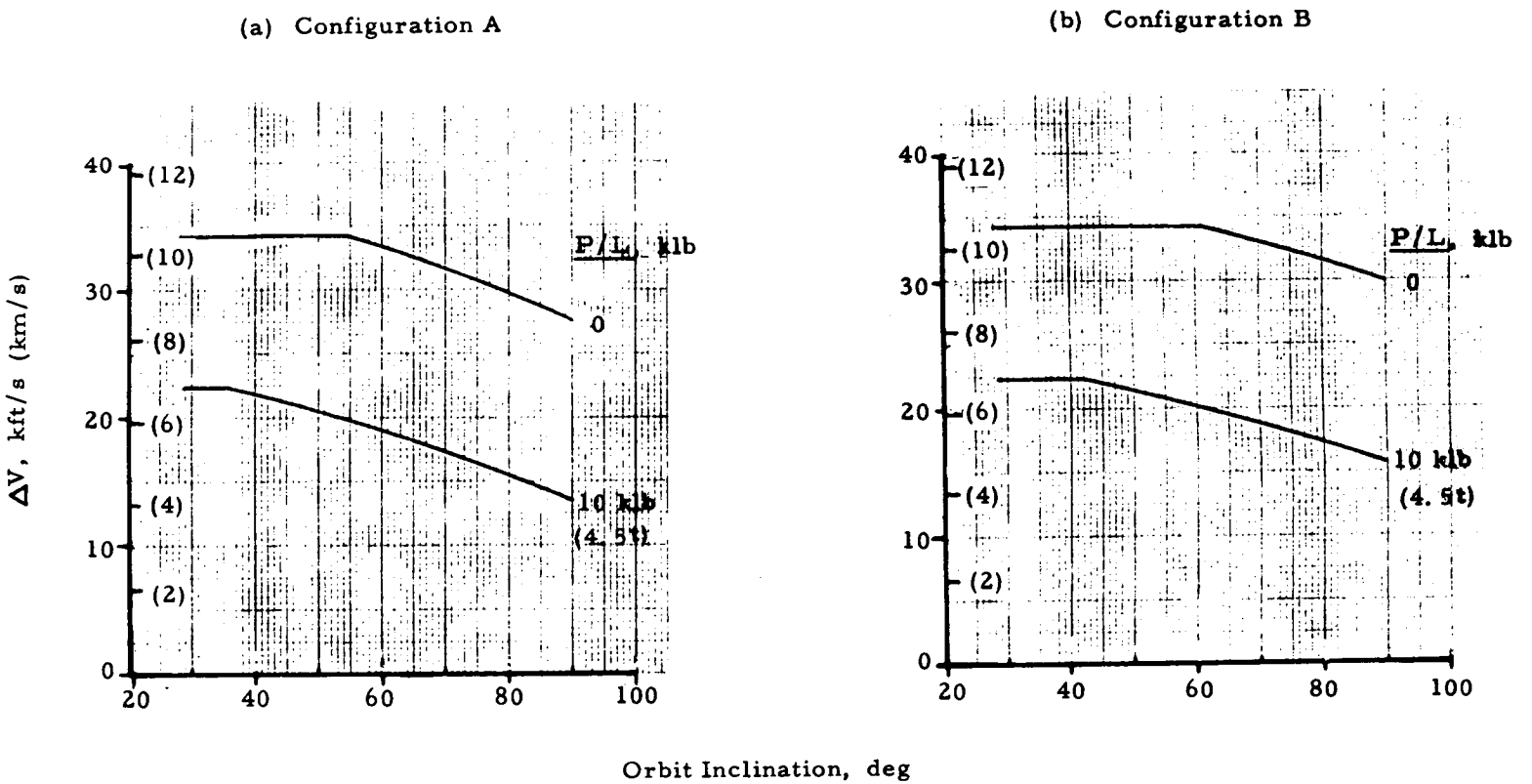

Figure E-5. Tug ΔV at Staging in 100 nmi (185 km) Circular Orbit

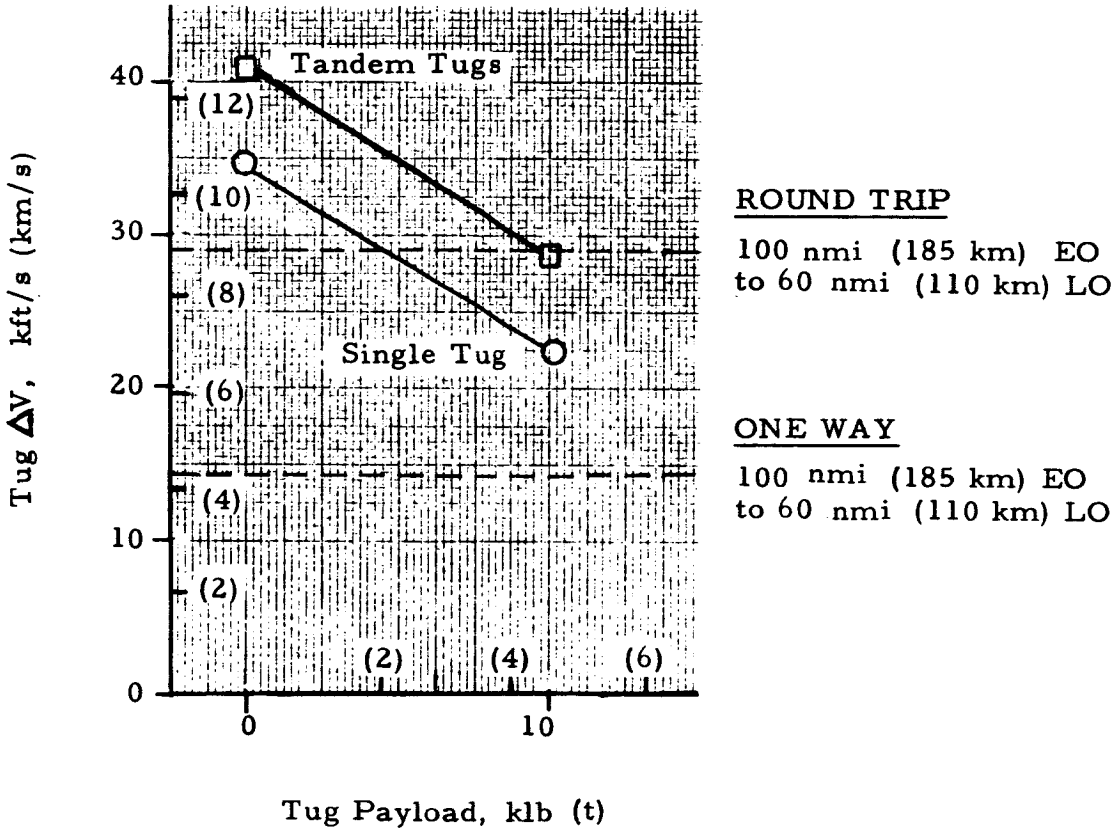

Figure E-6. Lunar Rescue Mission Capability of Shuttle-Launched Tug (Tug Launched/Retrieved at 100 nmi (185 km), 28.4°)

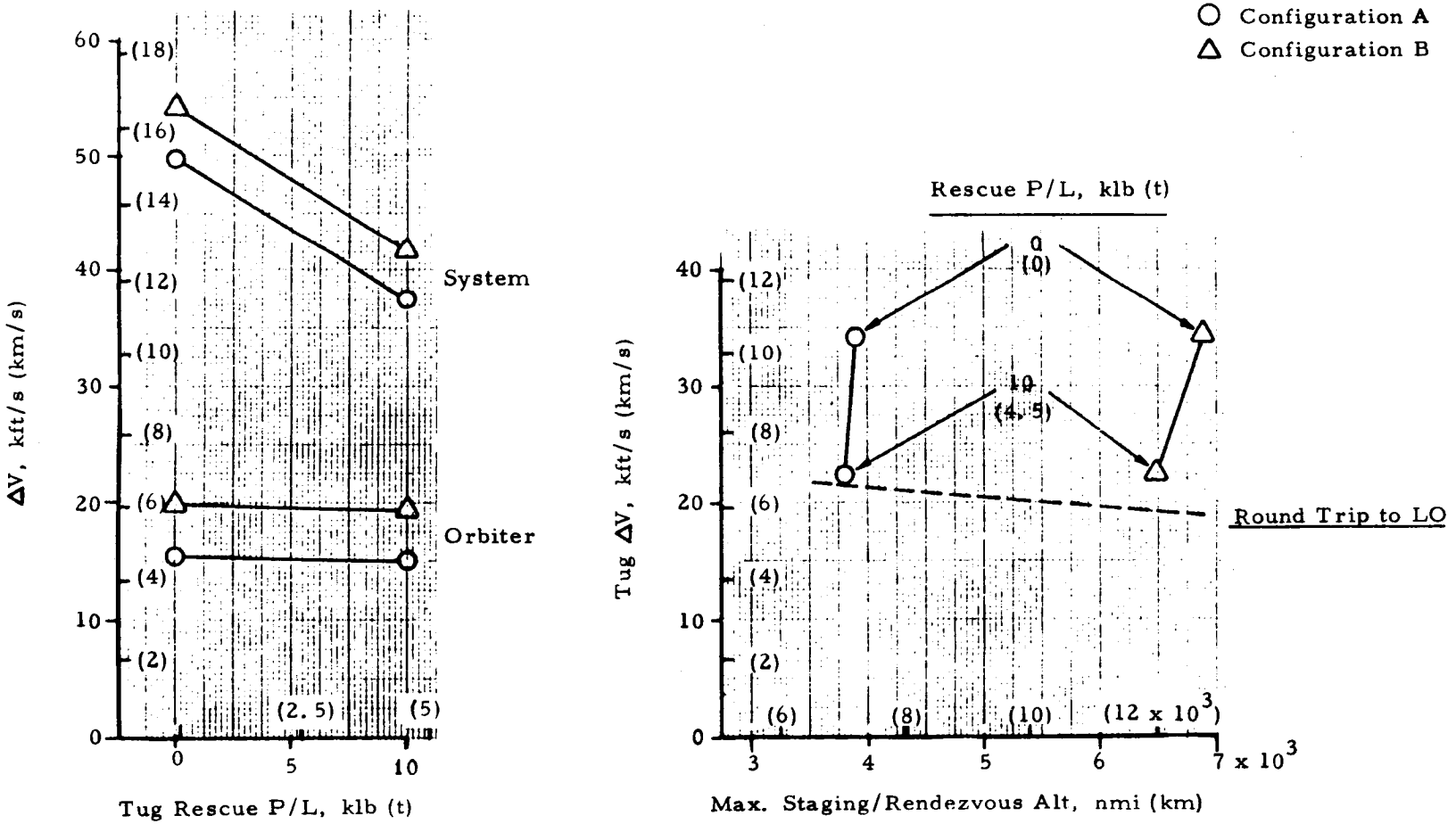

Figure E-7. Lunar Rescue Mission Capability of Refueled Shuttle-Launched Tug (Orbiter Refueled in LEO)

APPENDIX F

ORBITER REENTRY FROM ALTITUDES >100 NMI(185 KM)

APPENDIX F

CONTENTS

FIGURES

APPENDIX F*

ORBITER REENTRY FROM ALTITUDES > 100 NMI (185 KM)

F.1 INTRODUCTION

The "standard" Orbiter reentry is made from an altitude of 100 nmi (185 km) and a Thermal Protection System (TPS) to allow a crossrange of 1100 nmi (2040 km) is provided. Reentry from altitudes greater than 100 nmi (185 km) is accomplished by first transferring to a 100 nmi (185 km) orbit and then reentering from this lower altitude.

The maximum altitude from which the Orbiter can return utilizing a "standard" reentry depends on the ΔV available for transfer from the higher altitude to 100 nmi (185 km). For this same ΔV expenditure, reentry from an even greater altitude is possible if, instead of stopping at a parking altitude, direct reentry is undertaken. However, the TPS is not presently "designed" for this latter situation and the crossrange capability suffers.

An analysis of the maximum lower surface temperature generated during direct reentry from orbits > 100 nmi (185 km) for the limiting case of zero crossrange was reported in Reference F-1. Some of the results from that study are summarized in this Appendix.

F.2 ASSUMPTIONS

The analysis was made with an Orbiter having characteristics described in Reference F-2. The reentry platform area loading, W/S, was 48.3 lb/ft^2 (236 kg/m^2). Vehicle lift and drag characteristics are given in Figure F-1 as a function of angle of attack. The effects of viscous interaction were not considered.

---

*The material treated in this Appendix was originally presented in Ref. F-1.

The maximum allowable lower surface TPS temperature was held to 2200°F (~1480°K) at a point on the centerline at least 10 ft (3 m) downstream of the vehicle nose.

The lower surface TPS panel equilibrium temperature for direct reentry from altitudes > 100 nmi (185 km) was computed with a technique using the Eckert reference enthalpy method for both laminar and turbulent boundary layer heating. (Reference F-3 indicates that the Eckert reference enthalpy method of determining turbulent boundary layer heating is conservative.) Turbulent flow onset was assumed to occur at a Reynolds number of 10^6 with fully developed turbulent flow at 2×10^6.

Constraints imposed on the reentry trajectory were a maximum normal load factor of 2.5 Gs and a maximum skipout altitude of 400,000 ft (120 km).

F.3 ANALYSIS RESULTS

F.3.1 Reentry Altitude

As the altitude from which direct reentry is initiated is increased, an initial period of inverted flight or an initial period of inverted flight plus a steeper reentry angle are required to avoid skipout. The variation with altitude of the reentry angle and the period of inverted flight is given in Figure F-2.

Up to about 225 nmi (416 km), direct reentry can be accomplished without inverted flight or a reentry angle steeper than -1.0°. Between 225 and 355 nmi (416 and 656 km), an initial inverted flight period is required. Above 355 nmi (656 km), both an initial inverted flight period and an increase in the steepness of the reentry angle are required.

F.3.2 TPS Surface Temperature

The variation with initial orbital altitude of the peak lower surface TPS temperature during direct reentry is given in Figure F-3. Altitudes to 700 nmi (1300 km) were evaluated, and the peak temperature remained below 2200°F (~1480°K) over the entire range. By extrapolating the curve, it

appears that the temperature limit would be encountered at reentry from altitudes > ~750 nmi (~1390 km).

The time-temperature histories for several reentry trajectories are given in Figure F-4.

F.3.3 Deorbit ΔV

The total deorbit/reentry ΔV required for the single retrothrust burn direct reentry is shown in Figure F-5 as a function of orbital altitude. For comparison, the ΔV requirement for a "standard" reentry via a 100 nmi (185 km) parking orbit is also included.

The direct reentry mode requires only about 48% of the "standard" reentry ΔV. Thus, a larger on-orbit maneuvering margin becomes available and the rescue mission utility of the Orbiter is improved.

F.4 REFERENCES

F-1. Earth To Orbit Shuttle High Orbital Altitude Capability; Aerospace Corporation; TOR-0059(6759-02)-3; 31 July 1970.

F-2. STS Study Final Report: Volume III – Vehicle Operations and Performance; North American – Space Division; SAMSO TR 69-362. [Confidential]

F-3. A Comparison of Four Simple Calculation Methods for the Compressible Turbulent Boundary Layer on a Flat Plate; Aerospace Corporation; TOR-0066(5758-02)-3; 16 March 1970.

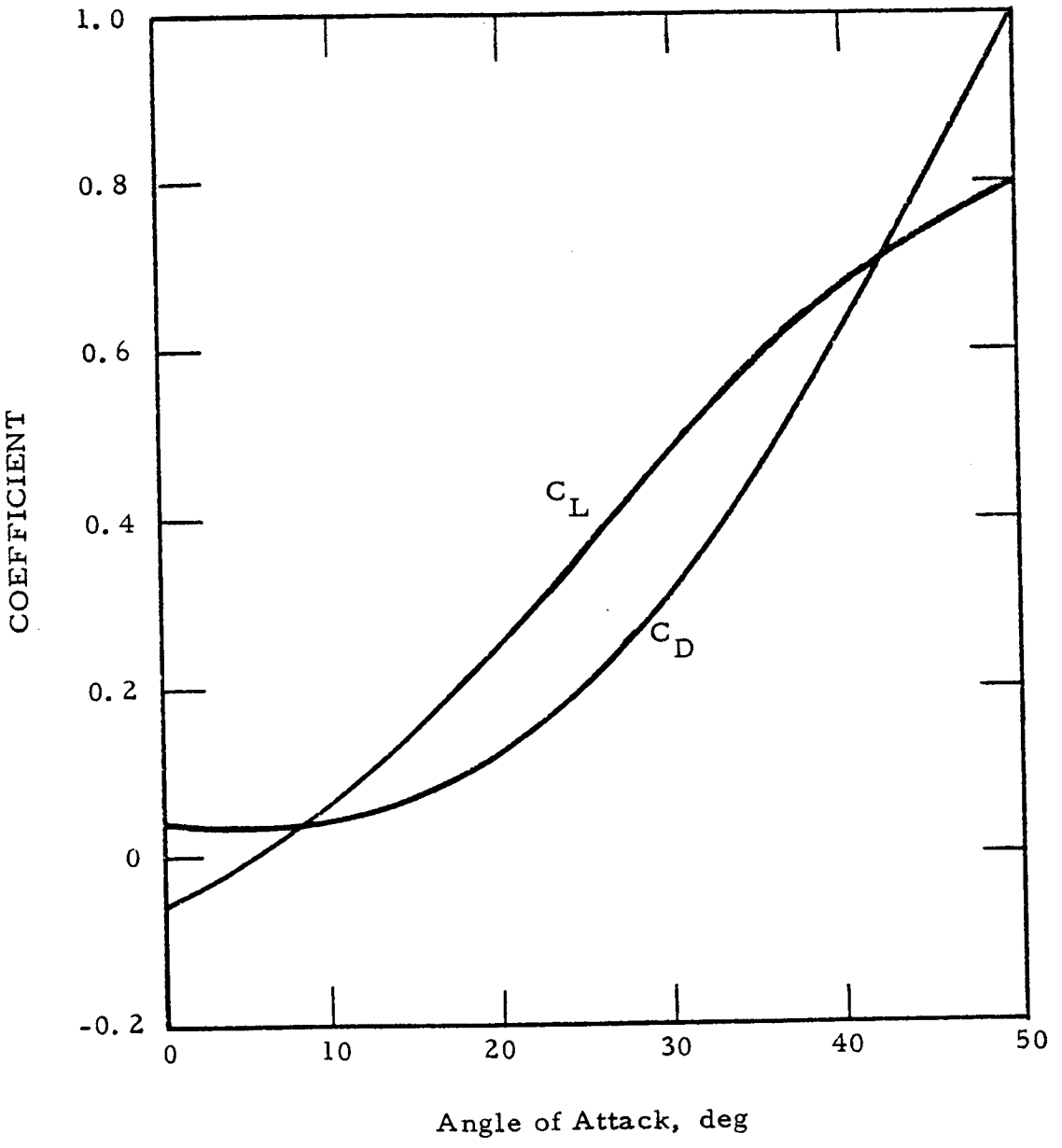

Figure F-1. Orbiter Lift and Drag Coefficient Variation with Angle of Attack (Ref. F-1)

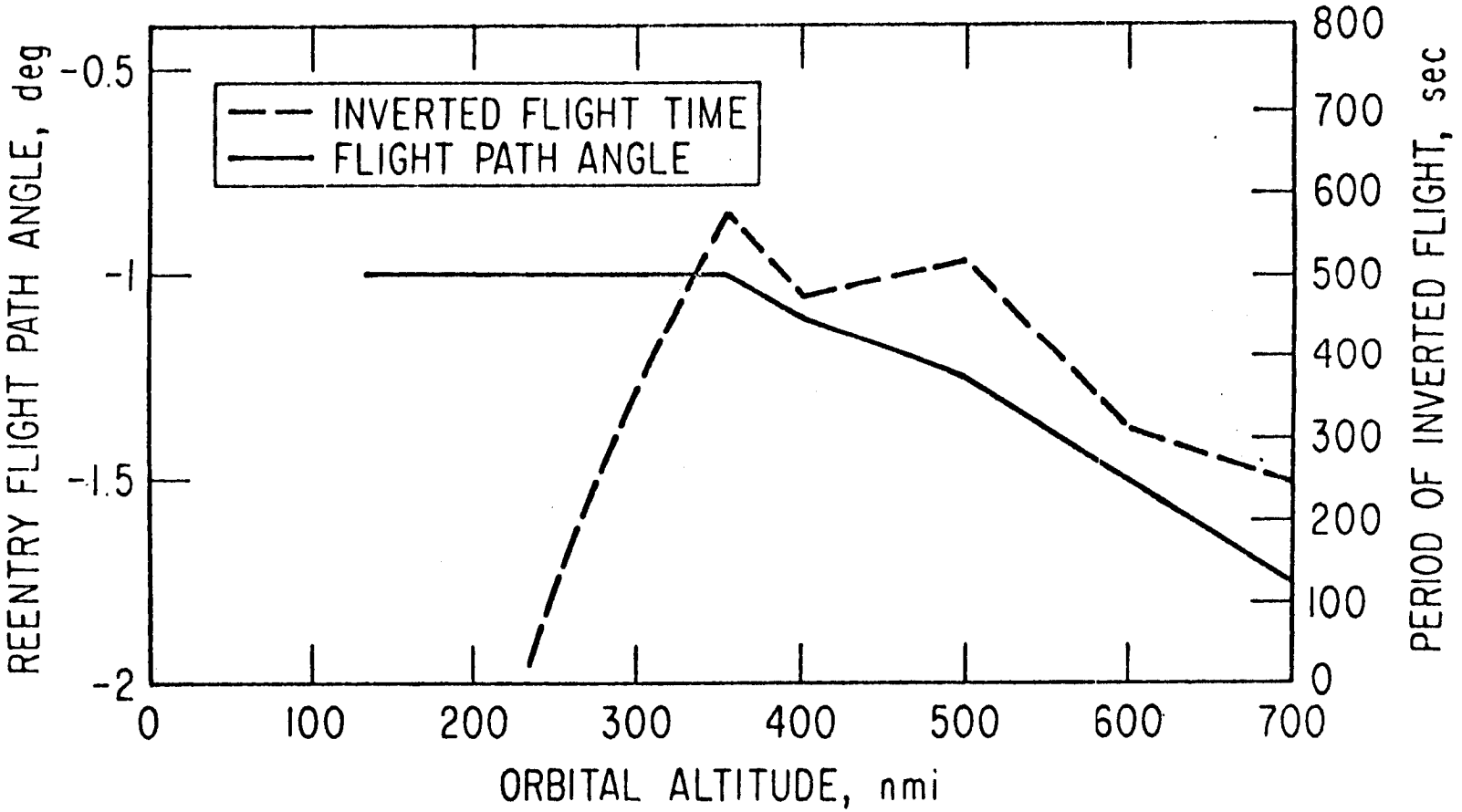

Figure F-2. Inverted Flight Time and Reentry Angle versus Oribtal Altitude for Direct Reentry with Zero Crossrange (Ref. F-1)

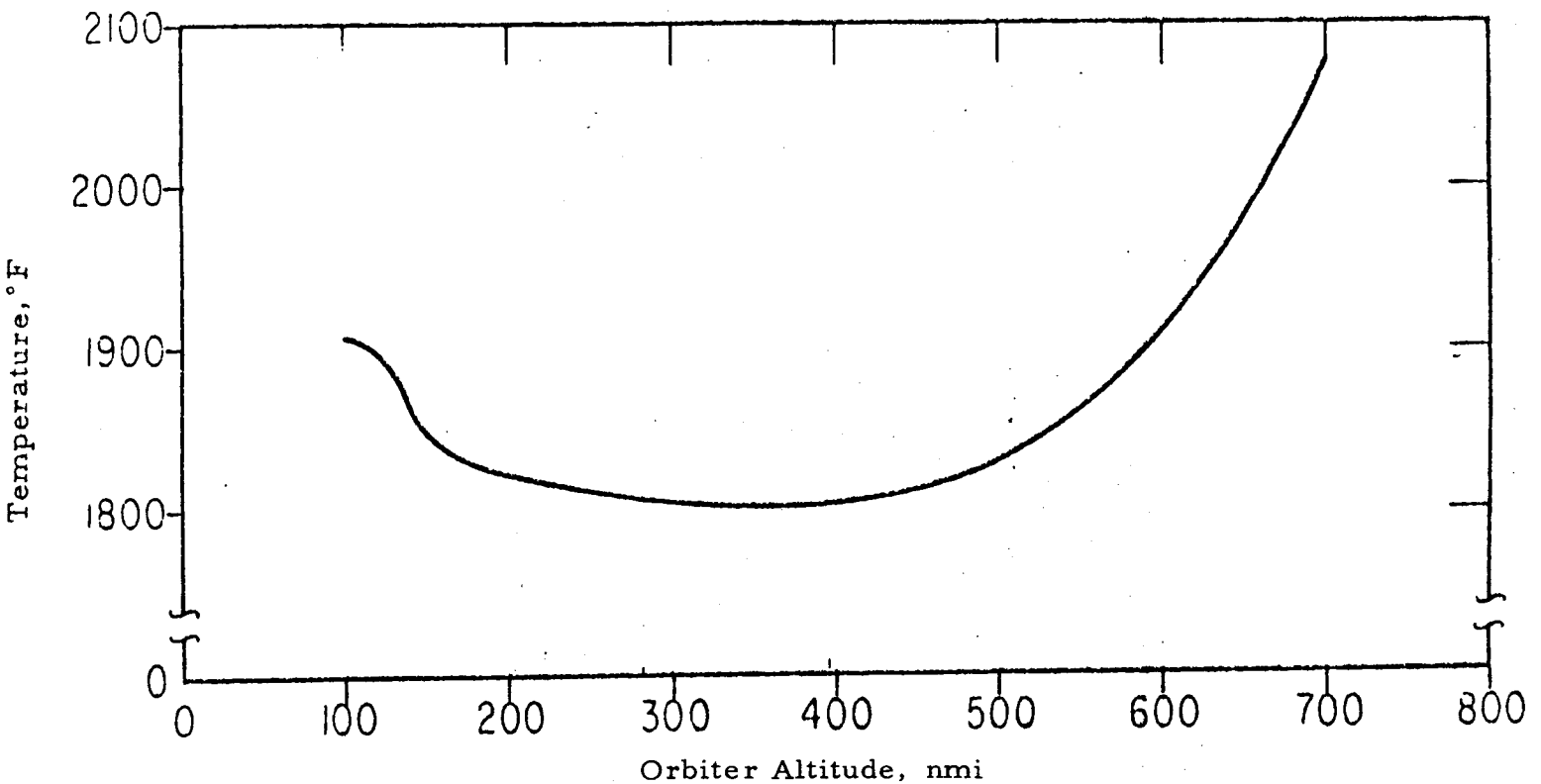

Figure F-3. Orbiter Lower Surface Peak Temperature for Direct Reentry with Zero Crossrange (Ref. F-1)

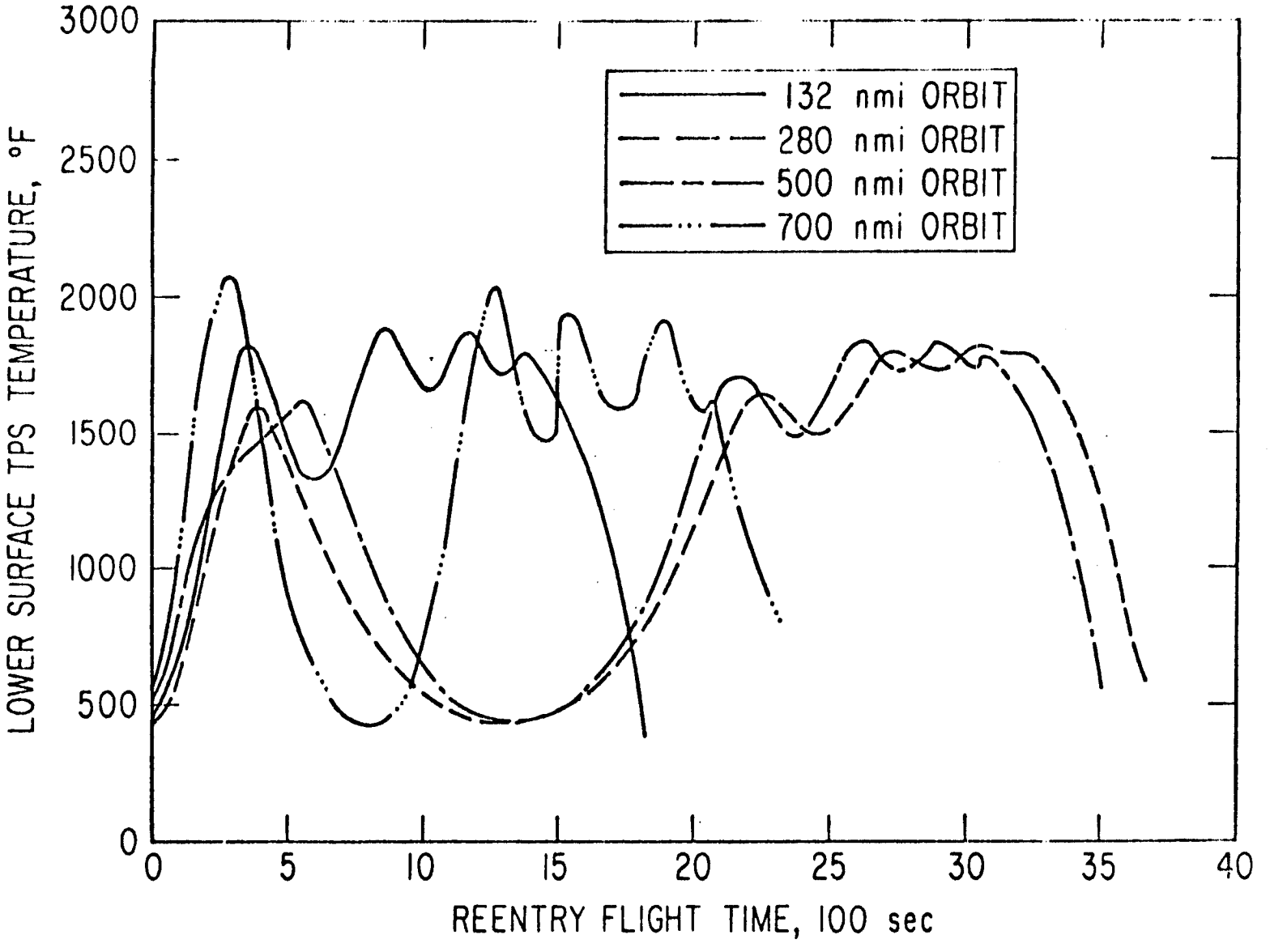

Figure F-4. Lower Surface Temperature – Time Histories for Direct Reentry with Zero Crossrange (Ref. F-1)

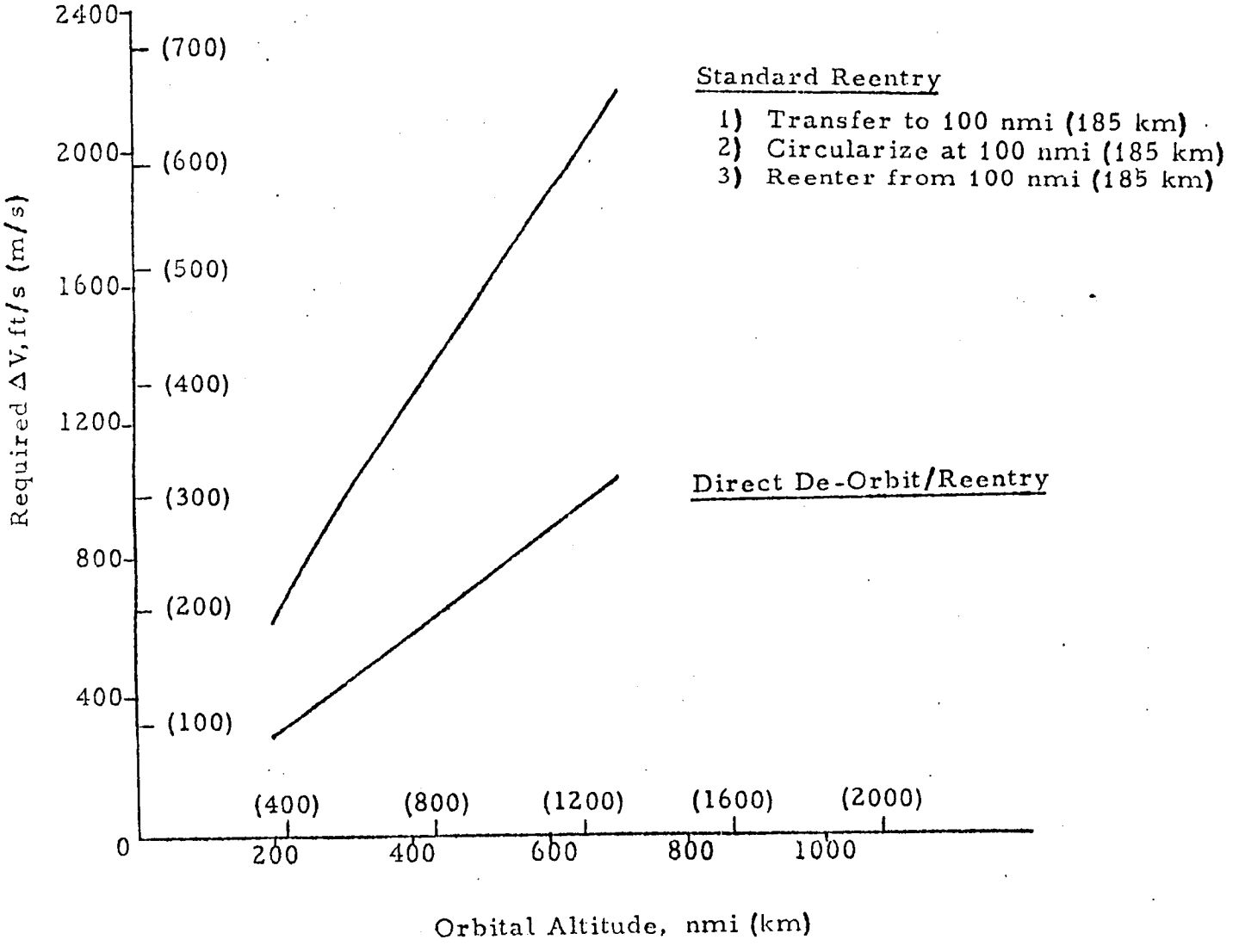

Figure F-5. Orbiter Reentry ΔV Requirement (Ref. F-1)

APPENDIX G

MULTIPLE-PASS GRAZING REENTRY FROM LUNAR ORBIT

APPENDIX G

CONTENTS

APPENDIX G

TABLES

FIGURES

FIGURES (CONTINUED)

APPENDIX G

MULTIPLE GRAZING REENTRY FROM LUNAR ORBIT*

G.1 ORBITAL MECHANICS**

G.1.1 Introduction

The flight mechanics aspects of multiple-pass grazing renetry for return from lunar orbit are described in the following paragraphs. This reentry mode utilizes successive passes into earth atmosphere to dissipate the high energy levels of the orbit. The aerodynamic deceleration which occurs at each perigee pass gradually reduces the entry velocity to the point where a reentry can be accomplished without exceeding the TPS capability of the vehicle.

G.1.2 Method of Calculation

Calculation of the grazing pass orbits was made as follows. First, a typical patched conic solution for the initial transearth trajectory was selected. The injection velocity was 3300 ft/s (1 km/s) and the transit time was 60.2 hours to perigee. The perigee altitude was selected to assure a vehicle lower surface centerline maximum temperature of 2200°F (~1480°K), based on perigee velocity. The patched conic transearth trajectory was projected to the point of entry into the significant atmosphere, assumed to be 100 nmi (185 km) above the surface of the earth. The deceleration due to the atmospheric density was integrated for that portion of the orbit where the altitude was less than 100 nmi (185 km). At the atmospheric exit point a two-body orbit projection was made to determine the next apogee and period, which are

*The lunar case was selected for analysis because velocity on the initial perigee pass is ~2500 ft/s (760 m/s) greater than the value for geosynchronous orbit return and therefore presents the more severe situation.

**The results reported in this section are based on the work of K. N. Easley.

reduced from the previous due to the energy dissipation of the atmospheric drag. A small velocity change was made at apogee to adjust the perigee altitude so that 2200°F (~1480°K) is reached, but not exceeded, on the following perigee. The orbit was projected to the atmospheric entry point where the integration of the drag effects was started. This process of calculating the orbit was repeated until the vehicle was captured; i.e., the orbit decayed to an impact trajectory.

The atmospheric portion of the computation was made using the following vehicle data.

$$L/D = 0.797$$

$$W/C_L S = 41.3 \text{ lb/ft}^2 \ (1980 \text{ N/m}^2)$$

$$\alpha = 50 \text{ degrees}$$

$$\beta = 90 \text{ degrees}$$

The angle of attack (α) is for maximum lift which, more importantly, provides maximum drag. A bank angle (β) of 90° was used to eliminate the necessity of compensating for positive or negative lift when computing the perigee altitude to meet the 2200°F (~1480°K) temperature. The small change in inclination can be assumed to be removed by banking in both directions. The use of 90° bank angle for planning also allows the flexibility of using the bank angle for control of the maximum temperature exposure.

G.1.3 Performance Results

G.1.3.1 Maximum Lower Surface Temperature

The discussion in G.1.2 refers to the nominal 2200°F (~1480°K) temperature case. The sensitivity of the lower surface maximum temperature to the perigee altitude was determined by slightly perturbing the altitude which gives 2200°F (~1480°K). This sensitivity is shown in Figure G-1. The variation in return time (total time to capture) as a function of maximum temperature was also computed and is presented in Figure G-2.

At a fixed maximum temperature, the perigee altitude decreases slightly with each pass. For the 2200°F (~1480°K) case, the perigee altitude varies between 46.6 and 42.2 nmi (86 and 78 km). On any given pass, a change in the targeted perigee altitude of about 1 nmi (1.85 km) results in a corresponding change of ~100°F (~56°K) in temperature. Even such a small temperature reduction translates into a large return time increase and is to be avoided.

G.1.3.2 Assisted Grazing Reentry

The return time data of Figure G-2 were computed with complete reliance upon the atmosphere for energy dissipation. Application of a retro ΔV at the first perigee pass can significantly reduce the return times, assuming ΔV capability is available. Figure G-3 illustrates the time savings as a function of ΔV for maximum allowable temperatures of 2200°F (~1480°K) and 1940°F (1333°K). Also shown are the return times for pure grazing (no ΔV) reentries. Note that no time savings is realized until a certain ΔV is used. This result is due to the assumption that the ΔV is applied at the first perigee. The first perigee cannot be within the atmosphere or the aft end of the vehicle would be subjected to heating in excess of its TPS capability since the attitude is dictated by the retro orientation. Therefore, a minimum retro ΔV which is equal to the deceleration due to drag on a first perigee pass in the atmosphere is required before any time savings result.

G.1.3.3 Reentry Phase

For the purpose of computing the return time data it was not considered necessary to include any detail on the final reentry to touchdown. Instead, a typical time of 0.5 hr was included to cover this phase. However, in order to assess the TPS requirements a typical final reentry was included. The particular trajectory was designed to provide 1100 nmi (2040 km) cross-range with short downrange on a reentry from 100 nmi (185 km). Figures G-4 and G-5 provide a trajectory profile and temperature history data. Use of this trajectory is consistent with an operating procedure of: (1) decay until a low earth orbit is achieved; (2) use ΔV to raise perigee to 100 nmi (185 km);

(3) loiter until a landing opportunity arises; and (4) deorbit and reentry similar to that from a normal LEO. The worst total heat input condition would be for zero loiter time.

G.1.3.4 Perigee Adjustment

As mentioned previously, small amounts of ΔV are applied at each apogee to adjust perigee to maintain the temperature at 2200°F (~1480°K) (or whatever limit is chosen). A tabulation of the ΔV used at each apogee to maintain 2200°F (~1480°K) is given in Table G-1. For the purpose of counting orbits, the second apogee is that which occurs following the first perigee pass. Also tabulated in Table G-1 are the perigee and apogee altitudes and period of the orbit for each apogee after the first grazing pass.

G.2 THERMAL PROTECTION*

G.2.1 Introduction

As discussed in Appendix F, the characteristics of the Orbiter thermal protection system (TPS) are established by low earth orbit reentry requirement. Because of the TPS inadequacy for direct lunar return and the inability of the Orbiter to return to low earth orbit with the ΔV available, multiple grazing earth reentry from lunar orbit is suggested. The orbital mechanics of a multiple grazing reentry maneuver is treated in G.1. The adequacy of the TPS for a "standard" Orbiter during such a maneuver is treated in this section.

G.2.2 TPS Characteristics

A Mark II type of Orbiter was considered (see Configuration B in Appendix B). Using material properties and design concepts from a recent Shuttle study (Reference G-1), wall thicknesses were established and temperature history along the centerline of the bottom surface was computed.

*The results herein are based on work by Y.S. Hong and J. Vasiliu.

Thermal properties of the primary TPS material, identified as REI, are plotted in Figure G-6. Behind the REI is an RTV bond and then the aluminum backface. The thickness and thermal characteristics of each material are given in Table G-2. This combination of materials and thicknesses meet the following criteria:

a. Normal low earth orbit reentry trajectory
b. Prereentry TPS surface temperature - 100°F (310°K)
c. Aluminum backface maximum temperature - 300°F (420°K)
d. Maximum surface temperature - 2200°F (1480°K)

G.2.3 REI Thickness Determination

The thickness of the Reusable External Insulation, as given in Table G-2, is based on a normal reentry analysis from low earth orbit. A lower surface maximum temperature profile for a normal reentry as represented by Figure G-5 was assumed. Also assumed was an initial surface temperature at 400,000 ft (120 km) altitude of 100°F (310°K). The aluminum backface temperature history for a range of REI thicknesses was then determined. Due to the large variation in REI thermal conductivity with pressure, appropriate adjustments were made to account for local pressure variation with time.

Table G-2. Thermal Protection System Design Properties (Ref. G-1)

Material	Thickness, in.	Thickness, mm	Density, lb/ft^3	Specific Heat, Btu/lb-°F	Thermal Conductivity, Btu/ft-hr-°F
REI	2.53	64.3	12	Fig. G-6	Fig. G-6
RTV	0.08	2.0	50	0.53	0.1
Aluminum Backface	0.06	1.5	178	0.2	111

The results obtained are plotted in Figure G-7. The peak temperatures were then crossplotted as a function of REI thickness, Figure G-8. As can be seen, a thickness of 2.53 in. (64.3 mm) holds the peak aluminum backface temperature to 300°F (420°K) during normal reentry.

G.2.4 Reentry from Lunar Orbit

As indicated in G.1.3.4, for unassisted lunar return there are a total of 11 grazing passes before reentry. The temperature history of the lower surface during the last 5 perigees and reentry is given in Figure G-9. Since the perigee heat pulse is very short compared to the cooling-off period, the effect on the aluminum backface peak temperature caused by not including the 6 initial perigee heat pulses is believed to be negligible. During the period of interest, the heat pulse duration is typically 200 - 400 sec, whereas the cooling off period between pulses is 10 - 20 ksec.

Two surface temperature histories are shown in Figure G-9. In one case, the initial surface temperature preceding each pulse was taken as 0°F (255°K). In the second case, this value was raised to 100°F (310°F).

Using the TPS thickness established for normal low earth orbit reentry (Table G-2) and allowing for an 1100 nmi (2040 km) crossrange, the aluminum backface temperature history was computed for both initial surface temperatures. The results are plotted in Figure G-10. Most of the temperature rise occurs during soakback after the reentry heat pulse. The temperature increase during the multiple pulses prior to reentry is relatively small.

The peak aluminum backface temperatures for unassisted multiple grazing reentry are summarized in Table G-3.

G.2.5 Crossrange Capability

It is evident from Table G-3 that to avoid exceeding the maximum backface design temperature of 300°F (420°K), the initial lower surface temperature must be held below 100°F (310°K) for each perigee pass. If this is not

Table G-3. Backface Temperature Summary*

	°F		°K	
Initial TPS surface temp.	0	100	255	310
Peak backface structure temp.	271	350	406	449

*Design conditions: 2200°F (~1480°K) max surface temp.
1100 nmi (2040 km) crossrange

feasible, a reduction in crossrange from 1100 nmi (2040 km) will achieve the same result.

Trajectories for various crossranges were unavailable. Consequently, the reentry heat pulse for a decreased crossrange was approximated by arbitrarily reducing the nominal pulse so as to obtain a maximum of 300°F (420°K) backface temperature. The reentry heat flux for both the original and adjusted cases is plotted in Figure G-11 as a function of time. The integrated flux during reentry is 11,900 Btu/ft^2 (135 x 10^6 joule/m^2) for an 1100 nmi (2040 km) crossrange and 9700 Btu/ft^2 (110 x 10^6 joule/m^2) for the reduced crossrange. The total time at peak heating is 850 sec and 690 sec, respectively.

A correlation, based on a large number of trajectory histories indicates that the time at peak heating is roughly proportional to the square root of the crossrange. Using this correlation, it is estimated that if the initial TPS surface temperature prior to each perigee is maintained at 100°F (310°K), the aluminum backface maximum design temperature of 300°F (420°K) will not be exceeded if the crossrange is reduced to 730 nmi (1350 km).

G.3 RADIATION EXPOSURE*

G.3.1 Introduction

Some of the modes of Shuttle operation suggested in this study introduce exposure to the trapped radiation environment of the earth not normally encountered under conventional Orbiter operation. A preliminary examination was made of the potential threat such exposure poses and the details of this examination and the conclusions reached are treated in this section of Appendix G.

G.3.2 Mission Model

Two situations within the capability of the Space Shuttle as augmented by the techniques treated in this study were considered:

a. Circular earth orbits inclined at 30^{o} and at altitudes from 300 to 19,300 nmi (555 to 35,800 km)

b. An unassisted, multiple grazing reentry from lunar orbit.

G.3.3 Radiation Environment

An electron and proton environment model from Reference G-2, Volumes II and V was used in computing the biological doses reported herein. The electron environment was assumed identical to the "projected 1968" model of Reference G-2 since this represents the situation at a solar maximum.

Only the "naturally trapped" geomagnetic particle environment has been considered. It should be noted that there are additional radiation sources which are potentially hazardous to Shuttle missions. They include:

a. Solar particle events

b. Enhanced electron environment from nuclear bursts in space

c. On-board nuclear sources

*This section is based upon material provided by R.G. Pruett.

The radiation from these sources was beyond the scope of the assessment reported herein. However, since radiation effects are additive by nature and harmful to humans, the contributions made by these sources must ultimately be considered.

G.3.4 Circular Earth Orbit

The radiation dose absorbed by a Shuttle crew in a 24 hour day is plotted in Figure G-12 as a function of circular orbit altitude and effective shielding thickness. Although plotted in rem/day, the calculations were actually made in rads and a Quality Factor (QF) of unity was used to convert to rem.

The term QF (References G-3, G-4, and G-5) has recently been adopted to designate the Linear Energy Transfer (LET) dependent factor when applied to radiation protection instead of relative biological effectiveness. For electrons, the QF is unity for any LET value. For protons, in the range encountered under the missions of interest (10 - 300 MeV) the LET is less than 3.5. According to Reference G-3, the QF for this latter case is also unity.

Three shielding thickness curves are plotted in Figure G-12, namely 1/2, 2, and 4 g/cm^2 of aluminum. The 2 g/cm^2 value is typical of current Orbiter design practice. The 1/2 g/cm^2 curve is representative of protection offered by an EVA suit. The 4 g/cm^2 curve is included to illustrate the protection achieved by doubling the Orbiter shielding thickness.

The data of Figure G-12 are for circular orbits inclined 30°. Other inclinations provide different dose values. The exact way in which the dose changes with inclination is complicated by the South Atlantic anomaly and to a lesser degree by the solar cycle. In general, increasing the inclination from 30° to 90° (polar orbit) causes a dose reduction to about half the 30° value. For altitudes above ~1000 nmi (1850 km)

reducing the inclination from 30^{o} to 0^{o} (equatorial orbit) increases the dose to about twice the 30^{o} value. Below 1000 nmi (1850 km), the effect of the South Atlantic anomaly is felt at inclinations $<20^{o}$. As a result, it is possible, depending on the specific orbital altitude, to have the dose in equatorial orbit fall below the 30^{o} value for that same altitude.

The skin dose parameter used as the ordinate is the dose at a depth of 0.1 mm at any point on the torso. It assumes that for the omnidirectional environment encountered due to selfshielding, one half of the particles never reach a given point on the body. This assumption is valid so long as bremsstrahlung is not a significantly large fraction of the total dose. If it is, the skin dose value represents the whole body dose as well.

In Figure G-12, the 4 g/cm^2 curve becomes the whole body dose above about 6000 nmi (11,000 km). The g/cm^2 curve is about 50% bremsstrahlung above 6000 nmi (11,000 km) and hence the whole body dose is about half the ordinate value. The whole body dose for the 1/2 g/cm^2 case is considerably less than the ordinate values of Figure G-12.

For altitudes to approximately 5000 nmi (9250 km) the dose with shielding thicknesses of 2 and 4 g/cm^2 is due almost entirely to protons. At greater altitudes, the dose is from electrons and/or bremsstrahlung. The dose with a shielding thickness of 1/2 g/cm^2 is due to a combination of protons and penetrating electrons up to about 5000 nmi (9250 km). Above this altitude the dose is due entirely to electrons.

In order to interpret the significance of crew radiation exposure to mission duration, some guidelines for permissible exposure and/or exposure rates must be defined. Current NASA constraints, as defined in Reference G-4, were utilized and are given in Table G-4 for ready reference.

Applying the skin dose limits from Table G-4 to the curves in Figure G-12, mission constraints can be readily established. For example, a 25-day mission would limit the average daily exposure to 3 rem/day (75 rem maximum for 30 days). With a 4 g/cm^2 shield, the mission altitude must be restricted to less than 580 nmi (1070 km) or greater than 4800 nmi (8900).

It is readily apparent from Figure G-12 that there are large regions of near-earth space which will impose severe restrictions to Shuttle rescue missions due to the radiation environment. Added Orbiter shielding is of limited benefit. Moreover, EVA in these regions will have to be carefully programmed and adequately monitored.

The problem is better illustrated by Figure G-13 where the time required to accumulate a 75 rem dose is plotted as a function of altitude. At 1000 nmi (1850 km), the maximum 30-day dose is accumulated in only 12 hours of EVA (0.5 day). At either 1500 or 8000 nmi (2800 or 14,800 km) this limit is reached in something less than 5 hours of EVA time.

Some type of onboard radiation monitoring system (as in past manned missions) is obviously also required for the Shuttle rescue mission. Preflight models of the trapped environment will probably not be known to an accuracy of a factor of ± 2. Individual crew activities will undoubtedly take them in and out of areas which are more heavily shielded than others. Also, there is risk of encountering a solar particle event of some unpredictable intensity and the possibility of intensified electron activity due to a nuclear detonation in space. All of these uncertainties make it clear that a system for keeping an accurate near real-time, record of the radiation exposure to each crew member is necessary if the dose limits of Table G-4 are to be observed. The choice of who performs an EVA during a rescue mission could depend on which crew member has received the least radiation exposure to that point in time.

G.3.5 Multiple Grazing Reentry from Lunar Orbit

When multiple grazing reentry from lunar orbit is employed, the Orbiter makes numerous passes through the trapped radiation belts. The total dose acquired depends, of course, on the number of passes, the orbit orientation about the earth, and the orbital dimensions and periods.

Weakest radiation intensities are encountered in elliptic orbits with polar inclinations. Coincidentally, a polar return orbit from the moon can always be achieved with no increase in ΔV over the trans-earth-injection value, References G-6 and G-7. It was assumed, therefore, that all successive grazing orbits have polar inclinations, and the radiation exposure was estimated on this basis. Although the orbit plane is polar, the angle between the orbit major axis and earth equator can vary over a significant range. An angle of 30^{o} was used in the analysis which follows.

A schematic drawing of the trapped radiation environment of the earth and portions of elliptic grazing traverses for the conditions stated in the previous paragraph is shown in Figure G-14 for the no-perigee-assist case. The no-perigee-assist case offers the maximum number of passes and thus the greatest accumulated exposure. It is clear from this diagram that portions of each orbit traverse the trapped radiation environment of the earth and hence some crew dose is experienced during these periods.

Apogee and perigee altitudes, the approximate period and the incremental radiation dose for each orbit are listed in Table G-5. The total crew dose of ~4 rem (behind a 2 g/cm^2 aluminum shield) over a 13.5 day period is well within the acceptable limits given in Table G-4.

If the inclination of the orbit major axis with the earth equatorial plan is reduced to zero degrees, the total dose is reduced by about 25%.

On the other hand, if no attempt is made to follow a minimum dose return and the orbit inclination is reduced from polar (90^{o}) to 0^{o}, the total dose increases by about a factor of four. In any event, it appears that a multiple grazing reentry from the moon would not produce excessive crew exposure so long as the minimum shielding is in the order of 2 g/cm^{2} and EVA is not conducted in the trapped belts.

G.3.6 Conclusions

The naturally trapped particle environment of the earth will not pose a threat to Orbiter multiple grazing reentry from lunar orbit.

Rescue missions involving EVA may be radiation limited over large portions of near-earth space.

G.4 REFERENCES

G-1. NR Space Shuttle Program, Orbiter Thermodynamics Design Data Book; January 1972; Space Division, North American Rockwell Corporation

G-2. Models of the Trapped Radiation Environment; NASA; SP-3024

G-3. Biological Factors in Manned Space Flight; Report of the Space Radiation Study Panel of the Life Sciences Committee; Wright H. Langham, Editor; 1967

G-4. Radiation Protection Guides and Constraints for Space Missions and Vehicle Design Studies Involving Nuclear Systems; Report of the Radiobiological Advisory Panel of the Committee on Space Medicine; NAS-NRC; 1970

G-5. Basic Radiation Protection Criteria; NCRP Report No. 39; 1971

G-6. Moon To Earth Trajectories; Jet Propulsion Laboratory; Technical Report No. 32-412C (Revision 1); 1 July 1964

G-7. Mission Analysis of OOS/RNS Operations Between Earth Orbit and Lunar Orbit; Aerospace Corporation; TOR-0066(5759-07)-5; 22 June 1970

Table G-1. Orbit Characteristics For Unassigned Multiple Pass Grazing Reentry; 2200°F (~1480°K) Maximum Temperature

Apogee No.	Orbit Adjust ΔV		Apogee Altitude		Perigee Altitude		Orbit Period
	ft/s	m/s	nmi	km	nmi	km	hr
1	—	—	208,000	385,000	—	—	—
2	0.01	0.003	137,000	254,000	46.6	86	134
3	0.05	0.015	67,000	124,000	46.4	86	50
4	0.07	0.021	42,000	77,800	46.1	85	26.7
5	0.12	0.037	29,000	53,700	45.8	85	16.6
6	0.17	0.052	20,500	38,000	45.5	84	11.2
7	0.23	0.070	15,000	27,800	45.1	83	8.0
8	0.32	0.098	10,800	20,000	44.7	83	5.8
9	0.46	0.140	7,600	14,100	44.1	82	4.3
10	0.69	0.210	4,900	9,070	42.4	79	3.2
11	1.14	0.348	2,500	4,630	42.2	78	2.3

Table G-4. Radiation Exposure Limits and Exposure Rate Constraints (Ref. G-4)

Constraints in Rem	Bone Marrow (5 cm)	Skin (0.1 mm)	Eye (3 mm)	Testes[2] (3 cm)
1 yr avg daily rate	0.2	0.6	0.3	0.1
30-day max	25	75	37	13
Quarterly max[1]	35	105	52	18
Yearly max	75	225	112	38
Career limit	400	1200	600	200

[1] May be allowed for two consecutive quarters followed by six months of restriction from further exposure to maintain yearly limit.

[2] These dose and dose rate limits are applicable only where the possibility of oligospermia and temporary infertility are to be avoided. For most manned space flights, the allowable exposure accumulation to the Germinal Epithclium (3 cm) will be the subject of a risk/gain decision for particular program, mission, and individuals concerned.

Table G-5. Lunar Return Multiple-Pass Orbit Characteristics and Radiation Exposure Behind 2 g/cm^2 Aluminum Shielding (No Perigee Assist)

Orbit No.	Apogee Alt.		Perigee Alt.		Approx Period, hr	Incremental Dose, rem
	nmi	km	nmi	km		
1	208,000	384,000	—	—	—	—
2	137,000	253,000	46.6	86	134	0.09
3	67,000	125,000	46.4	86	50	0.24
4	42,000	78,000	46.1	85	26.7	0.33
5	29,000	53,000	45.8	85	16.6	0.13
6	21,000	38,000	45.5	84	11.2	0.15
7	15,000	28,000	45.1	83	8.0	0.20
8	11,000	20,000	44.7	83	5.8	0.26
9	7,600	14,000	44.1	82	4.3	0.38
10	4,900	9,100	42.4	79	3.2	0.68
11	2,500	4,600	42.2	78	2.3	1.32
12	1,000	1,850	—	—	1.7	0.18
						Total Dose ≈ 4 rem

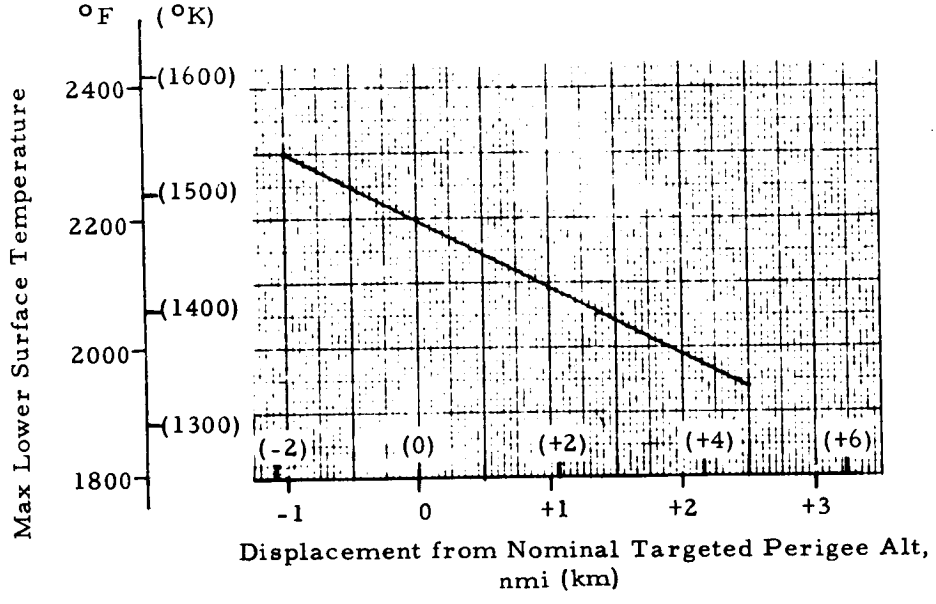

Figure G-1. Sensitivity Of Lower Surface Temperature To Perigee Altitude

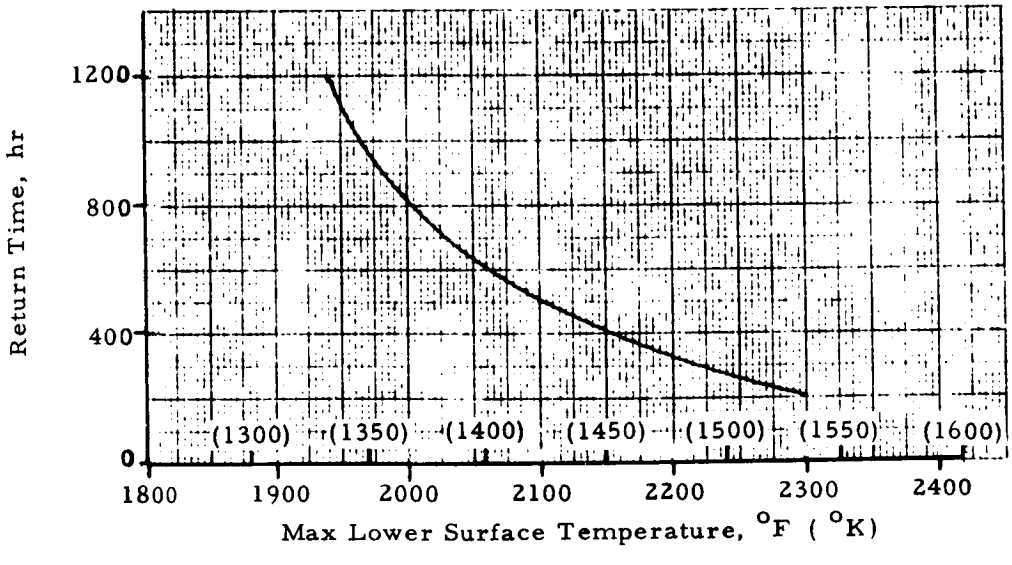

Figure G-2. Total Lunar Return Time for Unassisted Grazing Reentry

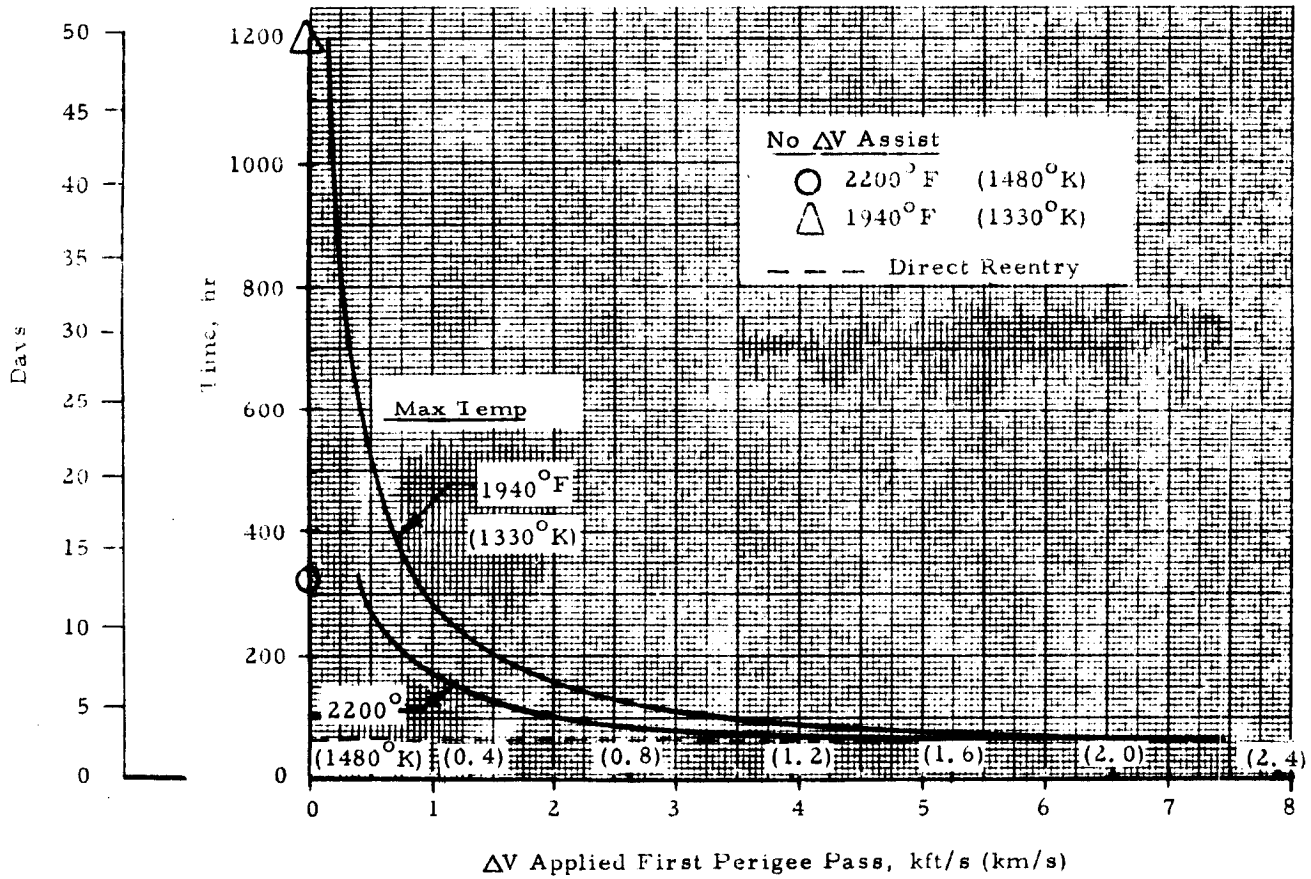

Figure G-3. Lunar Return Time for Assisted Grazing Reentry (Lunar Orbit To Touchdown)

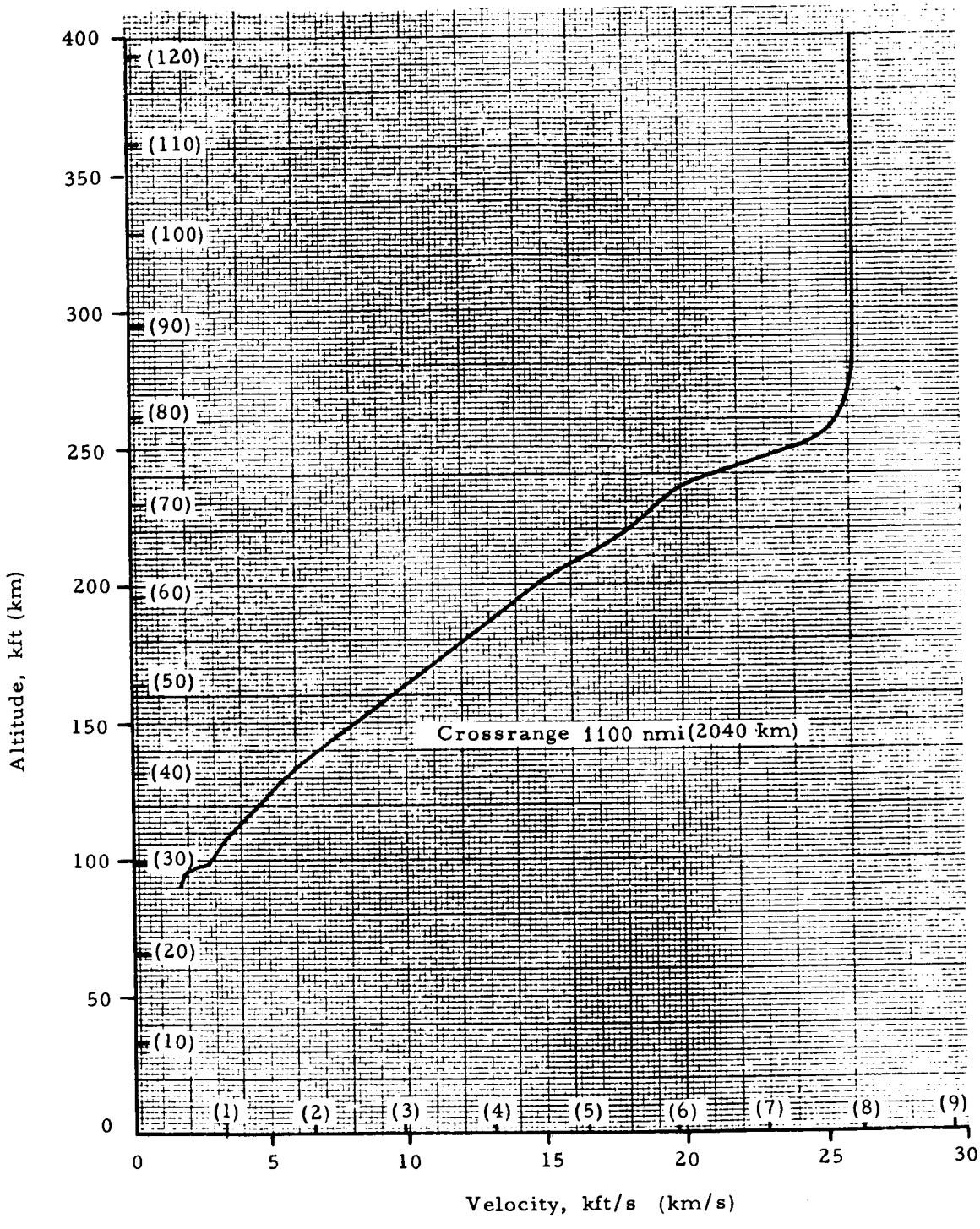

Figure G-4. Trajectory Profile For Final Reentry

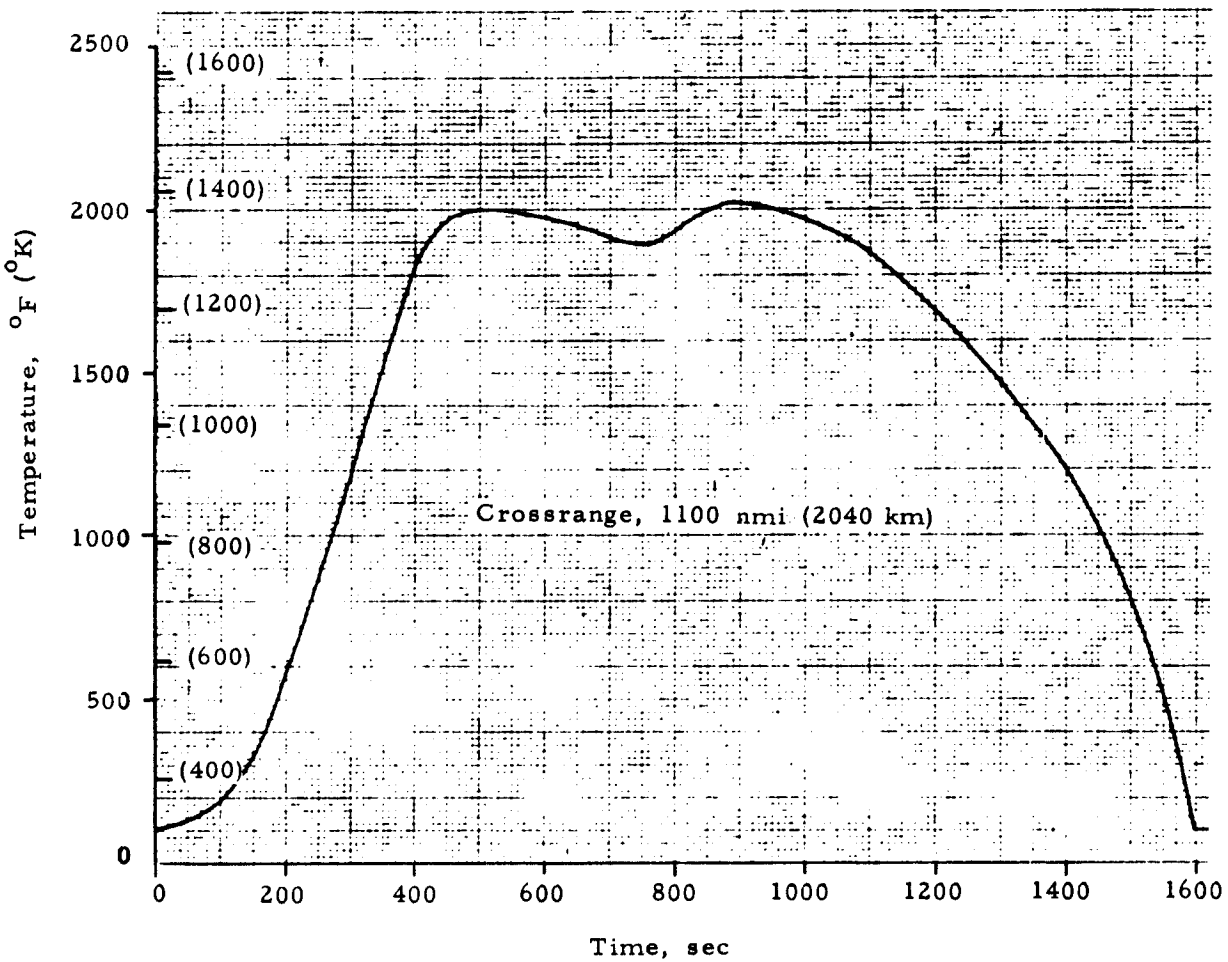

Figure G-5. Lower Surface Maximum Temperature History For Normal Reentry From 400,000 ft (120 km) Altitude

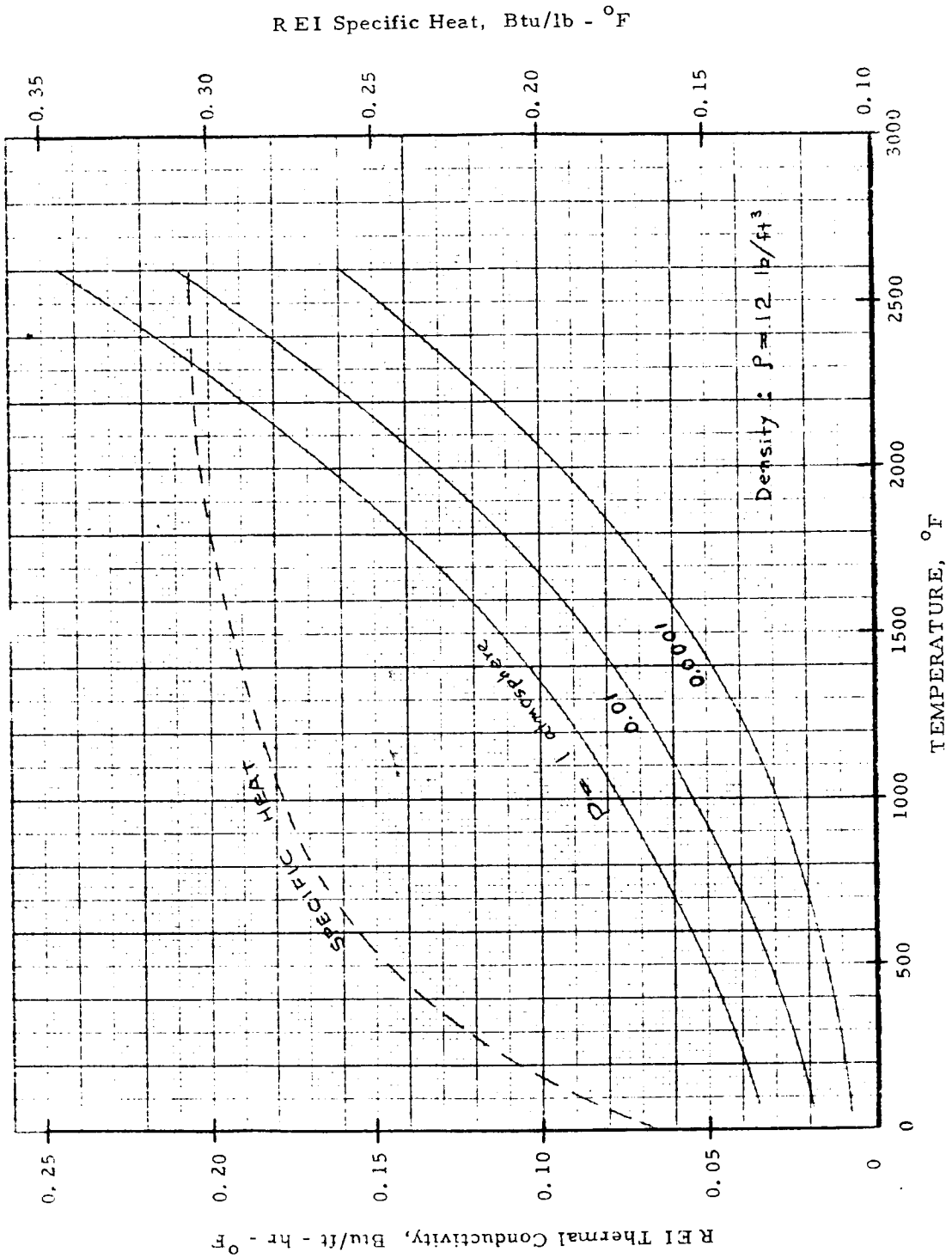

Figure G-6. Thermodynamic Properties of REI (Ref. G-1)

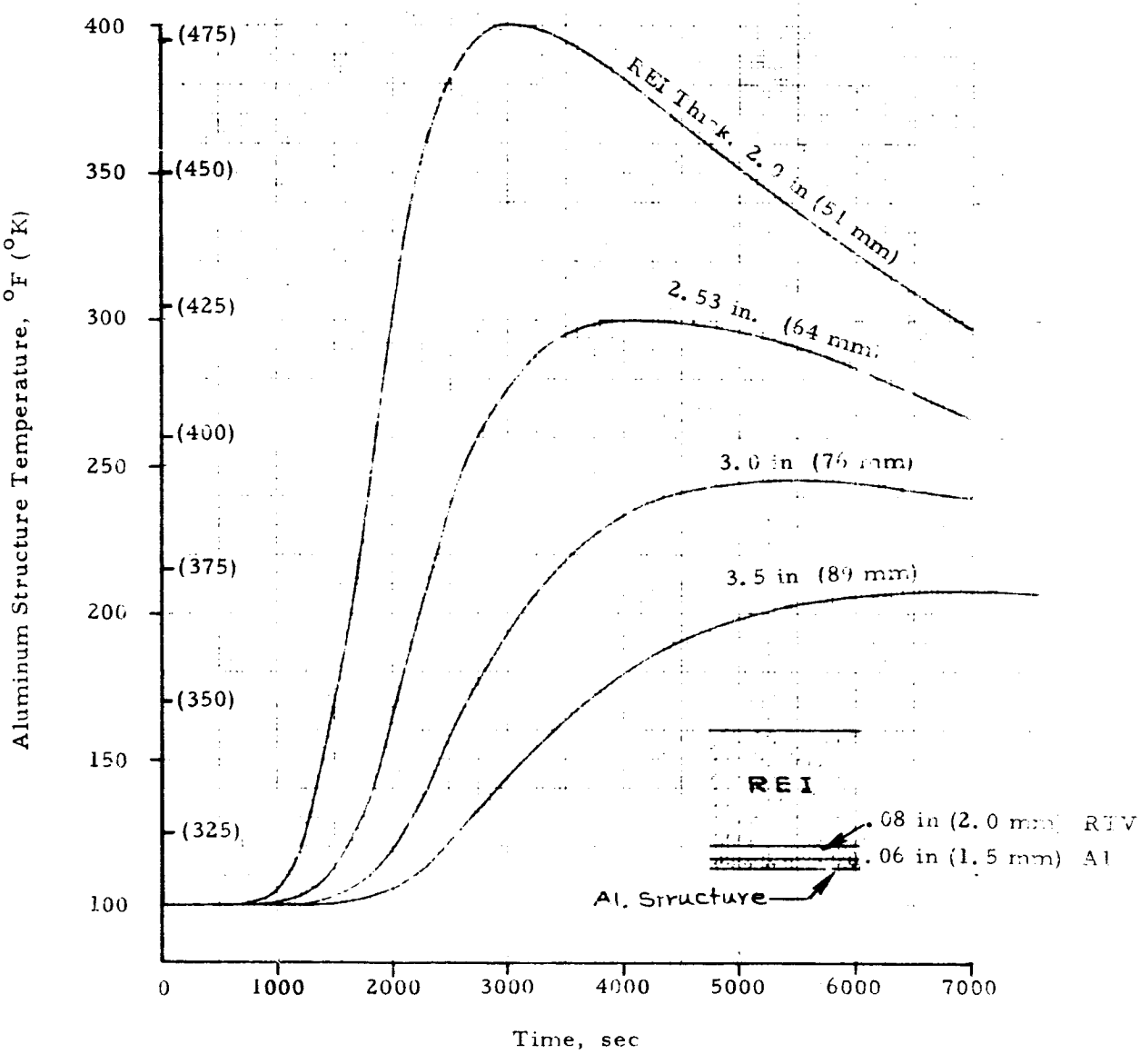

Figure G-7. Aluminum Backface Temperature History for Normal Low Earth Orbit Reentry

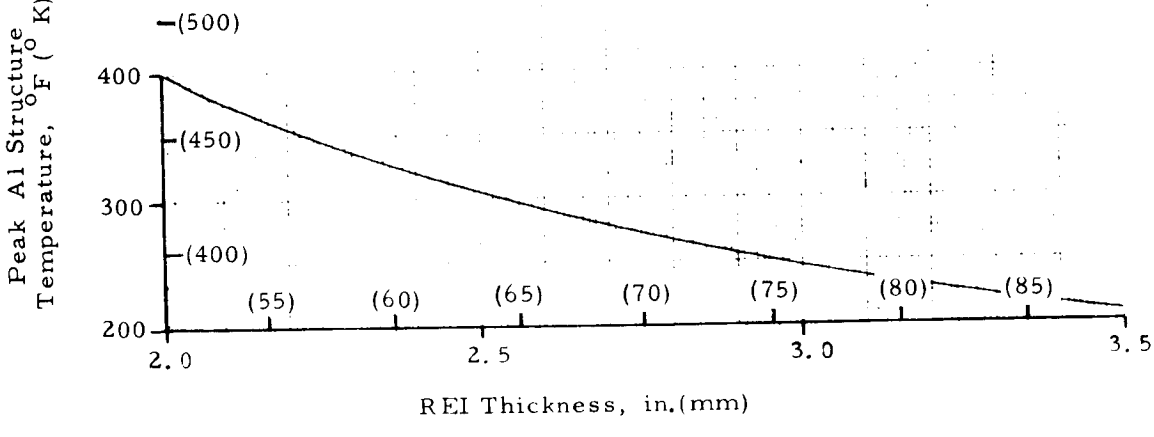

Figure G-8. Effect of REI Thickness on Aluminum Backface Peak Temperature

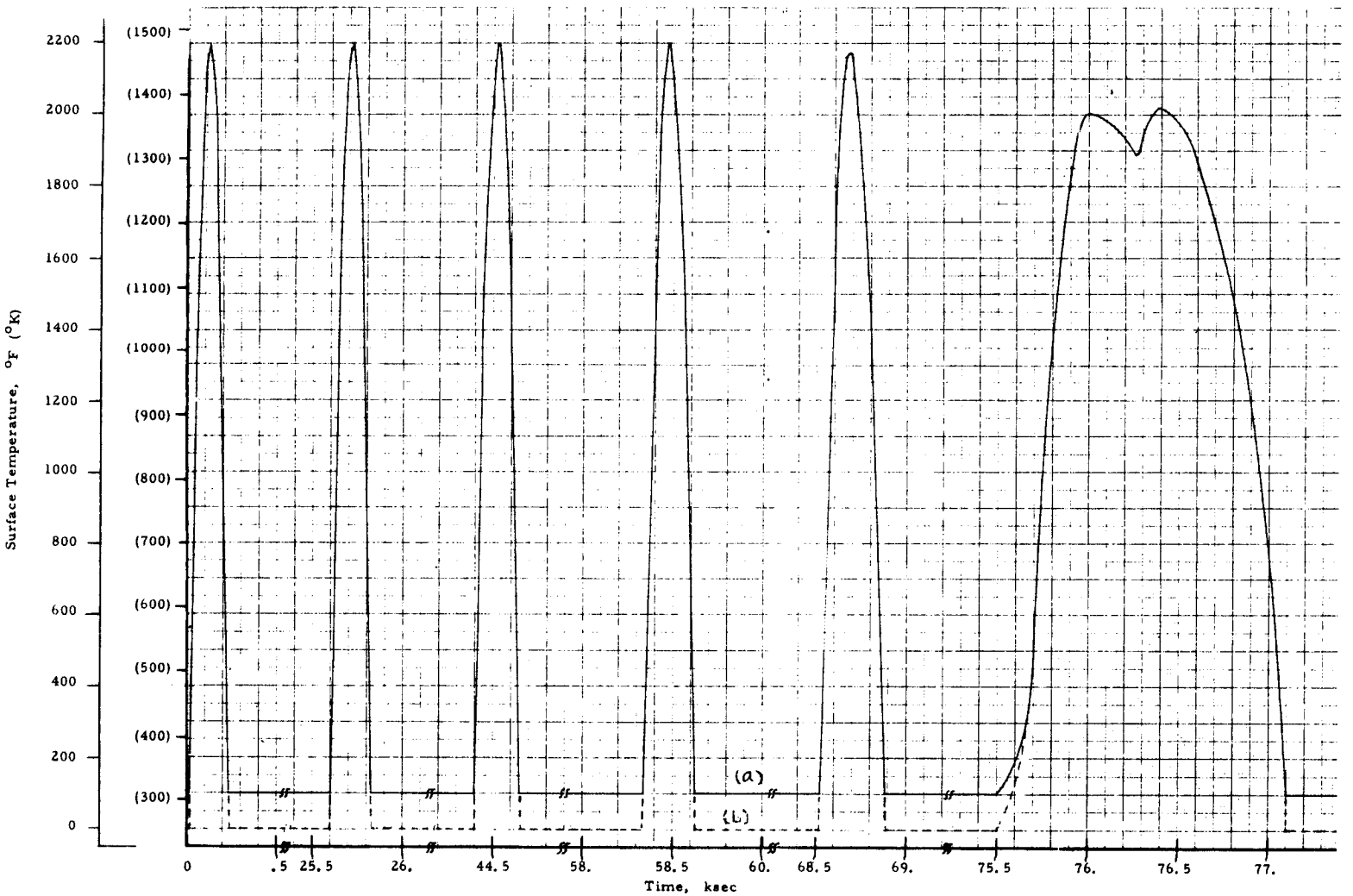

Figure G-9. Lower Surface Temperature History for Multiple Pass Grazing Reentry from Lunar Orbit (Starting with 7th Grazing Pass)

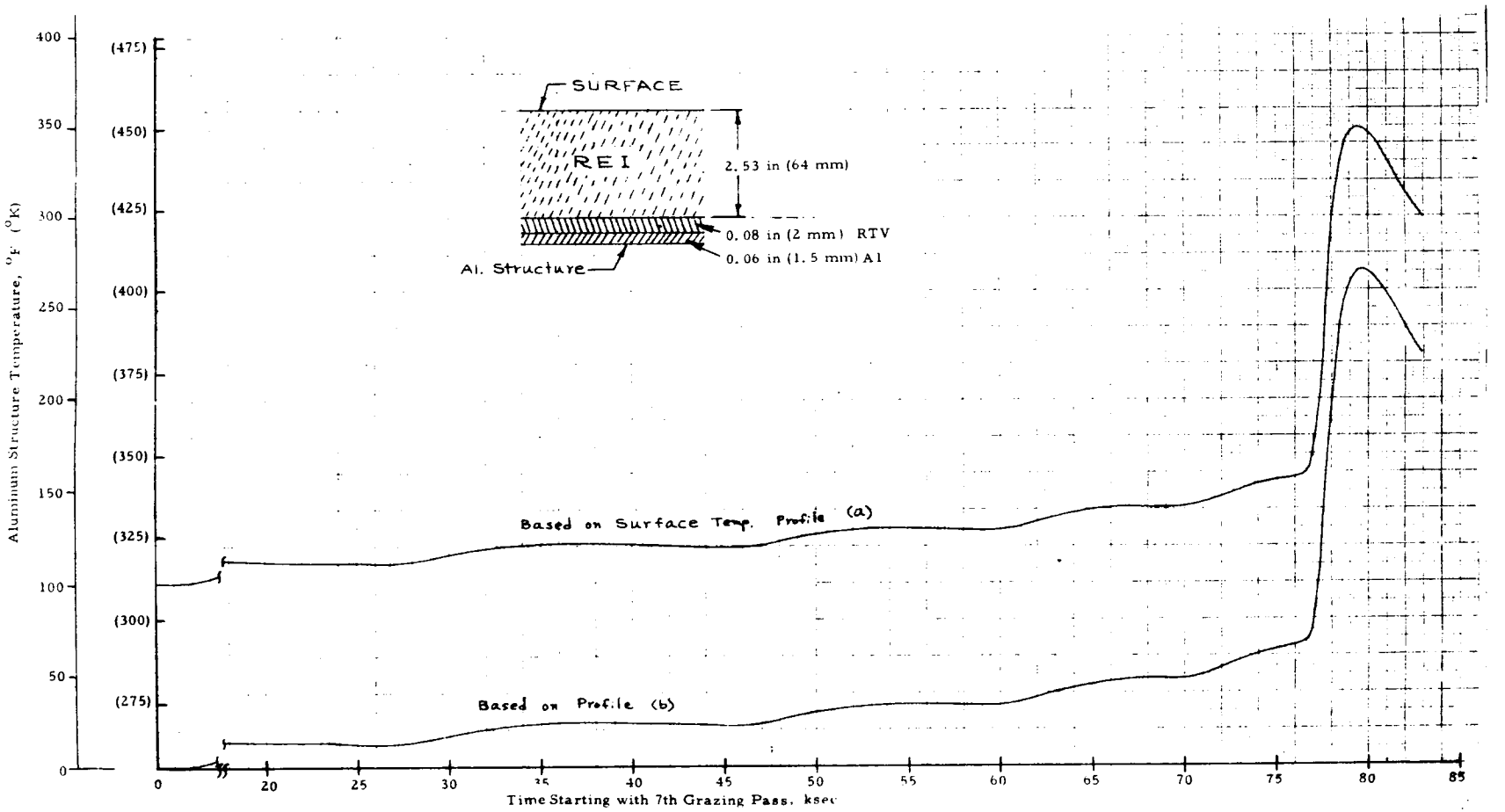

Figure G-10. Aluminum Backface Temperature History for Multiple Pass Grazing Reentry from Lunar Orbit with No Perigee Assist

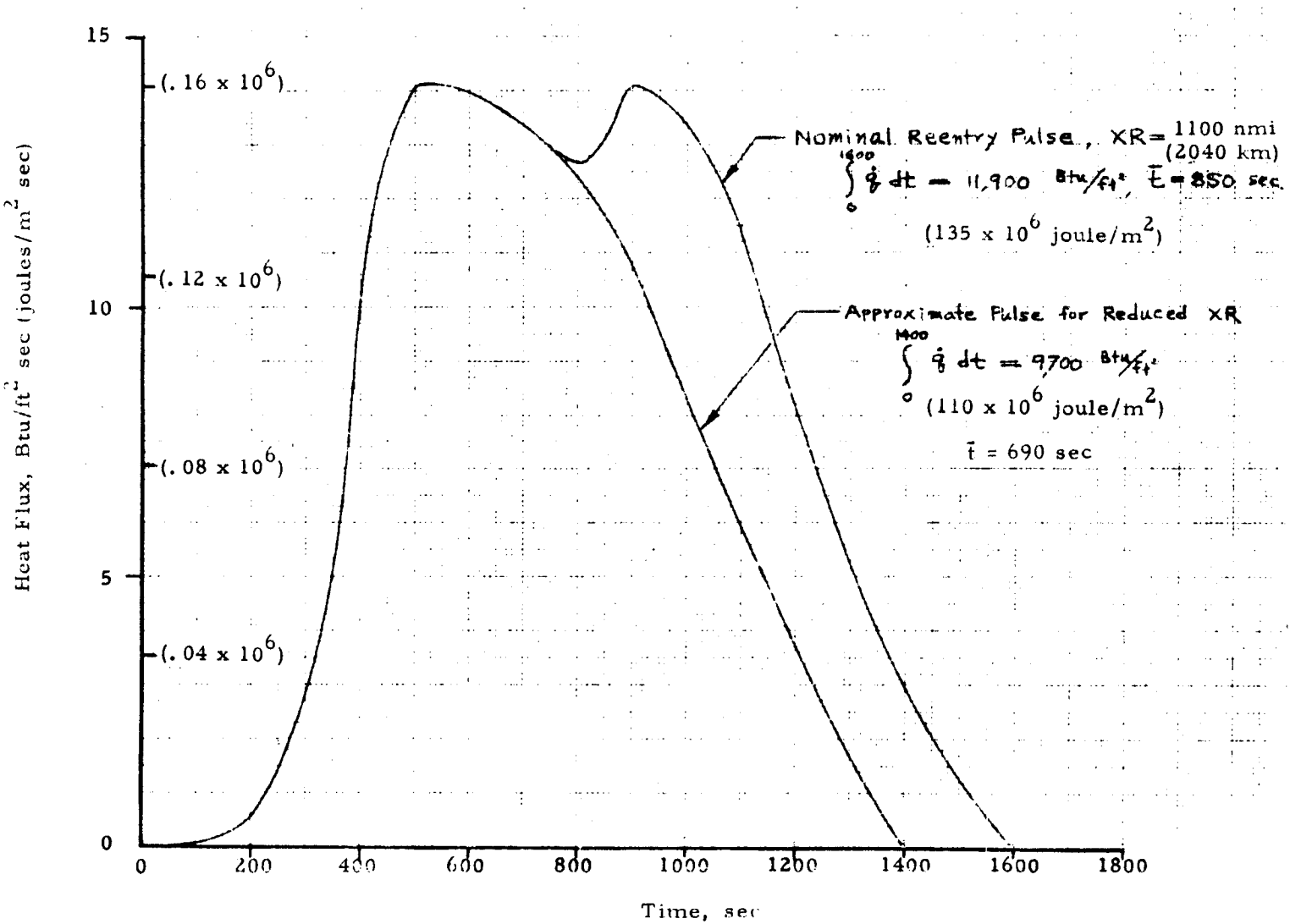

Figure G-11. Reentry Heat Flux History for Nominal and Reduced Crossrange Cases

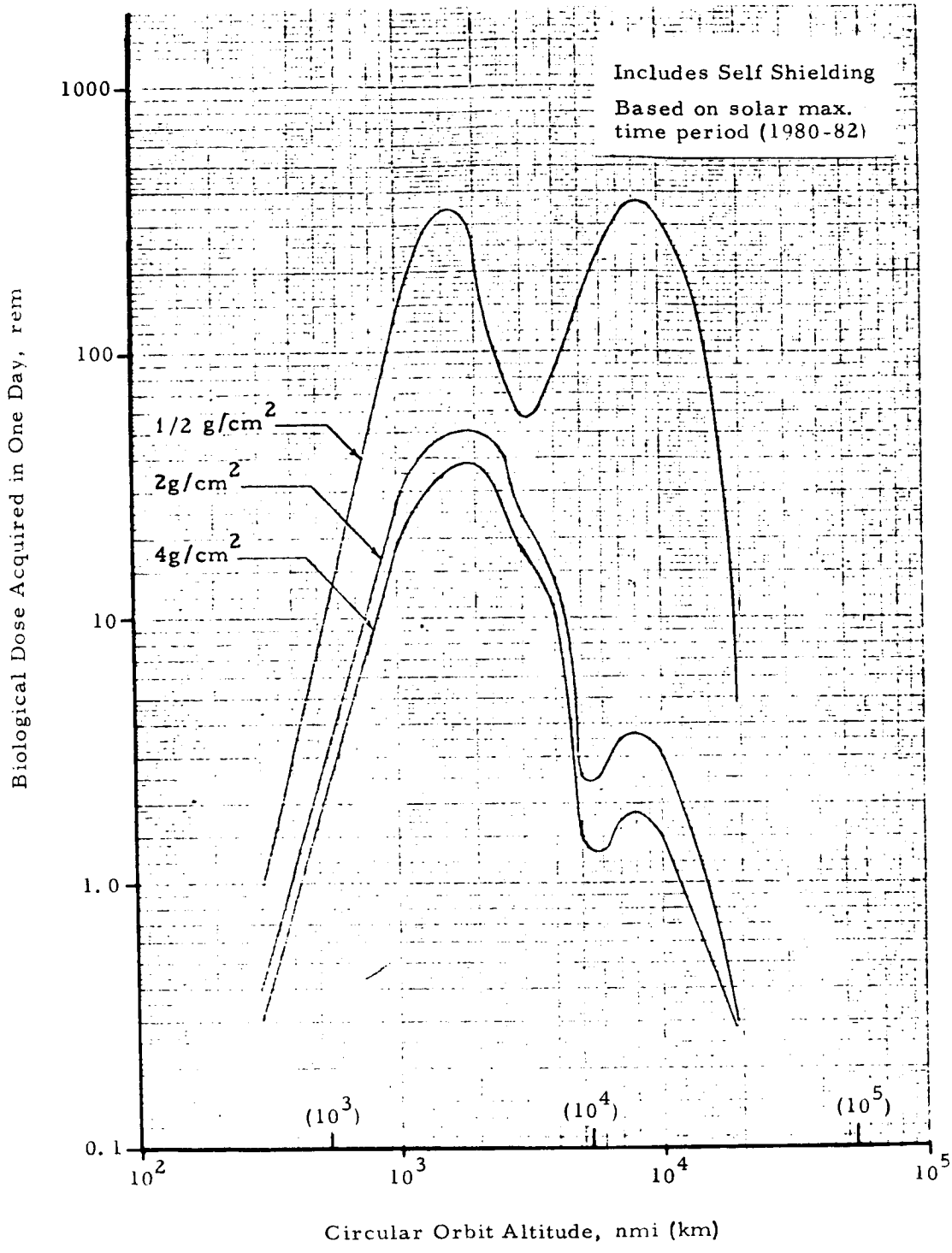

Figure G-12. Biological Dose (Skin) Due to Naturally Trapped Radiation Environment of the Earth for 30° Inclined Orbits

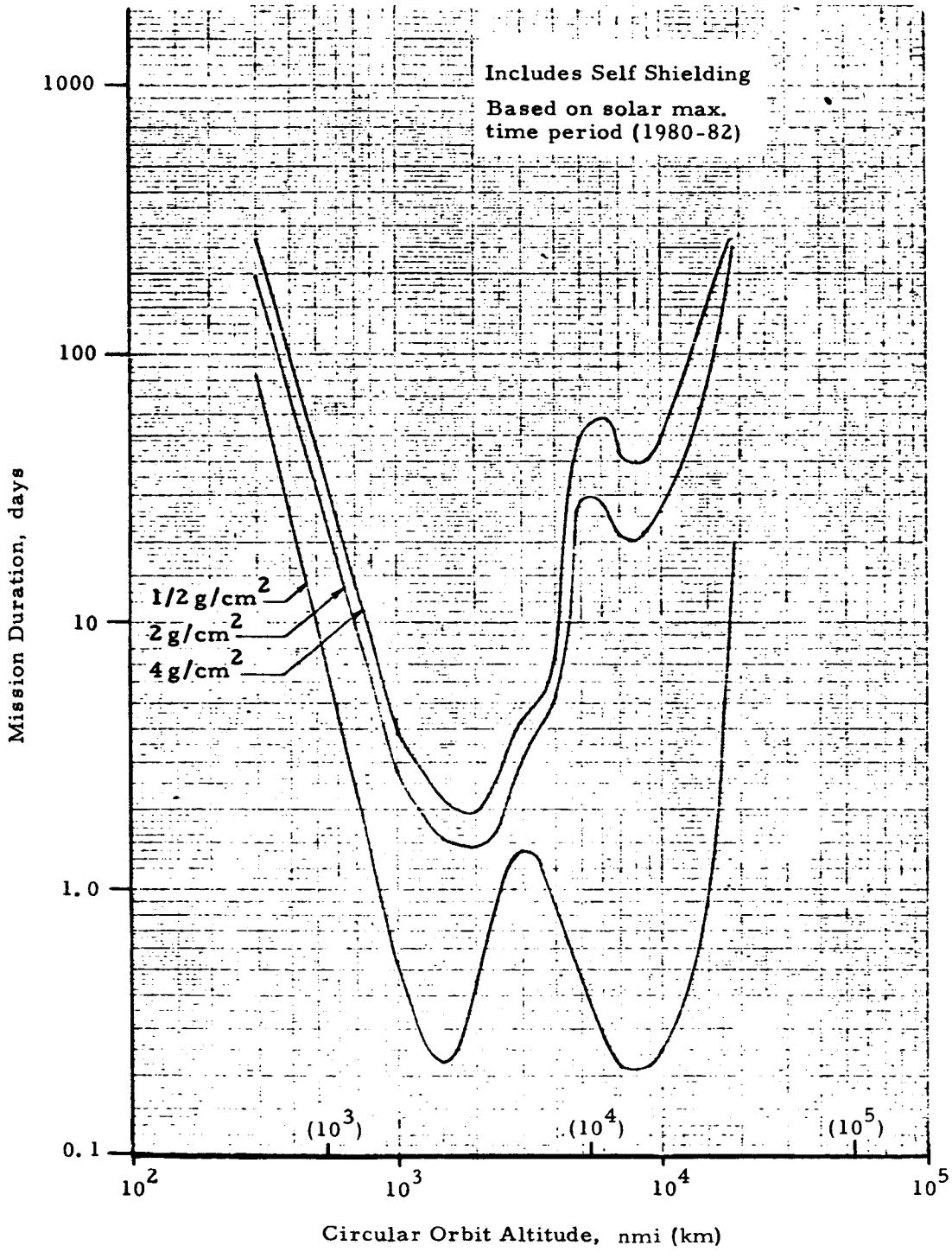

Figure G-13. Allowable Mission Duration in 30° Inclined Orbits for 75 Rem Maximum Skin Dose

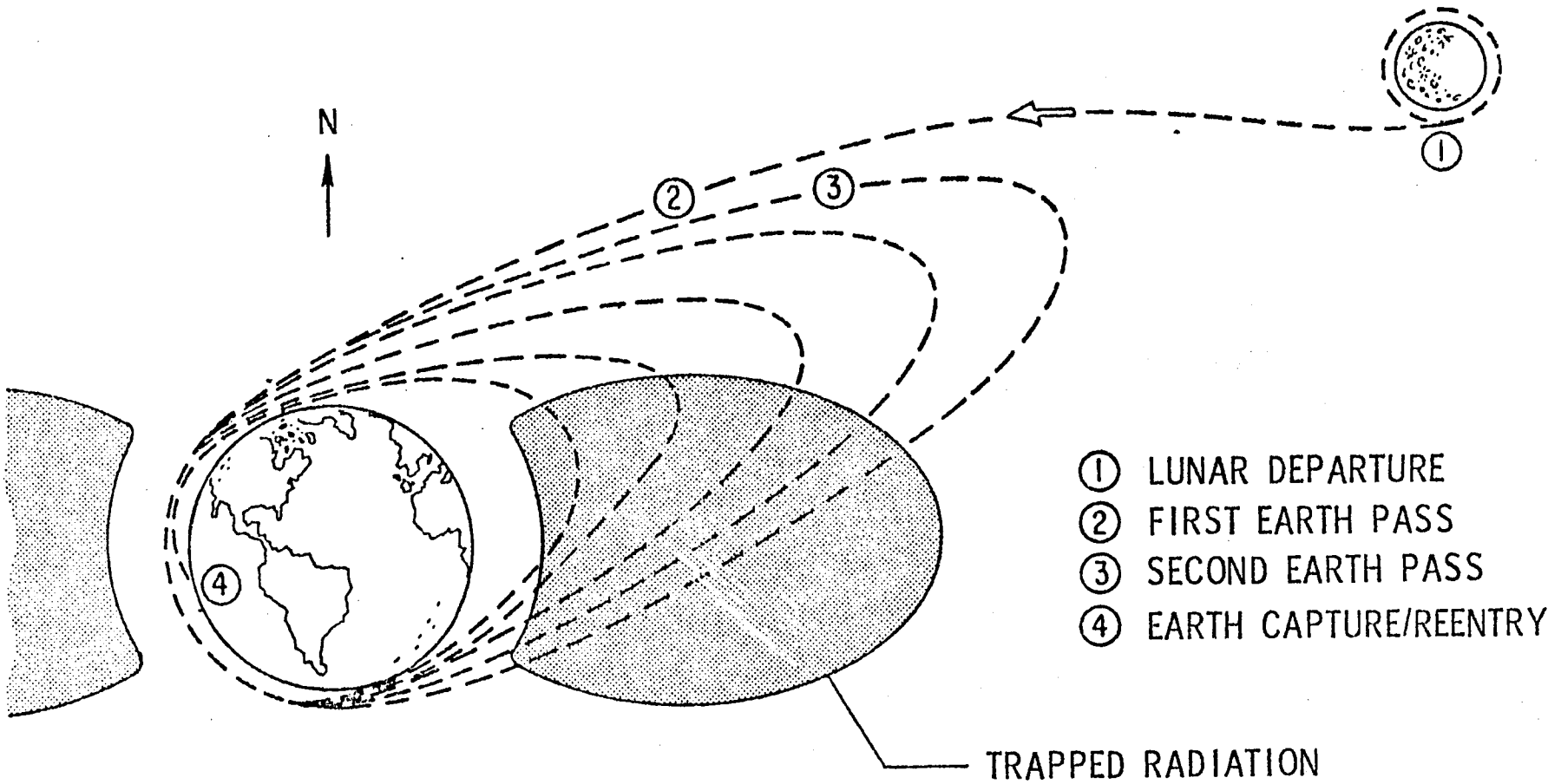

Figure G-14. Schematic Illustration of Unassisted Multiple Pass Grazing Lunar Return Through Trapped Radiation Field of the Earth (Polar Earth Orbits)

APPENDIX H

GROUND LAUNCHED ASCENT/RENDEZVOUS TIME

APPENDIX H

CONTENTS

APPENDIX H

FIGURES

FIGURES (cont.)

APPENDIX H*

GROUND LAUNCHED ASCENT/RENDEZVOUS TIME

(WORST-CASE)

H.1 MINIMUM ΔV ASCENT

In-plane ascent requires the least ΔV expenditure for reaching a given target altitude. Although establishing the proper phase relation between the distressed vehicle and an ascending rescue vehicle may require a parking delay at some intermediate orbital altitude, ideally, no increase in the total ΔV over direct ascent is necessary. Terminal rendezvous maneuvers are not considered.

H.1.1 Ascent Procedure

In-plane ascent requires that the launch occurs at the time the target orbit plane coincides with the launch site. Thus, the rescue vehicle enters the target orbit plane without further maneuvers. There are, in general, two launch opportunities every 24 hours. For example, for a 90° inclination orbit and launch from ETR, the in-plane opportunities occur every 12 hours; at a 55° inclination, times between launch are alternately 9 and 15 hours. For an easterly launch, the two launch opportunities merge and occur every 24 hours.

If ascent were immediately made to orbit altitude, the positions of the rescue vehicle and target would not necessarily coincide. In order to eliminate this difference in phase, a low altitude parking orbit is first established by the rescue vehicle. This altitude should be selected to be as low as possible without incurring significant adverse atmospheric drag effects. In this study, 100 nmi (185 km) was assumed. The orbital period at the low altitude parking orbit is less than that of the target at some higher altitude and therefore the

*The material in Appendix H was prepared by W. Fey.

rescue vehicle will gradually catch up with the target. When the proper phase relation has been achieved, a Hohmann transfer to target altitude is made and gross rendezvous is completed.

H.1.2 Method of Calculation

Worst-case times to rendezvous with a distressed vehicle were calculated for a range of inclinations and altitudes. It was assumed that subsequent to the declaration of emergency, the longest possible wait for the next launch opportunity occurred. In addition, the worst phasing situation was assumed, and a parking time sufficient for the relative phase of target and rescue vehicle to change by 360° was allowed. In addition to these times, allowances of 0.11 hr from lift-off to burnout in 50 x 100 nmi (93 x 185 km) orbit and 0.71 hr for Hohmann transfer from the 50 x 100 nmi (93 x 185 km) orbit to the 100 nmi (185 km) circular parking orbit were made. Also considered was the time for Hohmann transfer from parking orbit to target orbit.

H.1.3 Ascent/Rendezvous Time

The resulting worst-case times to rendezvous from an ETR launch are shown in Figure H-1(a) for altitudes to 20,000 nmi (37,000 km). Minimum time to rendezvous occurs at target altitudes around 5000 nmi (9300 km). At a given inclination, the rendezvous time depends upon the time for Hohmann transfer from parking orbit to target orbit altitude, which increases with increasing altitude, and the time spent in a parking orbit, which decreases with increasing altitude. The interaction of these two effects produces the minimum noted. Worst-case time to rendezvous decreases as inclination increases due to the time between launch opportunities which varies from 24 hours for an inclination of 28° to 12 hours at a 90° inclination.

The region up to an 800 nmi (~1500 km) target altitude, which is the approximate upper limit of Orbiter capability, is shown in Figure H-1(b). The effect of the long parking orbit times required for low target altitudes can be seen more clearly here; the time to rendezvous becomes quite long and approaches

infinity for a target at 100 nmi (185 km), since no phase change is accomplished if the rescue vehicle parks at the same altitude as the target. Fortunately, for low altitude targets the Orbiter will usually not need all of its ΔV capability to achieve target altitude and can use the excess to expedite rendezvous.

The time to rendezvous of Figure H-1 includes both the maximum waiting time for a launch opportunity and the maximum waiting time in the 100 nmi (185 km) parking orbit due to the worst possible phasing relation between the target and interceptor vehicles. At less severe phase relations, the rendezvous time may be significantly less.

Assuming no launch window delay, the total time for an in-plane ascent to a target at 270 nmi (500 km) is given in Figure H-2 as a function of the relative phase angle between the interceptor and the target. The variation is linear between an ideally phased situation with an ascent time of ~2 hours to the worst case with an ~23.5 hr ascent time. The curve is discontinuous between these two end points with the worst case representing a just missed ideally-phased condition.

H.2 ASCENT WITH EXCESS ΔV

H.2.1 Plane Change

Launching before or after the in-plane launch opportunity offers a method of rapidly changing the relative phase between the rescue vehicle and the target and thus reducing the intercept time. A velocity penalty is, however, imposed by this procedure. If ascent to the target altitude does not require the entire Orbiter ΔV available, the remaining propellant could be used to provide the needed ΔV for the plane change required to place the intercepter in the orbit plane of the target vehicle.

It was assumed that the plane change is made at apogee of the Hohmann transfer to target altitude and is combined with the injection velocity impulse in order to minimize the ΔV required. The procedure is illustrated schematically in Figure H-3.

Since the plane change along may require larger ΔV expenditures that may be available, parking orbit phasing at 100 nmi (185 km) may be combined with plane change to make optimum use of the available ΔV remaining.

H. 2. 2 In-Plane Elliptic Phasing Orbit

Another method of reducing some of the in-plane ascent/rendezvous times given in Figure H-2 is to employ an elliptic parking orbit which has a more favorable phase/period relation to the target orbit than does a 100 nmi (185 km) circular orbit.

If ΔV is available, such an elliptic orbit may be established and will, for some situations, allow the target to catch up with the rescue vehicle in less time than by the approach of H. 1. 1.

In estimating the ascent/rendezvous time, it was assumed that the rescue vehicle ascends to target altitude without parking at 100 nmi (185 km). Upon arrival at target altitude, a ΔV in excess of that required to circularize is added to establish an elliptic parking orbit with perigee at target altitude and apogee at some higher altitude. When sufficient phasing is accomplished, an impulse applied at perigee is used to circularize at target altitude. Due to the elliptic parking orbit, opportunities for rendezvous only occur when the rescue vehicle is at perigee. Adjustment so that the target coincides with the rescue vehicle at perigee can be made by variation of the parking orbit apogee. This ascent mode is illustrated schematically in Figure H-4.

H. 2. 3 Ascent/Rendezvous Time

H. 2. 3. 1 In-Plane Ascent

An example of such an in-plane ascent and intercept is treated in Figure H-5. The situation is a distressed vehicle in a 270 nmi (500 km) circular orbit of 55° inclination. Time from lift-off to gross rendezvous is shown as a function of relative phase between rescue vehicle and target. The waiting time for an in-plane launch opportunity has not been included.

Points (2) and (3) at 360° and 0° respectively, represent the ideally phased condition and require that no time be spent in a parking orbit. The time of approximately 2 hr is simply that corresponding to burnout in a 50 x 100 nmi (93 x 185 km) orbit plus Hohmann transfer to a 100 x 100 nmi (185 x 185 km) orbit followed by Hohmann transfer to a 270 x 270 nmi (500 x 500 km) orbit.

If the rescue vehicle parks at 100 nmi (185 km), the phase relative to the target follows line (1) – (2) and decreases at a rate of 16.7°/hr. This portion of the curve is that of Figure H-2 between 223 and 360°.

On the other hand, if parking is accomplished in 270 x 930 nmi (500 x 1700 km) orbit, which corresponds to an additional 2 kft/s (610 m/s) ΔV expenditure, the relative phase increases at a rate of 27.2°/hr (line (3) – (1)). At phase angles <223°, this parking orbit offers a lower intercept time than the 100 x 100 nmi (185 x 185 km) orbit. Above 223°, a greater time results.

The intersection of the two lines at ~223° phase difference (point (1)) represents the worst-case time-to-intercept condition of about 10 hr and the same delay occurs with either parking orbit.

The net effect of this intersection and the curve slope on either side of the intersection is that the preferred parking orbit will depend on the relative phasing between target and interceptor at the time the interceptor is launched. For certain conditions, significant reductions in the time-to-intercept for an in-plane launch are clearly available by means of an elliptic parking orbit with perigee at the target orbit altitude.

H.2.3.2 Out-of-Plane Ascent

As previously mentioned, interceptor launch before or after the time when the target orbit plane passes through the launch site yields a rapid adjustment of relative phase at the expense of a ΔV requirement. This effect is illustrated in Figure H-6 for the case of an available ΔV of 2 kft/s (610 m/s). The target characteristics are as before; namely, a 270 nmi (500 km) circular orbit inclined 55°.

The line on the right side of the figure which originates at point (4) and rises to (3') represents a launch 0.44 hr earlier than an in-plane launch and reduces the relative phase by 97°. Point (4) represents direct ascent to the target orbit followed by a plane change requiring 2 kft/s (610 m/s). To the right of point (4), the launch occurs not quite so early, ascent to 270 nmi (500 km) is also direct, and the required plane change is less.

To the left of point (4), along line (4) – (3'), the required relative phase decrease is greater than that possible with a launch 0.44 hr early. Here, parking in a 100 nmi (185 km) orbit is combined with a plane change at no ΔV penalty. After the final ascent to 270 nmi (500 km), the required plane change is made with the available 2 kft/s (610 m/s) excess ΔV.

The line (1) – (3) on the left side of Figure H-6 corresponds to a late launch with direct ascent to 270 nmi (500 km) followed by the necessary plane change. At point (3), the launch occurs approximately 0.5 hr after an in-plane launch opportunity and increases the relative phase by 123°. After direct ascent to 270 nmi (500 km), the plane change for rendezvous requires a 2 kft/s (610 m/s) ΔV expenditure. Between (3) and (1) the plane change ΔV requirement gradually drops to zero.

Line (3) – (3') represents a discontinuity between the early-launch and late-launch situation. Lines (1) – (1') and (2) – (2'), on the other hand, represent a trade-off situation combining late launch and phasing in an elliptic orbit above the target orbit. Line (1) – (1') represents the use of all available excess ΔV to establish the highest possible (longest period) elliptic parking orbit. Line (2) – (2') represents the use of 1 kft/s (305 m/s) for plane change and 1 kft/s (305 m/s) for a phasing orbit. For the worst-case situation, the use of the entire available excess ΔV for an elliptic phasing orbit appears to be the most advantageous approach.

This is borne out in Figure H-7 which shows the worst-case rendezvous time as a function of the relative amounts of ΔV applied to parking orbit and plane

change. This sort of optimization had to be performed for each ΔV considered for a particular target orbit altitude and inclination. It was found that for the smaller ΔVs, it was most advantageous to use all the ΔV for establishing the parking orbit. At some point when sufficient ΔV was available, however, it became most advantageous to use all the ΔV to produce plane change. There appeared to be no situations when a combined strategy was optimum.

H.2.4 Total Interception Time

These same trends can be observed in the results shown in Figure H-8(a) which shows worst-case time to rendezvous as a function of ΔV available for a target in 270 nmi (500 km) orbit of 55° inclination. In this case the ground wait for a launch opportunity is included. For this inclination, it is basically 15 hours but adjusted for the length of launch window provided as a function of ΔV. For ΔVs up to 2.45 kft/s (750 m/s), it is most optimum to use all the ΔV to obtain a phasing orbit of the longest possible period. From that point to one corresponding to a ΔV of 2.8 kft/s (850 m/s), the ΔV should all be used for plane change. At ΔVs in excess of 2.8 kft/s (850 m/s), the curve changes its character again and the time savings as a function of increased velocity are rather meager. At a ΔV of 2.8 kft/s (850 m/s) or greater, no time must be spent in parking orbit at either 100 nmi (185 km) or above target altitude. All phasing can be accomplished by waiting on the ground. Consequently, the rapid improvements in rendezvous time connected with shortening the phasing time are no longer possible. The further decrease in rendezvous time is a result of a widened launch window as increased velocity capability allows an earlier or later launch with its attendant higher plane change and ΔV requirement.

Similar data for a target altitude of 500 nmi (925 km) at an inclination of 55° is shown in Figure H-8(b) and for an altitude of 100 nmi (185 km), in Figure H-8(c). The curve at 100 nmi (185 km) is different from the others in that the worst-case time to rendezvous is infinite unless some ΔV is

available. The right hand portion of the curves, representing rendezvous times when sufficient ΔV is available so that no time is spent in parking orbit, are very similar for the three altitudes considered. This is the result of the trade-off of two factors. The Hohmann transfer time to target altitude increases as the altitude increases. However, the ΔV requirement for plane change at apogee of the transfer at target altitude decreases due to the lower velocity of the rescue vehicle and target. This results in a somewhat increased launch window and, hence, a decreased wait on the ground prior to a launch opportunity. The net effect is a very slight increase in time required for rendezvous at the higher altitude for a particular ΔV capability.

H.3 SHUTTLE CAPABILITY

When the data on times required for rendezvous as a function of available velocity are compared with vehicle capability, two conflicting trends are evident. The time to rendezvous tends to decrease for higher target altitudes but the ΔV available to be employed to shorten rendezvous time also decreases. Values for the basic ΔV capability of the four vehicles considered were taken from the results shown in Appendix B for the case of a 10 klb (4.5 t) rescue module. Both this baseline capability and that when additional propellant is loaded in the cargo bay (Appendix C) were considered, and results are shown in Figure H-9. A vehicle with ΔV capability rather limited shows a decrease in time to rendezvous as target altitude increases (up to the maximum altitude capability) while those vehicles which have somewhat more capability show little change in time to rendezvous as target altitude is varied.

H.4 ALTERNATE RENDEZVOUS PROCEDURE

An improved technique for rendezvous is believed possible by employment of a bi-elliptic transfer maneuver as described in References H-1 and H-2. Consideration of this method would require a more extensive analysis than that appropriate to the present study. The principal improvement would consist of performing the plane change in three portions; when entering the transfer ellipse from 100 nmi (185 km) altitude, at apogee of the exterior

phasing orbit and upon arrival at target altitude. These can be combined with the impulses for altitude change at these points and varied in magnitude in order to minimize the velocity requirement. In addition, the altitude of the exterior phasing orbit can be selected so that the rescue vehicle coincides with the target upon arrival at target altitude, without further adjustment.

H.5 REFERENCES

H-1. Baker, J.M., "Orbit Transfer and Rendezvous Maneuvers Between Inclined Circular Orbits," TOR-469(5540-10)-11, Aerospace Corporation; June 1965

H-2. Fey, W. A., "Extended Launch Windows for Ground-Based Rescue Missions," AAS Paper No. 71-304, AAS/AIAA Astrodynamics Specialists Conference; 1971

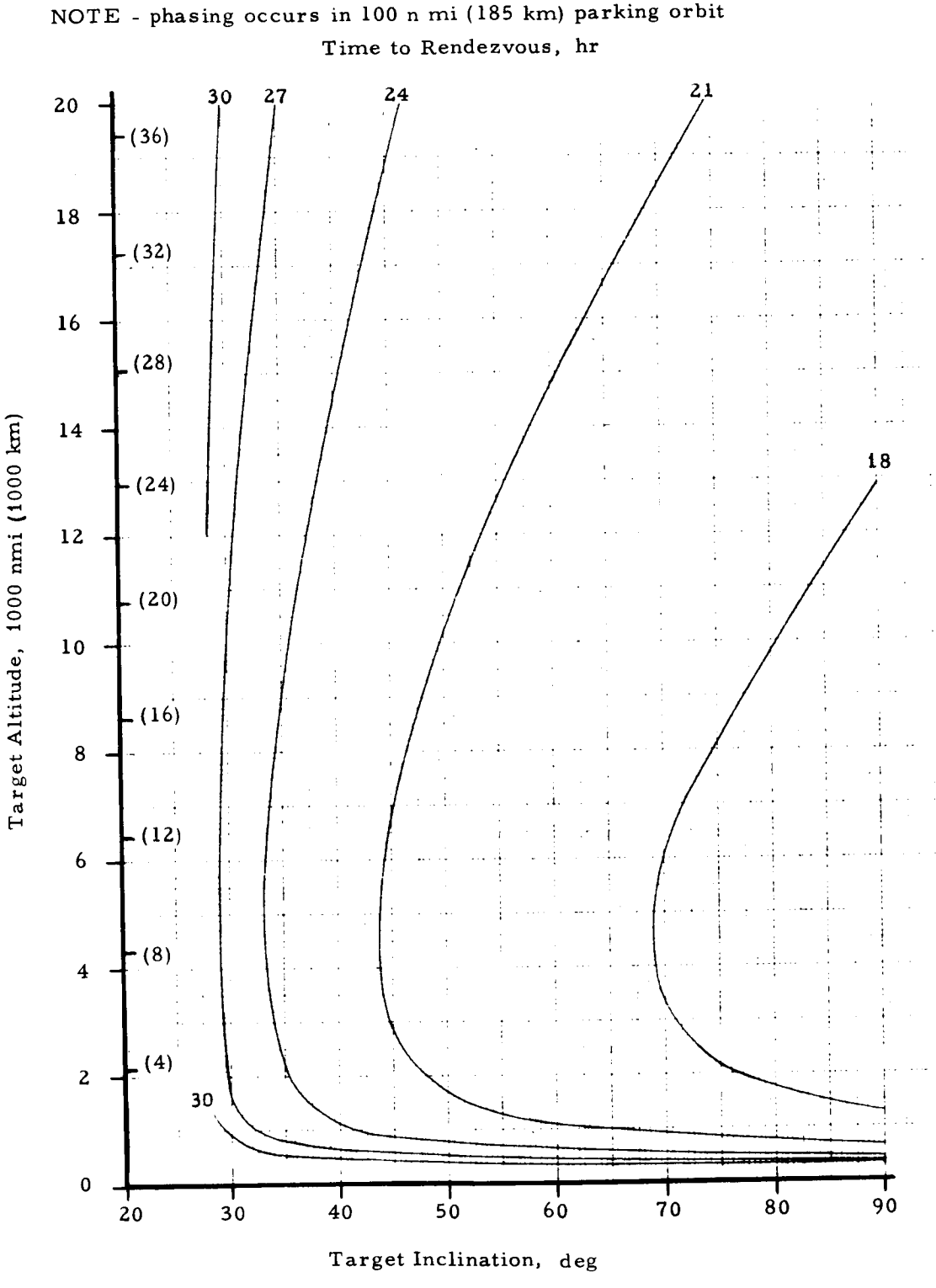

Figure H-1. Worst-Case Time to Rendezvous for In-Plane Ascent
(a) Target Altitude 100-20,000 nmi (185-37,000 km)

NOTE - phasing occurs in 100 n mi (185 km) parking orbit

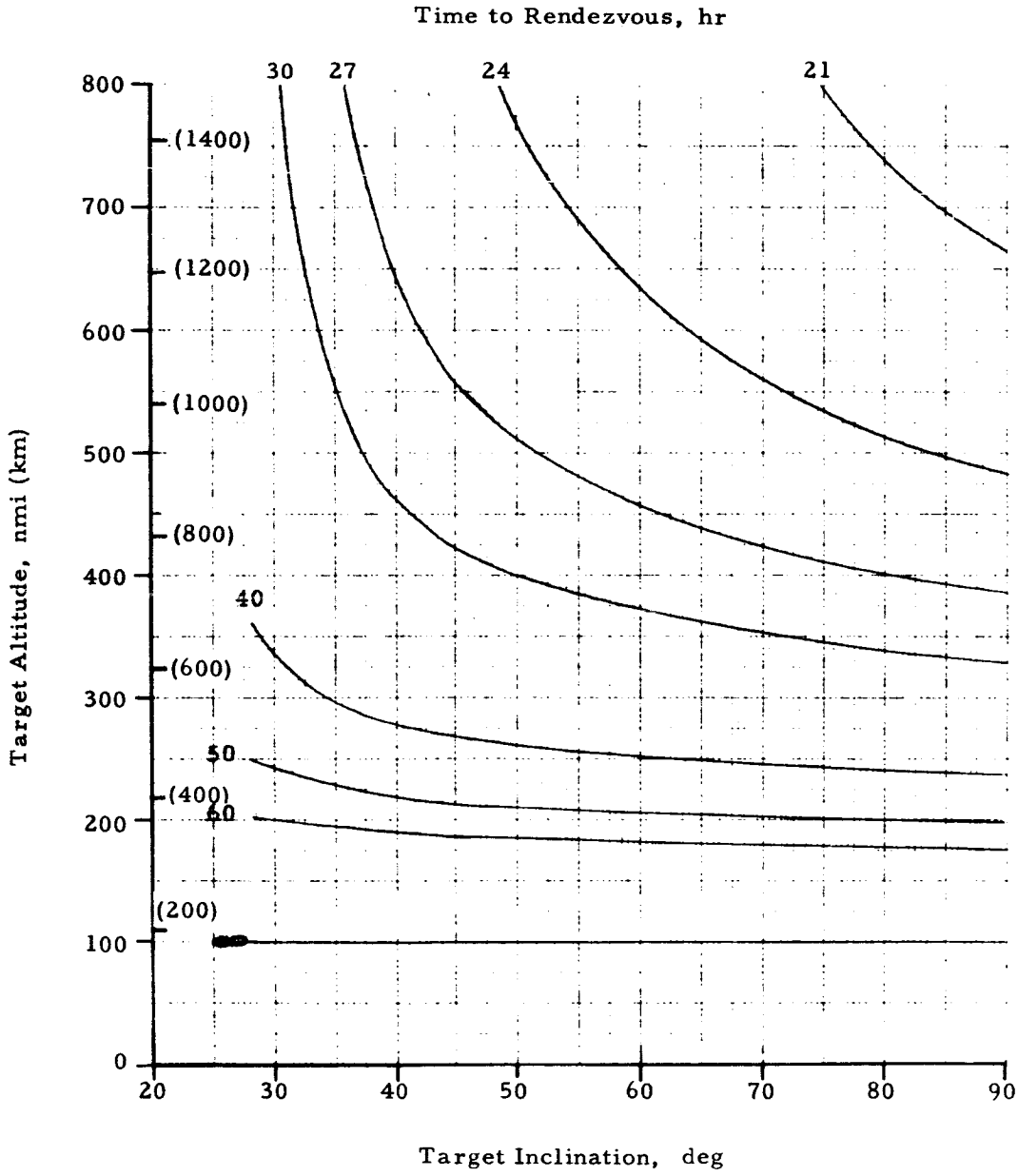

Figure H-1. Worst-Case Time to Rendezvous for In-Plane Ascent
(b) Target Altitude 100 - 800 nmi (185 - 1480 km)

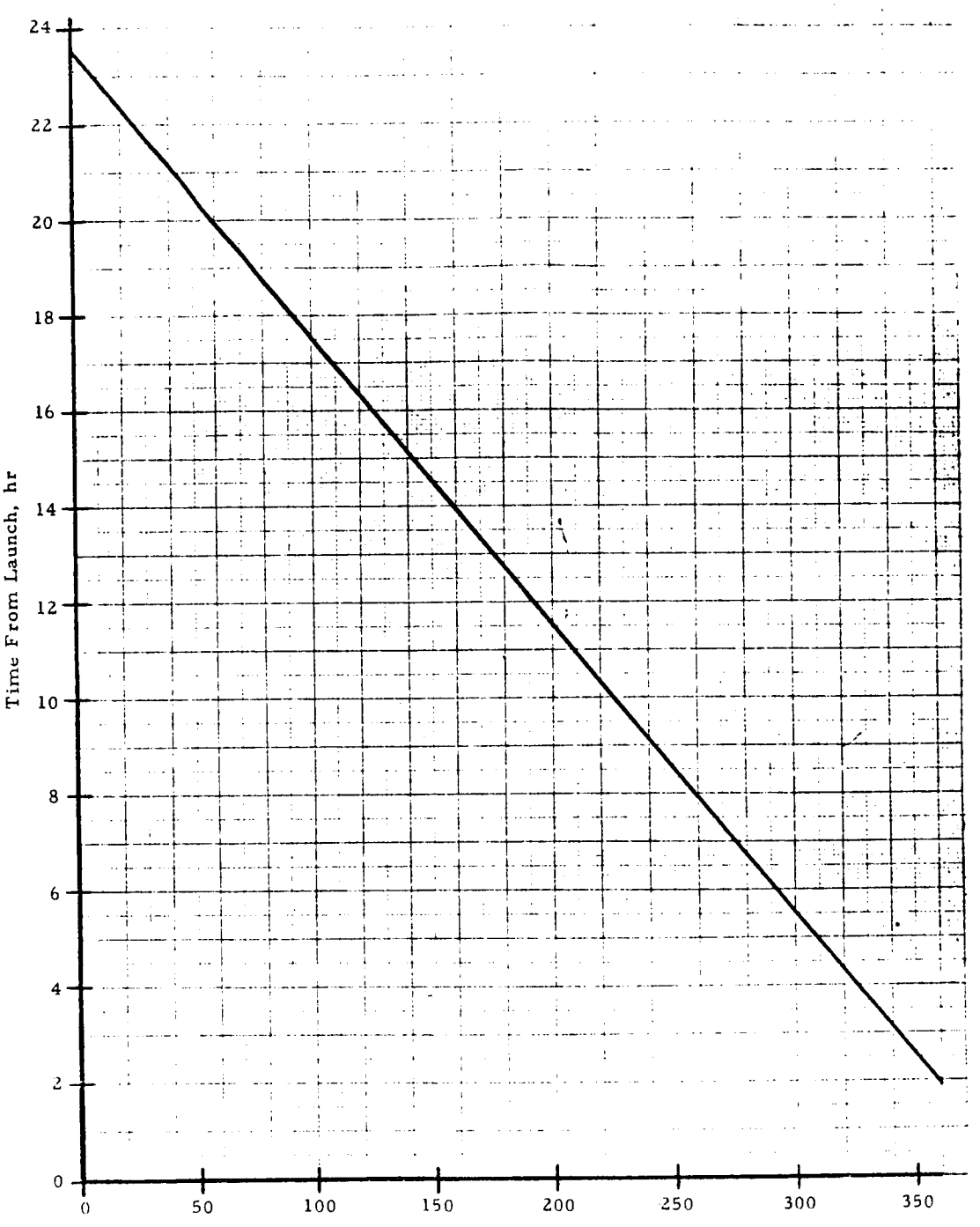

Figure H-2. Total Time from Launch to Intercept for In-Plane Ascent to 270 nmi (500 km) Target [100 nmi (185 km) Parking Orbit]

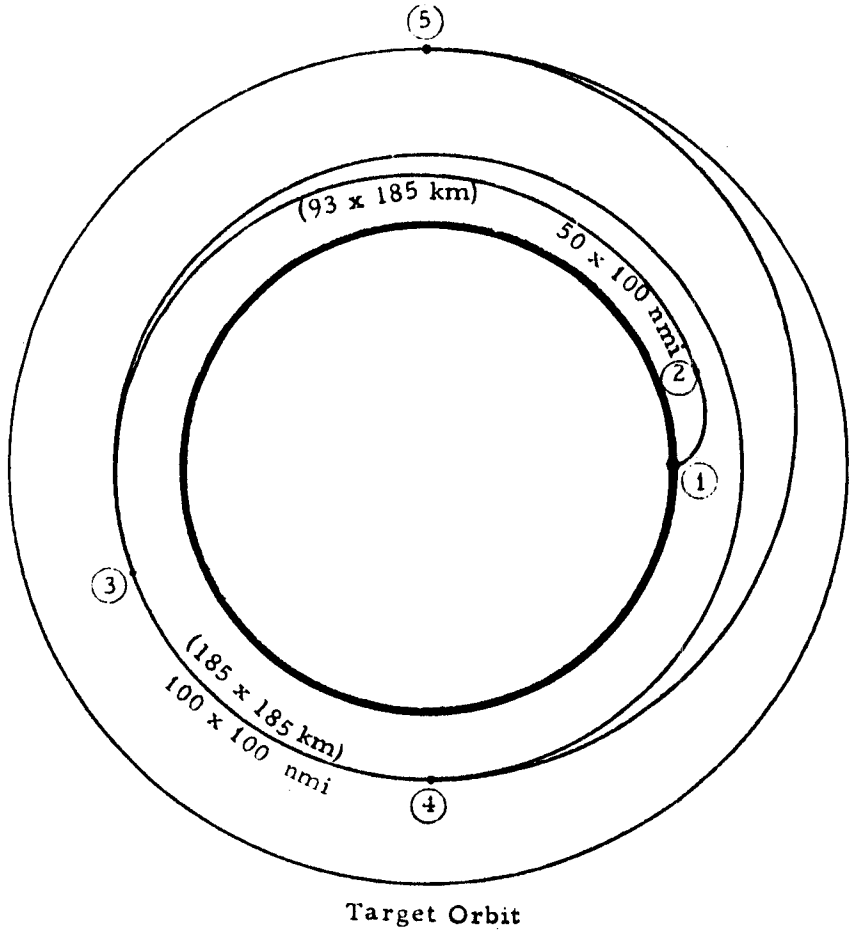

(1) Lift-off from ETR

(2) Burnout in 50 x 100 nmi (93 x 185 km) orbit

(3) Circularize and park in 100 nmi (185 km) orbit for phasing

(4) Inject from parking orbit into 100 nmi (185 km) x target orbit altitude. (Injection 180° from (4) is also permissible)

(5) Circularize and plane change to enter target orbit in phase with target

Figure H-3. Schematic Diagram of Rescue Vehicle Ascent with 100 nmi (185 km) Parking Orbit

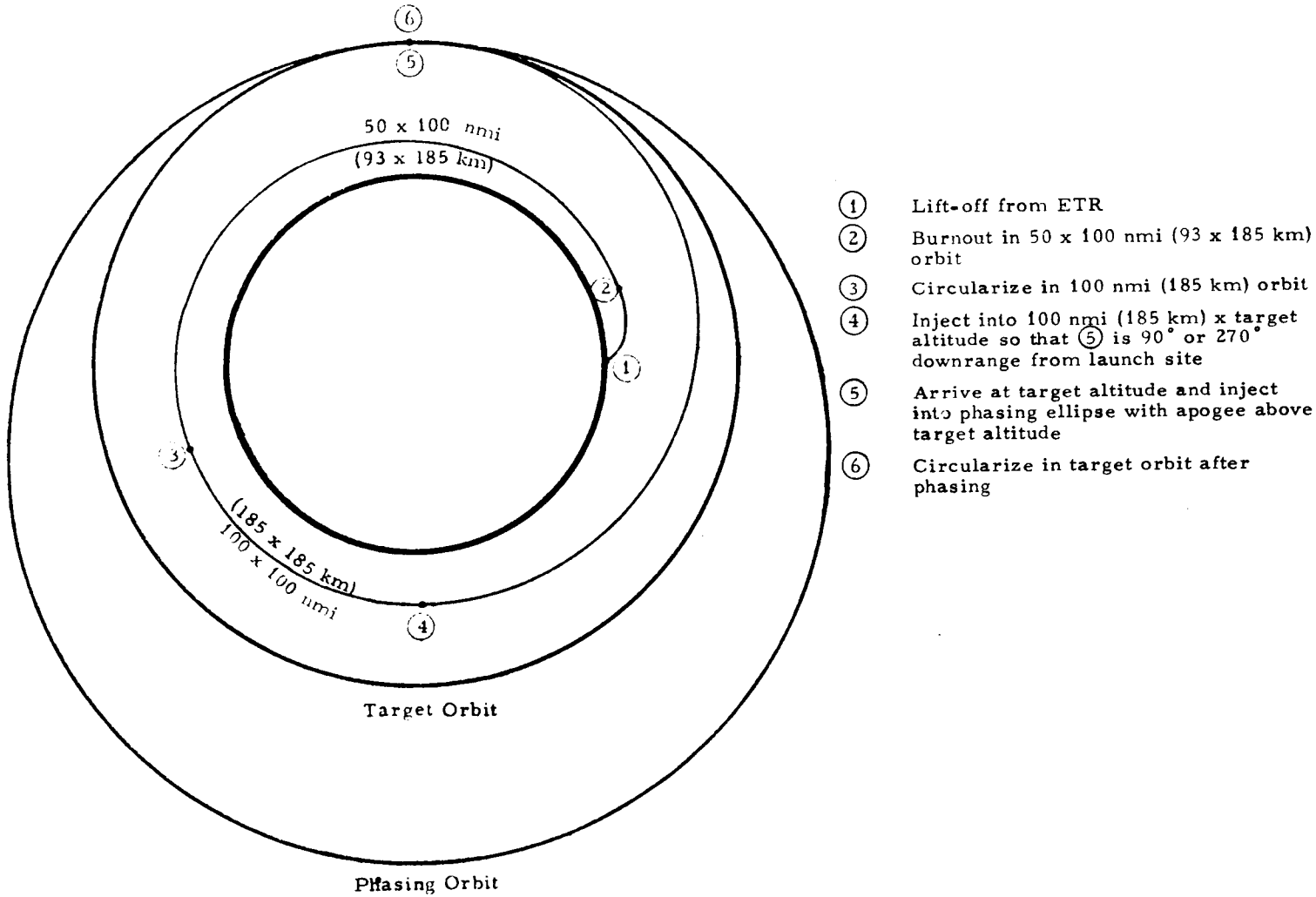

Figure H-4. Schematic Diagram of Rescue Vehicle Ascent Via Elliptic Parking Orbit with Apogee Above Target Orbit

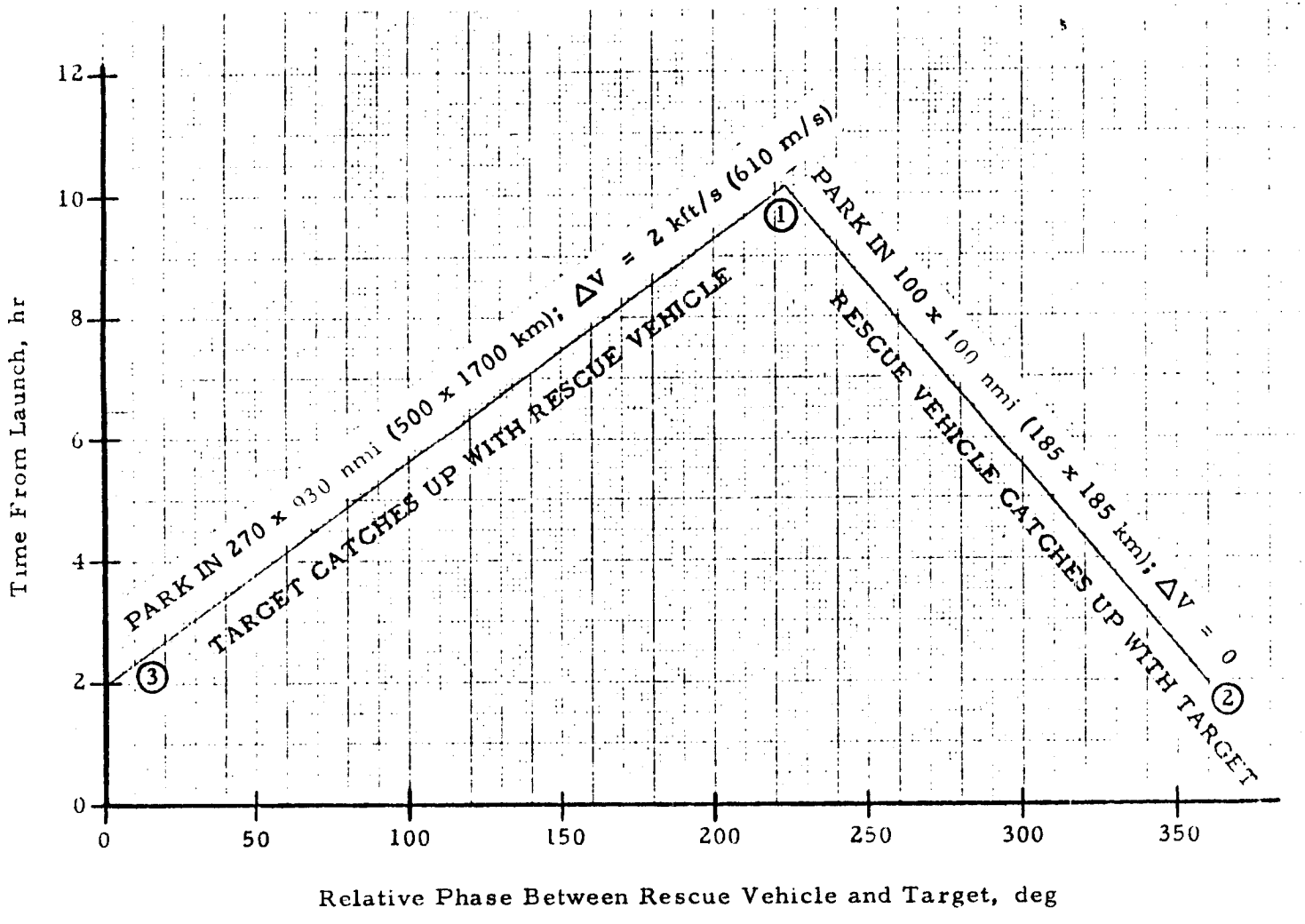

Figure H-5. Total Time From Launch to Intercept for In-Plane Ascent to 270 nmi (500 km) Target with 2 kft/s (610 m/s) Available Excess ΔV

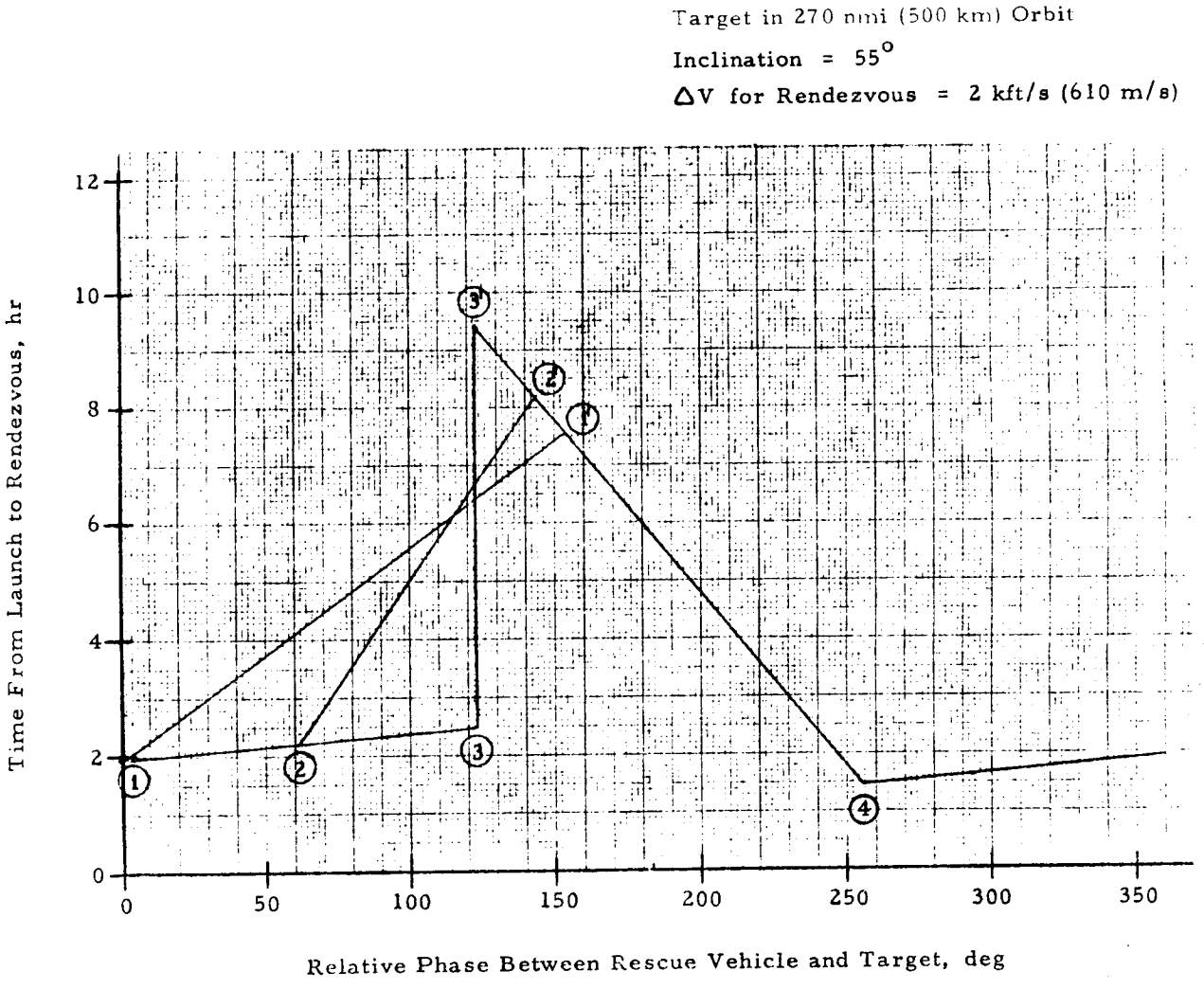

Figure H-6. Total Time from Launch to Intercept for Out-of-Plane Ascent to 270 nmi (500 km) Target with 2 kft/s (610 m/s) Available Excess ΔV

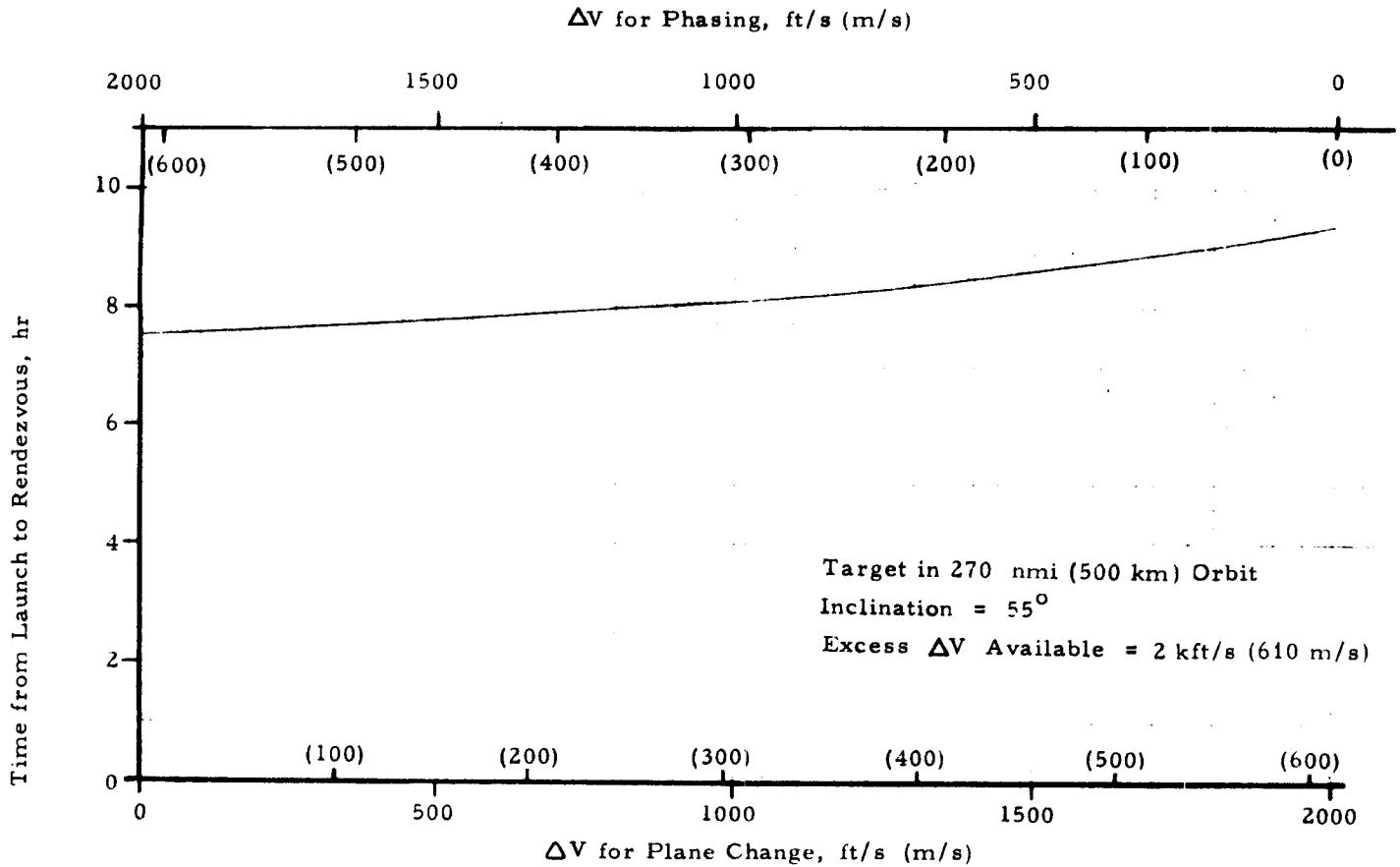

Figure H-7. Effect of Available ΔV Distribution Between Plane Change and Phasing on Worst-Case Time from Launch to Rendezvous

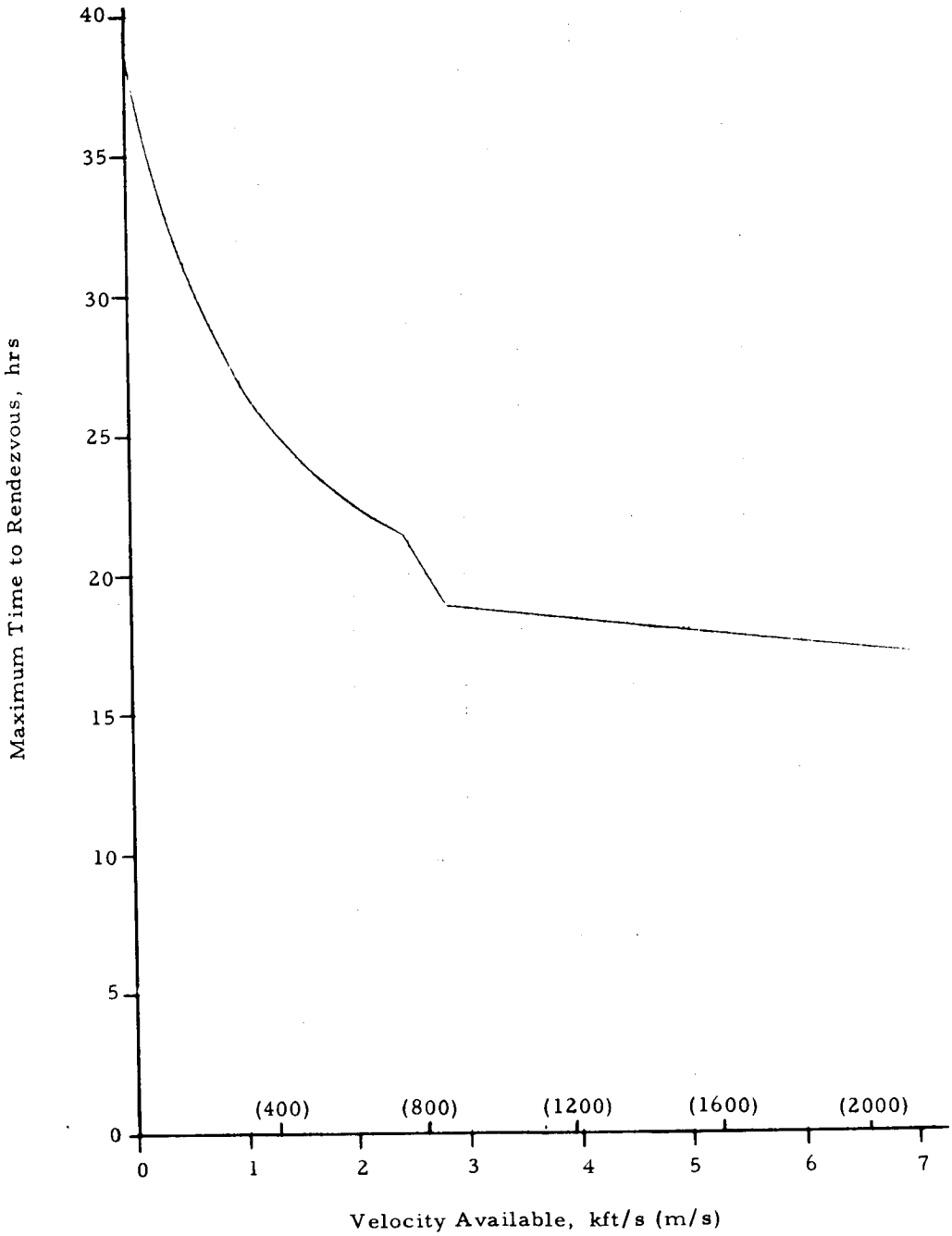

Figure H-8. Worst-Case Total Time to Rendezvous with Excess Available ΔV
(a) Target in 270 nmi (500 km), 55° Circular Orbit

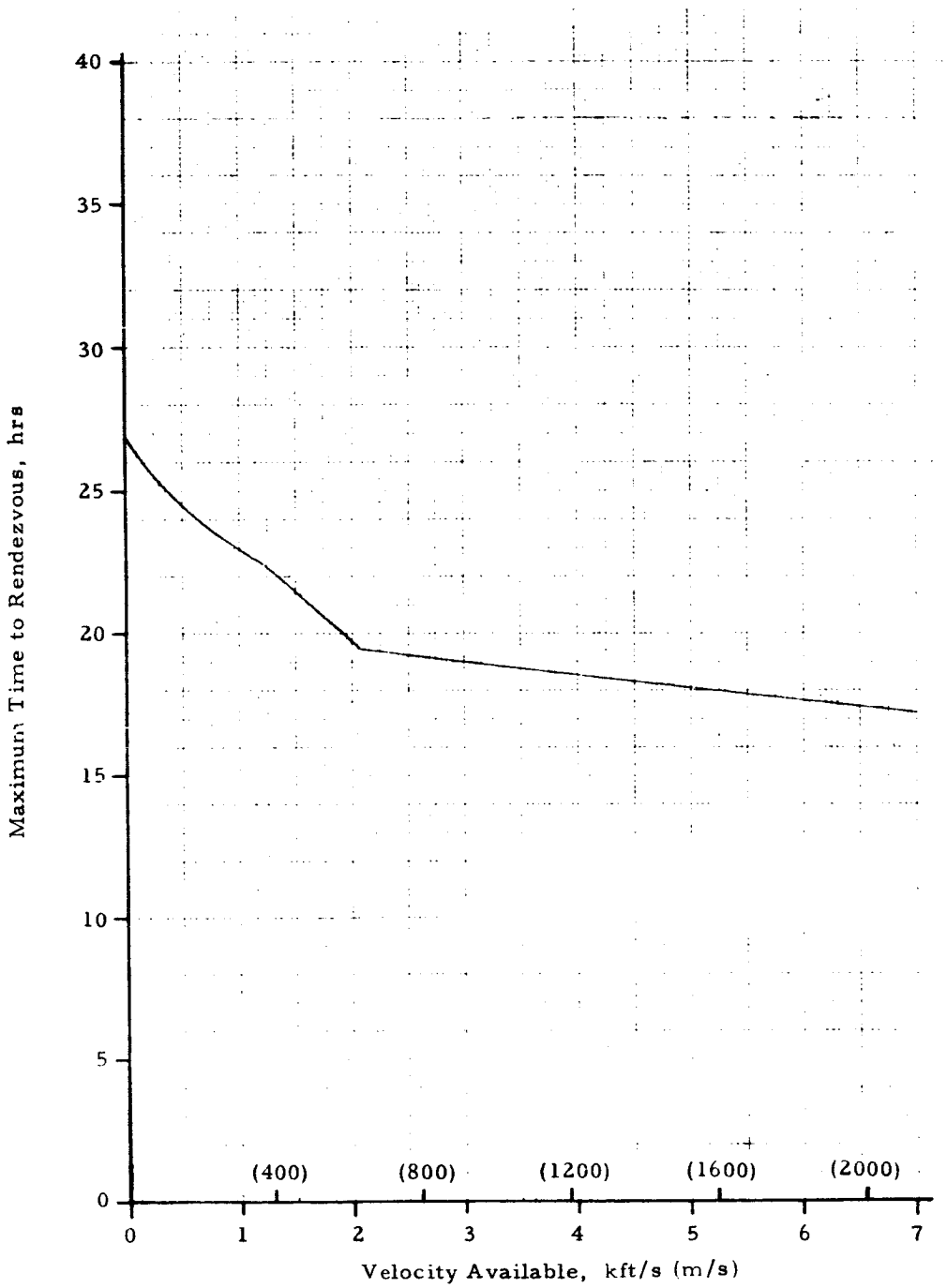

Figure H-8. Worst-Case Total Time to Rendezvous with Excess Available ΔV
(b) Target in 500 nmi (925 km), 55° Circular Orbit

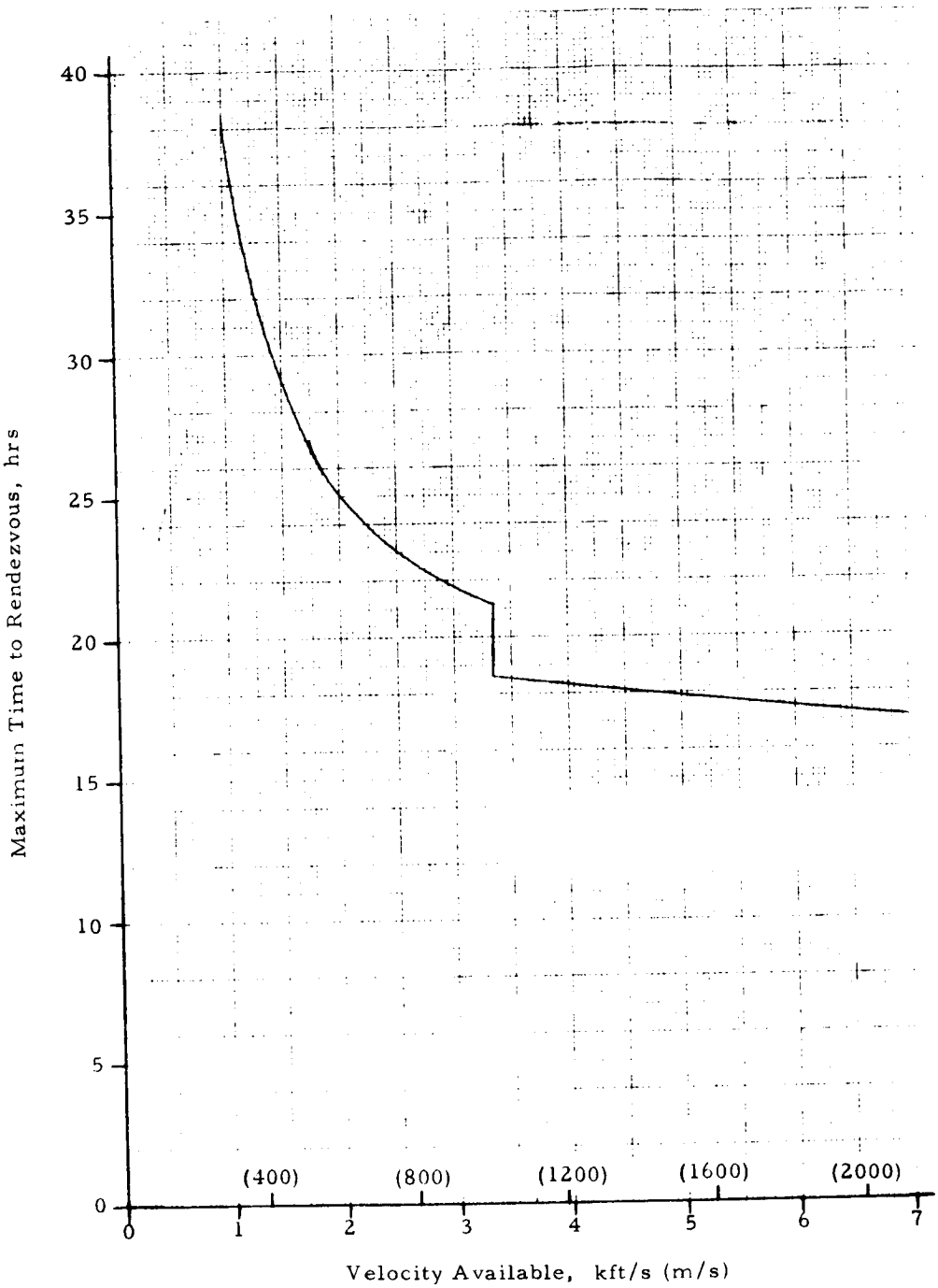

Figure H-8. Worst-Case Total Time to Rendezvous with Excess Available ΔV
(c) Target in 100 nmi (185 km), 55^{o} Circular Orbit

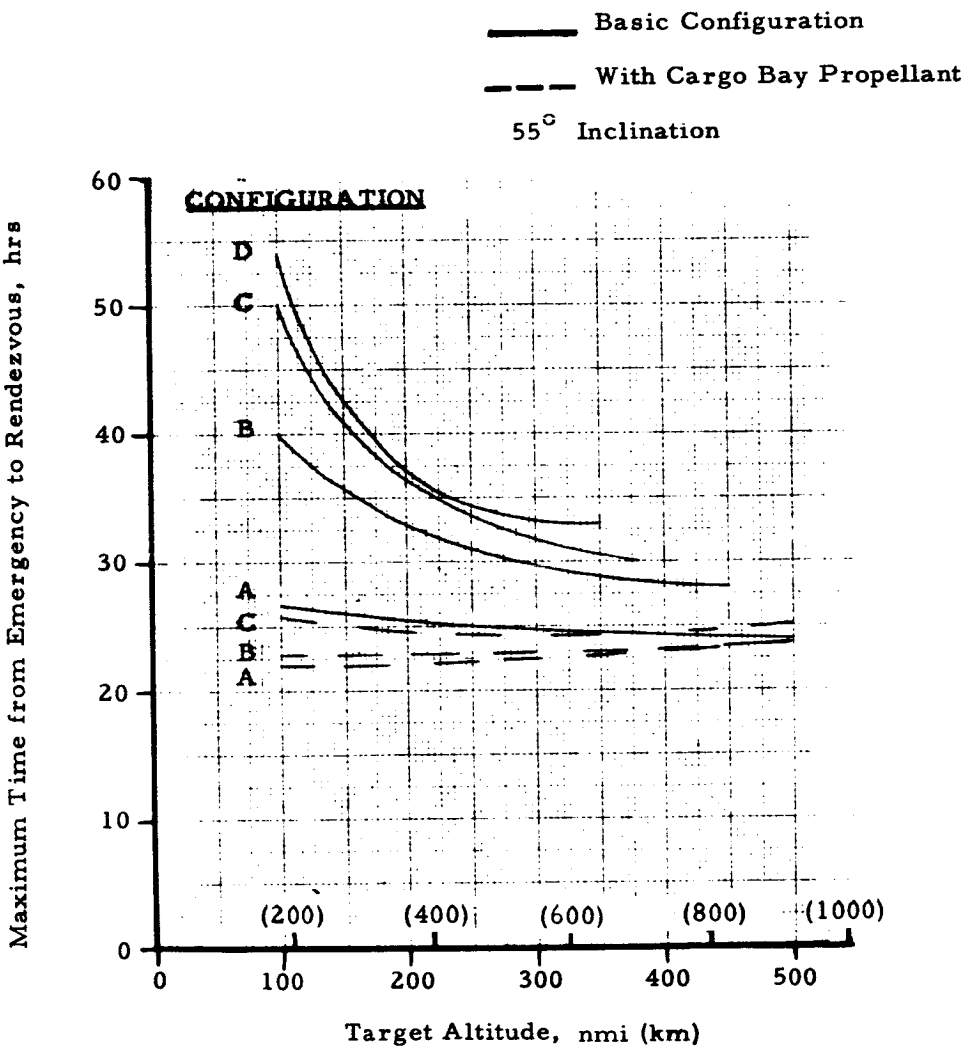

Figure H-9. Effect of Target Altitude on Worst-Case Total Time to Rendezvous for Shuttle Rescue Mission

APPENDIX I

COST ESTIMATES

APPENDIX I

CONTENTS

TABLES

APPENDIX I

COST ESTIMATES*

I.1 GENERAL

A number of methods for augmenting the basic rescue capability of the Earth Orbit Shuttle are discussed in Volume II, Part 1. Four EOS vehicles differing in design details were examined, and the costs associated with acquiring the improved capability were assembled for use in making summary comparisons

Three basic augmentation modes were assessed. They were:

a. Increased Propellant Loading
b. Orbital Refueling
c. EOS-Launched Tug

For cases (b) and (c), it was assumed that major items such as the means for orbital propellant delivery and storage and the Tug (sized for delivery into low earth orbit by the Shuttle) were already developed and in the inventory. Such major hardware items would not be acquired merely for rescue missions, but if available, could be used.

It was also assumed that is such hardware is in the inventory, then the necessary compatibility modifications for non-rescue missions have already been incorporated in the Shuttle. Only the incremental costs for rescue-mission-peculiar needs are to be considered.

On this basis, only the costs for case (a) need to be examined. However, Orbiter refueling in space presents interesting possibilities and only Orbiting Propellant Depot costs are available in the literature. The additional EOS costs to allow orbital refueling via propellant transfer as well as via tank exchange were, therefore, also examined.

---

*The material in this Section was provided by L. Raphael.

Wherever possible, cost estimates from previous studies on related hardware were used. If not available, estimates were made using the hardware definition and appropriate estimating data. In all cases, these estimates are "typical" values; because the hardware definitions are conceptual, the estimates are correspondingly, approximate.

Neither the cost of the propellant transferred to the Orbiter, nor the cost of the rescue payload were considered.

All costs are given in 1971 dollars.

I.2 INCREASED PROPELLANT LOADING

The costs associated with increased propellant loading for each Shuttle configuration are given in Table I-1. These values are basically the cost of developing and procuring the cargo bay tank in which the added propellant is carried. Thus, both the non-recurring and recurring costs, which are based on tank weight, will decrease with tank size.

The numbers given cover the cost of a superinsulated tank, capable of long-term cryogenic propellant storage, as well as fill, vent and drain lines, added pumps, valves and regulators, and the necessary electrical interfaces. RDT&E includes the procurement of one ground test tank and one flight test tank. Fee is included in all costs. The unit total cost includes not only the manufacturing costs but also sustaining costs such as spares, engineering, tooling support, and program management.

The non-recurring cost represents the major expense and, depending on Shuttle configuration, falls between 52 and 115 million dollars if the tank is sized to completely fill the cargo bay. When allowance is provided for a 10 klb (4.5 t) rescue payload, this cost range is reduced to 60 - 93 million dollars. The total unit cost is between 2 to 3% of the non-recurring cost.

The estimated direct operating cost per Shuttle flight for a program of ~800 flights is given in Table I-2 for each of the four Shuttle configurations. The increment which should be added to these values for the increased complexity of a launch with a fueled cargo bay tank is small and was not determined.

I.3 ORBITAL REFUELING

I.3.1 General

Except for Configuration A, there are two general modes of refueling the Shuttle second stage in low earth orbit. One is by direct propellant transfer from a donor into the empty Orbiter main tank. The donor could be an Orbiting Propellant Depot or one or more logistic vehicles. The other refueling mode is by actually exchanging the empty tank for a full one. This latter approach is only feasible with drop-tank Orbiter configurations or a cargo bay tank.

The cost investment in the fuel donor (not considered in this study) is independent of the refueling mode. The same amount of propellant would be required on orbit for either tank exchange or propellant transfer. Also, the tank refueled and then exchanged for an empty tank was assumed left in orbit on a previous mission which did not require refueling.

I.3.2 Propellant Transfer Mode

The estimated cost for modifying the Earth Orbit Shuttle second stage to accommodate propellant transfer into the main tank and then to resume operation after refueling is given in Table I-3a. The same procedures and modifications are involved for all four Shuttle configurations and the same RDT&E and added unit cost estimates resulted. The modifications include propellant fill lines at the docking juncture between the Orbiter and donor, valves, regulators, and an appropriate electrical interface. Also, the main engine system would have to be modified to allow engine restart and single-engine operation.

I.3.3 Tank Exchange Mode

More extensive modifications would be required to both the Orbiter and the separable main tank for the on-orbit tank exchange case. The tank attachment mechanism would have to be revised to allow separation and reattachment with complete integrity of all lines and circuits. In addition, a high-performance cryogenic insulation would have to be added to the tank and covered with a shroud in order to allow a reasonable on-orbit propellant storage period. As before, a modified main engine system is assumed to allow engine restart and single-engine operation.

As a result of these more extensive modifications, the main tank exchange refueling mode although less time consuming in operation would be much more expensive to acquire and use. The estimated costs for the necessary modifications, both non-recurring and added recurring, are given in Table I-3b. RDT&E includes the cost of procuring one ground test and one flight test main tank. Fee is included in all costs. The added increment to the unit cost of a "standard" EOS includes manufacturing as well as sustaining costs such as spares, engineering, tooling support, and program management.

The estimated non-recurring cost varies slightly with EOS configuration; 300 million dollars is a representative value. The added EOS unit cost is about 4% of this value.

I.3.4 Propellant Delivery Cost

The amount of propellant needed to refuel an Orbiter main tank depends upon the tank capacity. Except for secondary effects such as boil off and transfer time, the amount of propellant delivered to orbit would not vary with refueling mode. It was assumed, therefore, that the same number of propellant delivery logistics flights would be required whether direct propellant transfer, tank exchange, or an orbiting propellant depot are involved.

Cost was estimated for two alternate methods of propellant delivery. One involved delivery via Shuttle logistic flights and the other via logistic flights with an Expendable Second Stage (ESS).

The cost of a single Orbiter refueling by EOS and by ESS is given in Table I-4 for low earth orbit and an inclination of 28.4^{o}. The cost is based on the number of logistic flights required for each configuration and the cost per flight.

The direct operating cost of a Shuttle logistic flight is given in Table I-2. The cost per flight of an ESS configuration was obtained from Reference I-1 and adjusted to 1971 dollars.

The propellant delivery cost for refueling an Orbiter may reach and could even exceed $100M, irrespective of whether an EOS or an ESS is used, especially if propellant cost and hardware amortization are considered. Clearly, the cost of one Orbiter refueling could exceed the expense of acquiring this capability. Even for the tank exchange mode, the cost of a single refueling is about one-third the cost of RDT&E.

I.4 REFERENCE

I-1. Space Shuttle Phase A/B Study: Expendable Second Stage on a Reusable Booster; North American Rockwell Corporation - Space Division; SV 71-36; August 1971

Table I-1. Estimated Added Costs for Increased Propellant Loading (Millions of 1971 Dollars)

Configuration	Tank Size ft (m)	Tank Weight, klb	(t)	RDT&E	Unit Total*
A	15 x 60 (4.6 x 18.3)	11.0	(5.0)	114.45	3.19
	15 x 40 (4.6 x 12.2)	7.5	(3.4)	93.10	2.39
B	15 x 60 (4.6 x 18.3)	11.0	(5.0)	114.45	3.19
	15 x 40 (4.6 x 12.2)	7.5	(3.4)	93.10	2.39
C	12 x 40 (3.7 x 12.2)	4.8	(2.2)	80.59	1.67
	12 x 20 (3.7 x 6.1)	2.3	(1.0)	59.70	0.93
D	10 x 20 (3.0 x 6.1)	1.6	(0.7)	52.03	0.70

*Includes manufacturing, spares, engineering, tool support, and program management costs for added modifications

Table I-2. Estimated Shuttle Direct Operating Cost*
(Millions of 1971 Dollars)

Configuration	Cost/Flight
A	4.5
B	7.5
C	7.0
D	4.0

*~800-flight program; does not include hardware amortization

Table I-3. Estimated Orbital Refueling Costs
(Millions of 1971 Dollars)

(a) Propellant Transfer Mode

	RDT&E	Added Unit Cost*
All Configurations	45	1.5

(b) Main Tank Exchange Mode

Configuration	Drop Tank Weight klb	(t)	RDT&E	Added Unit Cost*
B	35.0	(16)	318.22	13.80
C	31.0	(14)	301.78	12.50
D	23.4	(11)	270.30	9.93

*includes manufacturing, spares, engineering, tooling support, and program management costs for added modifications

Table I-4. Estimated Propellant Delivery Cost*
(Millions of 1971 Dollars)

(a) Earth Orbit Shuttle Delivery

Configuration	No. of Flights	Cost/Flight**	Cost/Refueling
A	9	4.5	40.5
B	11	7.5	82.5
C	12	7.0	84.0
D	13	4.0	52.0

(b) Expendable Second Stage Delivery

Configuration	No. of Flights	Cost/Flight***	Cost/Refueling
A	3	33	99
B	4	33	132
C	4	33	132

* To low earth orbit and 28.4° inclination

** ~800-flight program; does not include hardware amortization

*** Reference I-1; adjusted to 1971 dollars

APPENDIX J

PARALLEL-BURN SPACE SHUTTLE CONFIGURATION

APPENDIX J

CONTENTS

APPENDIX J

FIGURES

APPENDIX J*

PARALLEL-BURN SPACE SHUTTLE CONFIGURATION

Work on this task was completed before the issuance of the RFP for development of the parallel-burn configuration of the Space Shuttle (Reference J-1) and the final report for this task was essentially completed well before the awarding of the initial Shuttle development contract. The four Space Shuttle concepts treated in the main body of this report (see Appendix B) were selected at a point in time when a wide range of Shuttle configurations were being investigated by industry and government. Since it was not possible at that time to identify a preferred Shuttle configuration, these four concepts were examined in order to provide information on space rescue capabilities for a spectrum of candidate systems. Appendix J was prepared in order to bridge the gap between the four configurations considered in this study and the selected Space Shuttle design. In the sections which follow, the parallel-burn Space Shuttle is described, basic performance capability of the system is presented, and characteristics and utility as a space rescue vehicle are discussed.

J.1 SPACE SHUTTLE DESCRIPTION

As presently conceived, the parallel-burn Space Shuttle system consists of a reusable Orbiter vehicle with an external propellant tank and two recoverable Solid Rocket Motors (SRMs) which burn in parallel with the Orbiter main engines. Figure J-1 (from Reference J-2) shows a typical Shuttle design with the elements mated for vertical launch. The Space Shuttle is to provide the performance capabilities for the three reference missions discussed in Section J-2. The Orbiter vehicle is capable of crossrange maneuvering during entry, controlled aerodynamic flight, horizontal landing, and utilizes

* This appendix was prepared by A. E. Goldstein.

an expendable main propellant tank for the boost phase. Representative weight, thrusts, and other characteristics of the system are given in Figure J-2. These data will most likely change as vehicle design matures.

The baseline Orbiter illustrated in Figure J-3 (from Reference J-2) is a manned, reusable, delta-winged space vehicle. The main fuselage contains the crew compartment, a payload bay capable of accommodating single or multiple payloads of up to 15 ft diam by 60 ft (4.6 m x 18 m) long, support systems, an Orbital Maneuvering System (OMS), and the main propulsion system engines. Protection against aerodynamic heating is provided during ascent and reentry by an external Thermal Protection System (TPS). Aerodynamic flight is controlled through the elevons and rudder, while space-attitude control is accomplished through Reaction Control System (RCS) thrusters which are attached to the vehicle as modules. The Orbiter vehicle is capable of docking to a space station or other compatible orbiting element during daylight or darkness.

Propellants for the Orbiter main engine are LO_2/LH_2 and are contained entirely within the expendable drop tank. The OMS provides propulsion after orbit has been attained and the main propellant tank has been jettisoned. This system burns storable propellants which are carried within the Orbiter.

The Orbiter crew compartment houses the flight crew, passengers, controls, and displays, as well as most of the avionics and environmental control system. An upper deck provides crew stations to accomplish all flight operations of the Orbiter and control of the manipulator system. Provisions for payload monitoring, passenger accommodation, electronics, environmental control/life support systems, and pressure suits and other EVA equipment can be included on the lower deck. The entire compartment is temperature, pressure, humidity, and atmosphere controlled to provide a sea level type "shirtsleeve" environment for the personnel and equipment.

Although the Orbiter can be flown in an emergency by a single crewman, a crew of four can be accommodated in the pressurized cabin for a baseline mission duration of seven days. Up to six additional persons can be accommodated for shorter duration missions with minor changes to the cabin interior. The Orbiter design also has the capability to extend the orbital stay-time up to 30 days.

J.2 BASIC PERFORMANCE CAPABILITY

J.2.1 General

The reference missions defined in the NASA RFP (Reference J-1) are described in the following paragraphs. For performance comparisons, Missions 1 and 2 are launched from the Kennedy Space Center (KSC) into an insertion orbit of 50 x 100 nmi (90 x 185 km) and Mission 3 is launched into the same insertion orbit from Vandenberg AFB (VAFB). The mission on-orbit translational ΔV capability (in excess of that required to achieve the insertion orbit and that required for on-orbit and entry attitude control) is stated for each mission and includes on-orbit ΔV reserves. The Reaction Control System (RCS) translation ΔV required for each mission is used to accomplish all rendezvous and docking maneuvers after terminal phase initiation.

Mission 1 is a payload delivery mission to a 100 nmi (185 km) circular orbit. The mission will be launched due east and requires a payload capability of 65,000 lb (29.5 t) with the Orbiter vehicle airbreathing engines removed. The Orbiter vehicle on-orbit translational ΔV requirement is 950 ft/s (290 m/s) from the Orbital Maneuvering System (OMS) and 120 ft/s (37 m/s) from the RCS.

Mission 2 is a resupply mission to an orbital element in a 270 nmi (500 km) circular orbit at 55 deg inclination. The payload requirement is 25,000 lb (11.3 t) with the airbreathing engines. The Orbiter vehicle on-orbit translational ΔV requirement is 1,400 ft/s (427 m/s) from the OMS and 120 ft/s (37 m/s) from the RCS.

Mission 3 is a payload delivery or retrieval mission to a 100 nmi (185 km) circular polar orbit and return to launch site in a single revolution. The payload requirement is 40,000 lb (18.1 t) with Orbiter vehicle airbreathing engines removed. The Orbiter vehicle on-orbit translational ΔV requirement is 500 ft/s (152 m/s) from the OMS and 150 ft/s (46 m/s) from the RCS.

J.2.2 Basic Vehicle Performance

Basic Shuttle performance capability is given in Figures J-4 and J-5 (from Reference J-3). Because of the similarity in design (single external propellant tank) and in system sizing mission requirements, the low altitude payload delivery capability of the parallel-burn Space Shuttle is nearly identical to that of Configuration B (see Appendix B). Moreover, on-orbit performance characteristics for equal propellant weights will also be similar to those of Configuration B, since the Orbiter dry weights are fairly close and the main and OMS rocket engines are identical for the two systems.

Figure J-4 shows Shuttle gross payload capabilities as a function of inclination for various circular orbital altitudes. The OMS propellant necessary to exactly provide the on-orbit ΔV required for each mission is listed at the right side of each curve. The corresponding circular orbit altitude that the Shuttle can reach, circularize, and retrofire (assuming direct reentry) while maintaining a 120 ft/s (37 m/s) reserve for rendezvous and contingencies is given at the left of each curve. Figure J-5 presents the corresponding payload capability as a function of circular orbit altitude reached.

The performance capabilities reflected in these figures are based upon the entire payload being carried throughout all of the ΔV maneuvers. The variation in payload between altitudes is due to trading payload for OMS propellant (until the OMS tanks are full). The OMS is not used at any time in the launch phase; i.e., prior to the Shuttle reaching its injection orbit.

The current Orbiter design approach is for two sets of OMS propellant tanks having a total capacity of 950 ft/s (290 m/s) of on-orbit ΔV with a 65,000 lb (29.5 t) payload, to be integrally mounted in the Orbiter. Up to three more sets of these propellant tanks, with add-on adaptions, can be put in the payload bay to provide a total capacity of 2500 ft/s (760 m/s) in the OMS. Each of the add-on tank sets adds 1200 lb (550 t) of inert weight to the Orbiter.

J.2.3 Rescue Mission ΔV

As with the other Shuttle systems considered in this study, the excess OMS propellant over that necessary to circularize the Orbiter in the final orbit and deboost can be used to perform on-orbit maneuvers and to expedite rendezvous with a stricken spacecraft. The on-orbit velocity capabilities corresponding to this excess propellant are given in Figure J-6 as a function of orbit altitude and inclination for payload weights of 0 and 10 klb (4.5 t). Two sets of curves are plotted in Figure J-6. The lower set corresponds to the basic configuration utilizing only the integral OMS propellant tanks with a total capability of 950 ft/s (290 m/s). The upper set of curves represents Orbiter operation with add-on tanks mounted in the payload bay to yield a total OMS capability of 2500 ft/s (760 m/s).

Shuttle rescue mission performance capability given in Figure J-6 is predicated upon injection of the Orbiter into a direct transfer elliptical orbit, rather than into the standard 50 x 100 nmi (90 x 185 km) injection orbit. Initially, the Shuttle can boost both the specified payload and a full OMS propellant tank(s) to the apogee of the desired elliptical transfer orbit. The OMS system provides the ΔV necessary to circularize at the apogee altitude and for direct deboost of the Orbiter and payload. The excess on-orbit ΔV remaining for rescue mission purposes is set by the OMS tank capacity and is the difference between the full ΔV capability and that required for Orbiter circularization and deboost. OMS propellant must be off-loaded, however, when the fully loaded weight exceeds the Shuttle payload capability to the desired orbit altitude/inclination combination. A break in the curves given

in Figure J-6 occurs at the point where OMS propellant off-loading is initiated, and the available ΔV decreases more rapidly as the altitude increases.

J.3 PERFORMANCE WITH INCREASED PROPELLANT LOADING

J.3.1 Additional OMS Propellant

Carrying additional propellants within a tank inserted in the Orbiter payload bay is an obvious way of improving Shuttle performance. The tank and propellant are treated as Orbiter payload and the added propellant load is adjusted to maintain the total cargo weight within Shuttle boost capability limits. The installation provides its own pressurization and transfer equipment, and the added propellant is fired through the OMS engines.

As described in the previous section, this mode of performance augmentation is already incorporated in the design of the Space Shuttle. It was pointed out that the basic Shuttle has an integral OMS propellant capacity of 950 ft/s (290 m/s) and that three sets of payload bay add-on tanks are provided to increase the capacity to a total of 2500 ft/s (760 m/s). Figure J-6 shows the rescue mission ΔV available with this higher OMS propellant loading. However, even greater on-orbit ΔV can be obtained at low orbit altitudes and inclinations with additional OMS propellant.

A comparison between the rescue mission ΔV available in a 100 nmi (185 m) orbit using integral OMS tanks with the maximum ΔV which can be obtained with added OMS propellant in the payload bay is given in Figure J-7. Data are shown for orbit inclinations of 28.4°, 55° and 90°. The rescue payload weight is 10 klb (4.5 t) for all cases.

The maximum on-orbit ΔV increase through the addition of OMS propellant at liftoff is about 2000 ft/s (610 m/s) and occurs at an orbit inclination of 28.4°. Less ΔV gain is observed at higher inclinations. Clearly, increased OMS propellant loading offers only small Shuttle performance augmentation possibilities and utility of this scheme is primarily limited to low earth orbit applications.

J.3.2 Orbital Refueling

Refueling the Orbiter in low earth orbit provides a means for obtaining a very large increase in available on-orbit ΔV. Techniques for providing large quantities of propellants in low earth orbit, mechanics of propellant transfer, etc. are discussed in Appendix D. These refueling techniques and procedures are also applicable to the parallel-burn Shuttle configuration.

In the orbital refueling case, propellant may be transferred from a donor directly into the Orbiter external propellant tank (emptied during boost phase) and/or payload bay mounted tanks, or the empty drop tank may be exchanged for a full tank previously refueled and maintained in a ready state in low earth orbit. All propellant acquired by refueling, even that in the cargo bay tank, is fired through the Orbiter main engines.

The ΔV available after orbital refueling of the Orbiter expendable propellant tank is given in Figure J-8 as a function of the rescue payload weight. Also indicated on the figure is the additional ΔV which could be gained by fueling a 40-ft long (12.2 m) propellant tank mounted in the payload bay [20 ft (6.1 m) of cargo bay length was reserved for the rescue payload]. A large on-orbit ΔV is clearly available with the orbital refueling mode of operation, even with a large rescue payload weight.

The velocity requirements for a lunar mission originating in low earth orbit are also given in Figure J-8 to illustrate the rescue mission capability of the refueled Orbiter. The upper dashed line represents the on-orbit ΔV required to accomplish a round trip between a 100 nmi (185 km) circular earth orbit and a 60 nmi (110 km) circular lunar orbit, while the lower dashed line represents the ΔV required for ascent to lunar orbit from low earth orbit plus trans-earth injection from lunar orbit. A lunar round trip from low earth orbit appears feasible with a 10 klb (4.5 t) rescue payload when added cargo bay propellants are used in addition to a refueled Orbiter drop tank.

J.4 PERFORMANCE WITH ADDED STAGES

Adding a stage to an existing launch system is the most frequently employed technique for augmenting capability. In the case of the Space Shuttle, the Orbiter payload bay can accommodate an upper stage of significant capability in addition to an appropriate rescue payload. Such a stage converts the two-stage Space Shuttle into a three-stage system. Characteristics and performance capabilities of candidate third stages are given in Appendix E where it was concluded that a Space Tug is the most effective third stage addition to the Shuttle. It should be noted that the basic performance of the parallel-burn Space Shuttle with a Tug as the upper stage is the same as that previously given in Appendix E for Configuration B.

Although the Tug would be designed to be reusable, neither the Tug nor the rescue payload would have reentry capability. Both are delivered to low earth orbit by the Space Shuttle and are returned from low earth orbit by the Orbiter. On a rescue mission, the Space Tug and the rescue payload would probably be simultaneously delivered into low earth orbit by the same Shuttle and returned from orbit by the same Orbiter.

A further step in using the Space Tug to augment Shuttle capability is to join two Tugs in tandem and launch them from low earth orbit. To acquire this four-stage capability, each fully-fueled Tug is separately carried into low earth orbit by individual Shuttles and then joined in space. As in the case of the three-stage system, the rescue payload and one of the Tug stages would be simultaneously delivered to orbit by the same Shuttle. The two Tugs are staged so that both are capable of independently returning to low earth orbit.

The on-orbit ΔVs available from both single and tandem Space Tug configurations launched from a 100 nmi (185 km) circular orbit are shown in Figure J-9 for rescue payloads of 0 and 10 klb (4.5 t). The dashed line represents the ΔV required for a round trip to lunar orbit from a 100 nmi (185 km) circular earth orbit. A round trip to geosynchronous orbit requires approximately the

same ΔV. The three-stage, single Tug configuration, has a lunar orbit round trip capability of approximately 5 klb (2.3 t). By using a four-stage (tandem Tug) configuration, payload capability can be raised to approximately 10 klb (4.5 t).

J.5 CONCLUDING REMARKS

In general, it appears feasible to extend the utility of the Space Shuttle as a Space Rescue Vehicle. Not only low earth orbit applications can be considered, but lunar and geosynchronous mission applications may also be possible. All four modes of performance augmentation considered for the Shuttle offer some rescue utility. The degree of utility depends, of course, on the specific augmentation mode, the nature of the Rescue Vehicle, and vehicle destination. Each augmentation mode is considered technically feasible and each has a unique capability and region of applicability.

Increasing the OMS propellant loading at liftoff by means of a cargo bay tank is useful primarily in low earth orbit. An additional ΔV of approximately 2000 ft/s (610 m/s) could be provided for a due east launch and the Orbiter could reach an orbital altitude of about 800 nmi (1500 km). Also, useful in low earth orbit emergencies is a fully fueled Tug and a Manned Rescue Module, both simultaneously placed in orbit by the same Orbiter. This system can provide a ΔV capability of approximately 22 kft/s (6.7 km/s) above in a 100 nmi (185 km) orbit.

An Orbiter with external drop tank can be used to deliver a fully fueled Space Tug plus a 10 klb (4.5 t) rescue payload into either lunar or geosynchronous orbit. However, the remaining ΔV is not sufficient to return the Orbiter and payload to low earth orbit. Since the Orbiter is not designed for direct reentry from such high energy missions, an alternate earth return technique such as multiple grazing reentry (see Appendix G) must be considered. Both lunar and geosynchronous orbit round trips from low earth orbit appear possible with a 10 klb (4.5 t) rescue payload. If Orbiter refueling is combined

with an added cargo bay propellant tank, some rescue orbit maneuvering capability is also achieved.

An alternate means of achieving lunar and geosynchronous orbit round trip capability is to use the Space Shuttle to deliver and launch a Space Tug in low earth orbit. This three-stage system has a lunar orbit round trip capability of about 5 klb (2.3 t). A tandem-Tug, four-stage configuration requires two Shuttle flights to low earth orbit, but raises the payload capability to about 10 klb (4.5 t).

J.6 REFERENCES

J-1. "Space Shuttle Program Request for Proposal (RFP) Number 9-BC421-67-2-40P," Released to industry on March 17, 1972.

J-2. "Space Shuttle Fact Sheet," National Aeronautics and Space Administration, May 1972.

J-3. "Space Shuttle Performance Capabilities Revision 1," NASA MSC Internal Note No. 71-FM-350, May 16, 1972.

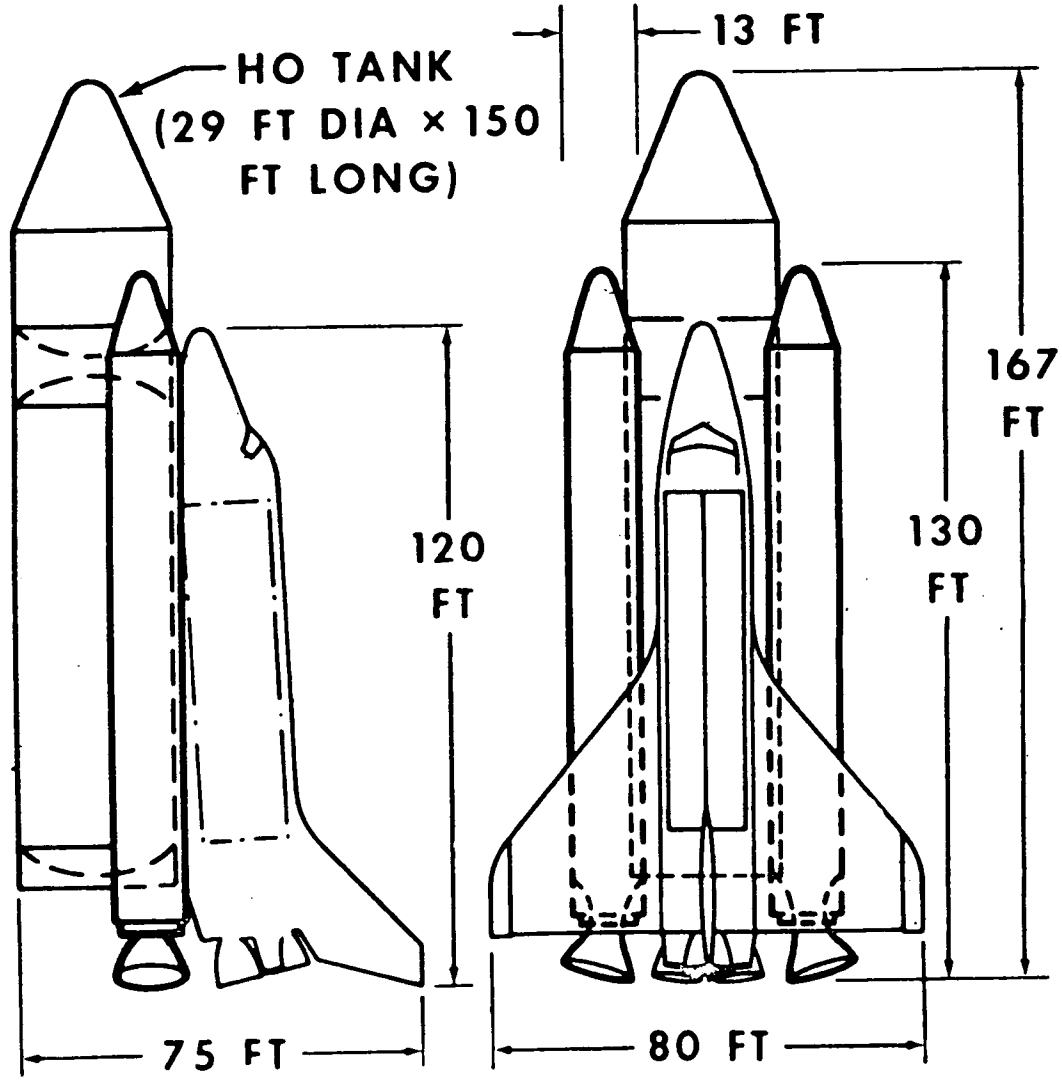

Figure J-1. Typical Parallel-Burn Shuttle Configuration (Reference J-2)

WEIGHTS

	klb	(t)
Payload (East)	65	(29)
Gross Lift-off	4560	(2070)
Orbiter Lift-off	1900	(860)
Booster Lift-off	2260	(1025)
Orbiter (Dry)	160	(73)
Drop Tank (Dry)	71	(32)

PROPULSION

	Booster	Orbiter
Number of Engines/Propellants	2/Solid	2 Hi Pc LO_2/LH_2
Vacuum Thrust, klb (10^6N)	3650 (16) ea.	470 (2.1) ea.
Vacuum Impulse, sec	262	455
Expansion Ratio	10:1	80:1

RELATIVE STAGING VELOCITY

≈5 kft/s (1.5 km/s)

Figure J-2. Typical Parallel-Burn Space Shuttle Characteristics

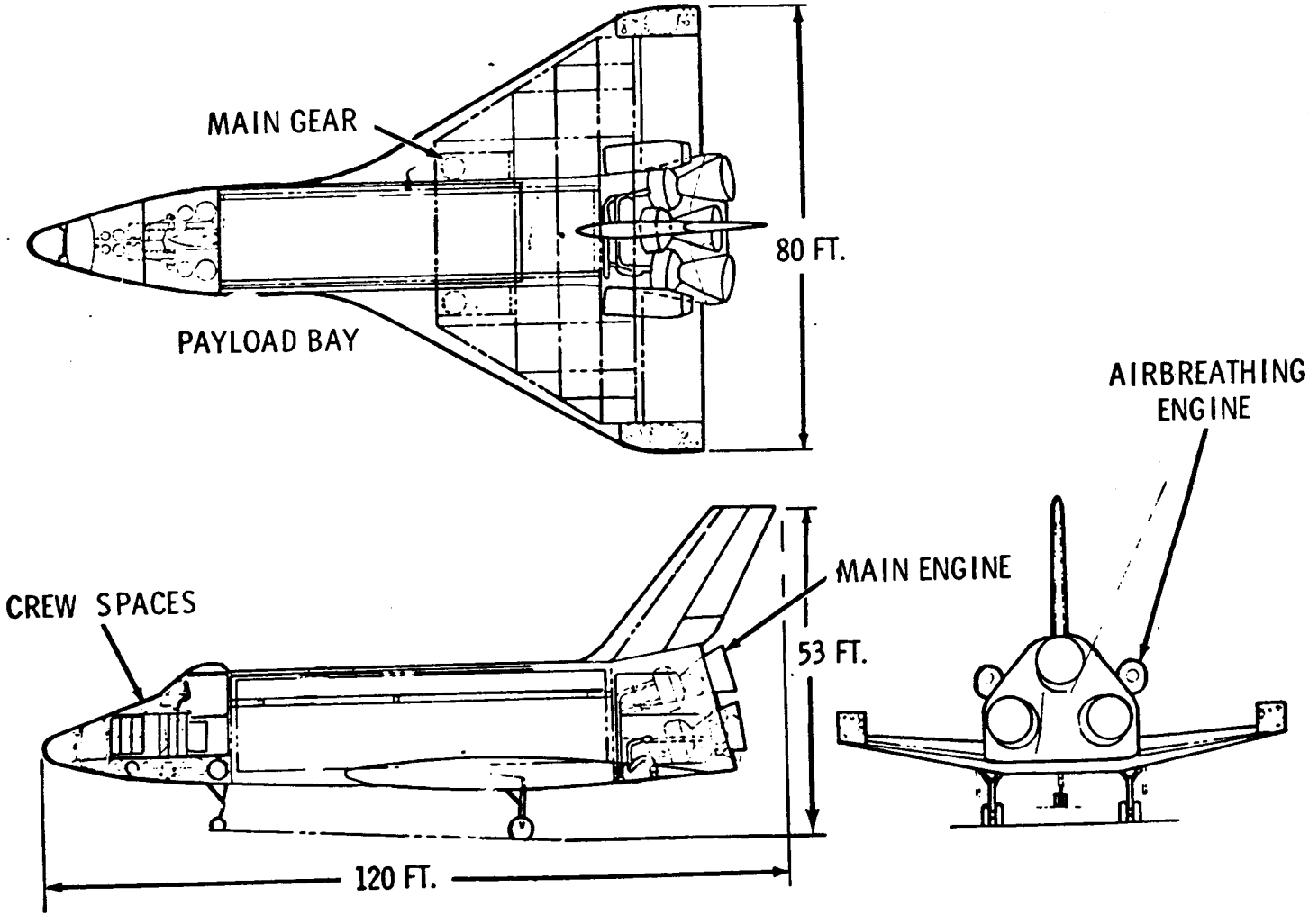

Figure J-3. Space Shuttle Orbiter - Typical Design (Reference J-2)

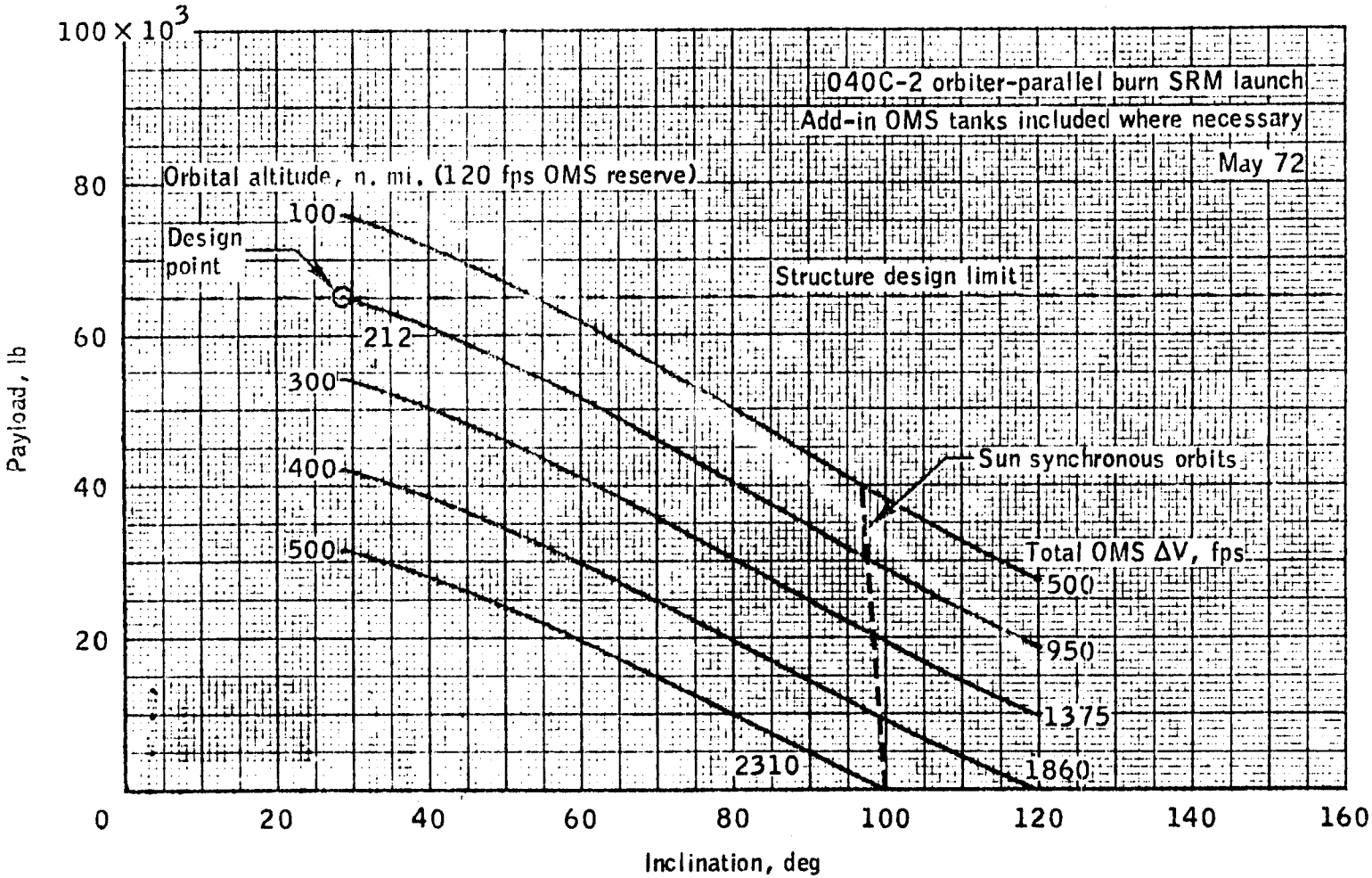

Figure J-4. Variation of Space Shuttle Payload with Orbit Inclination (Reference J-3)

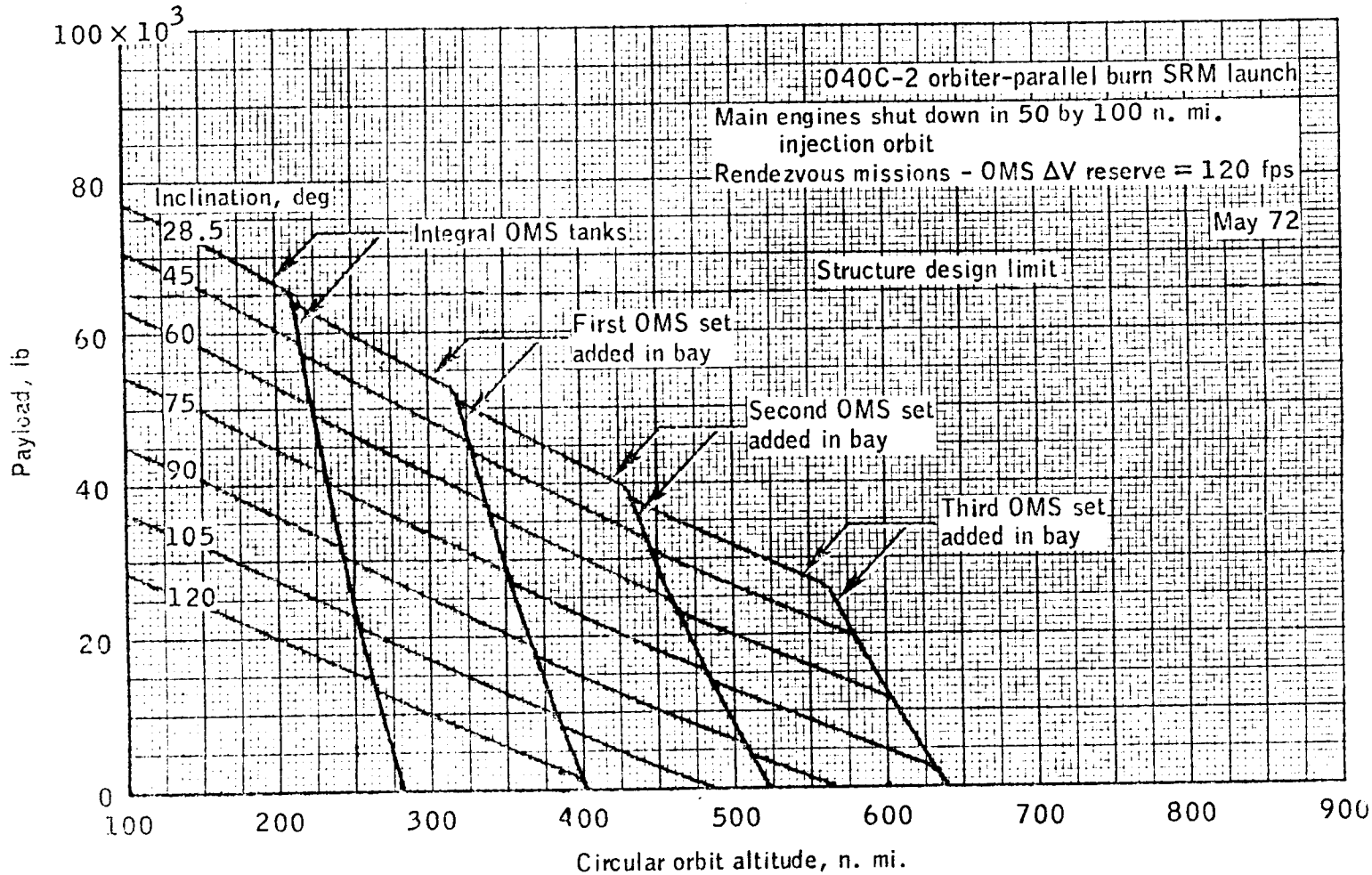

Figure J-5. Variation of Space Shuttle Payload with Circular Orbit Altitude (Reference J-3)

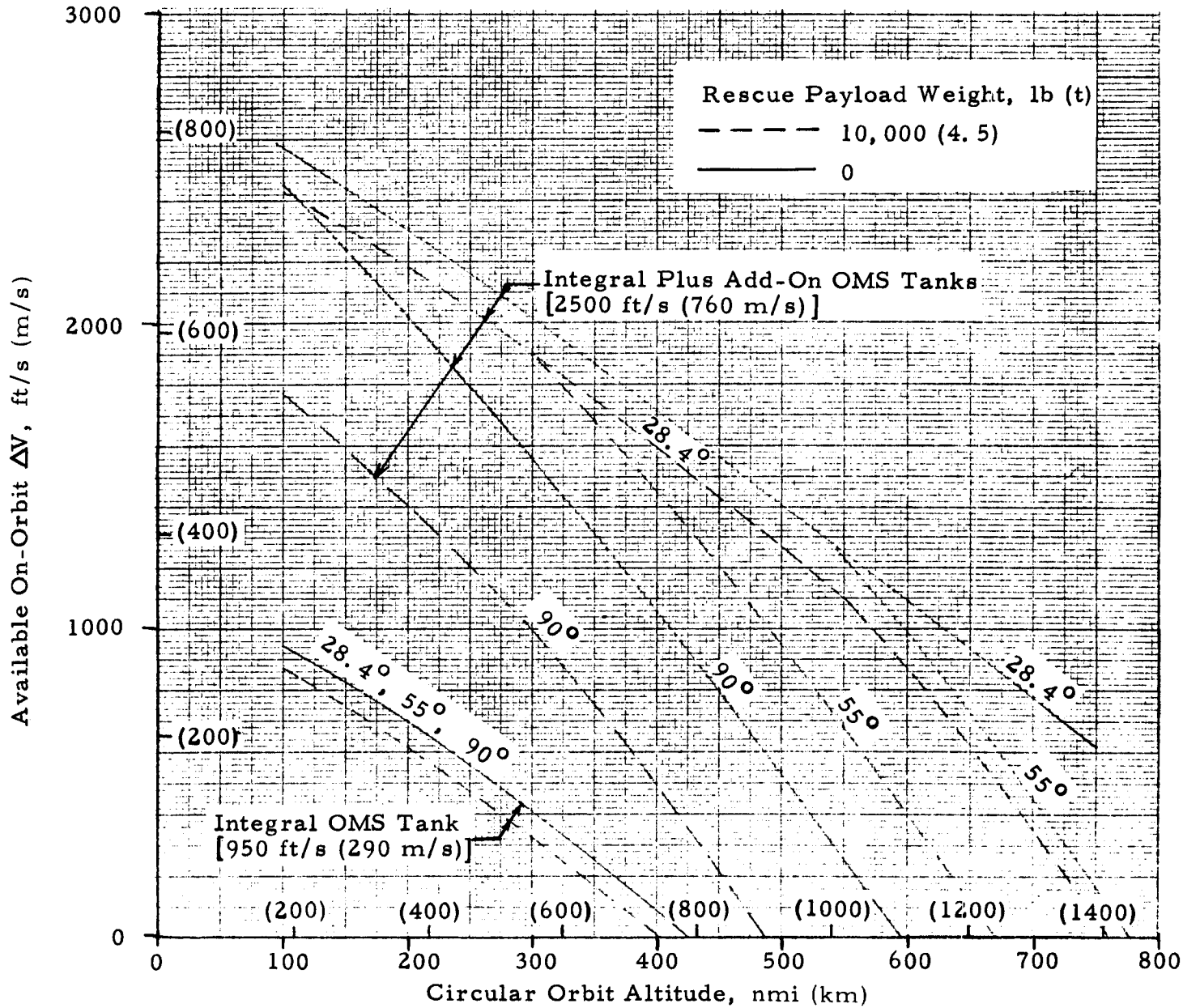

Figure J-6. Basic Space Shuttle Rescue Mission ΔV Capability

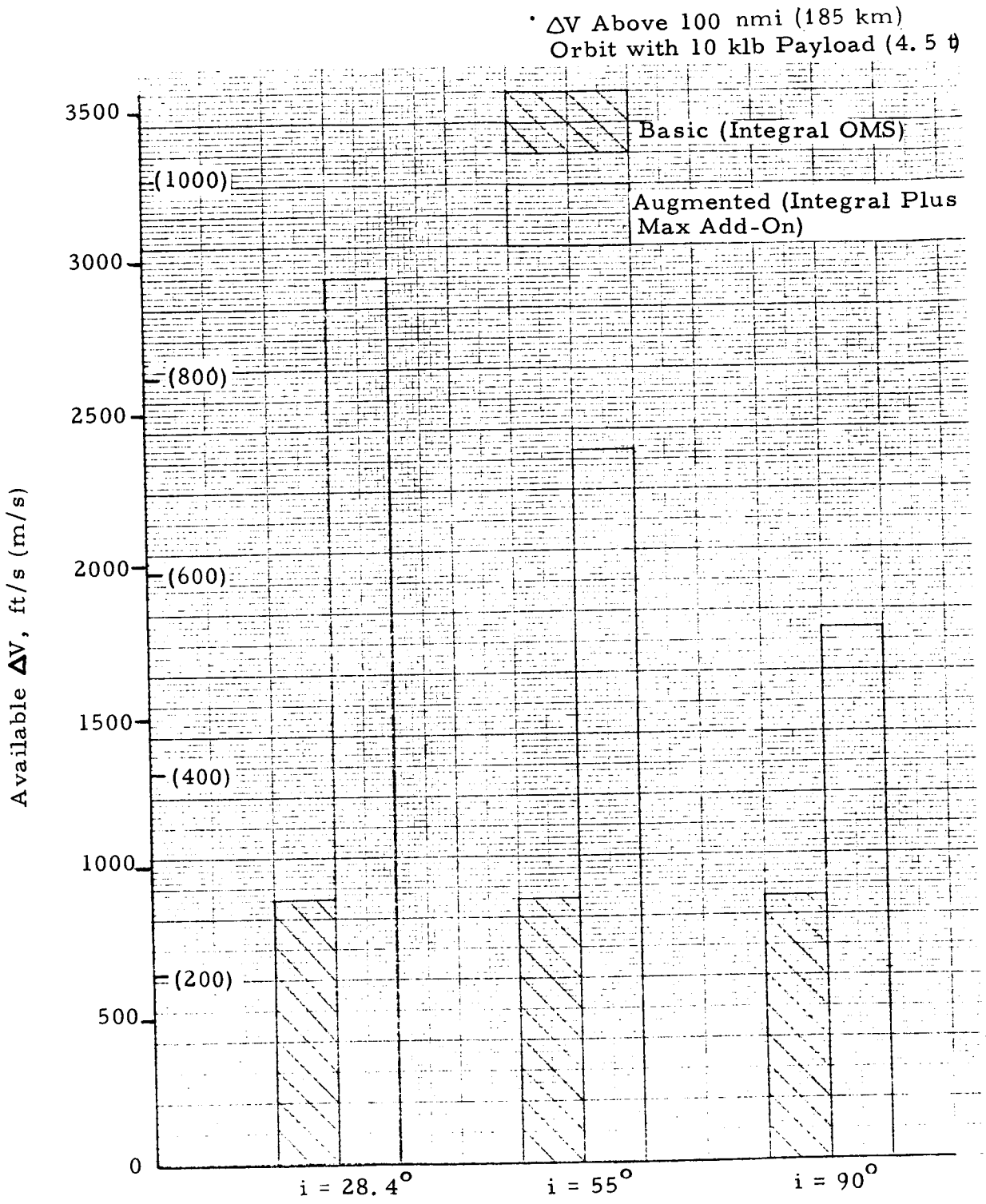

Figure J-7. Increased OMS Propellant Loading

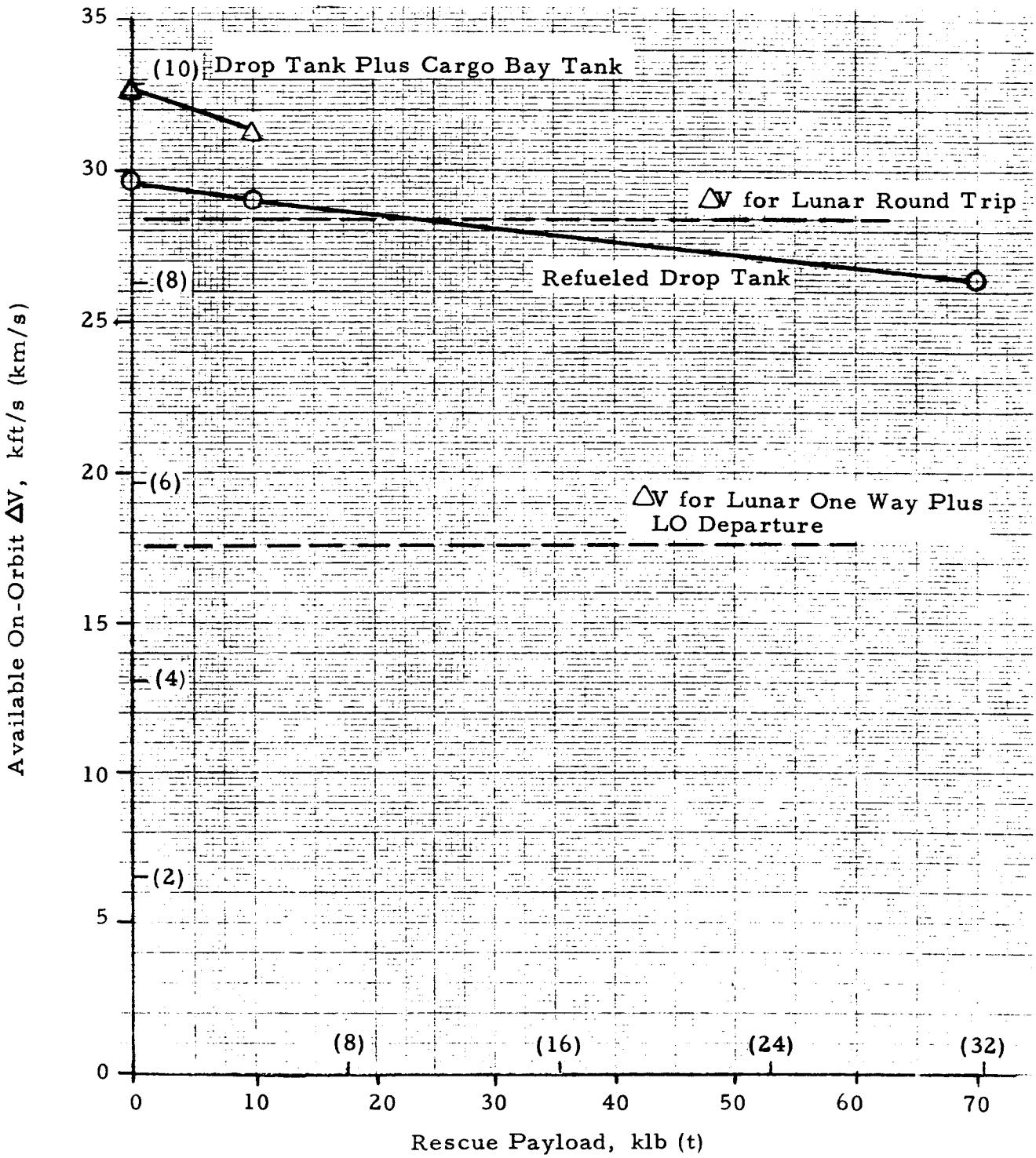

Figure J-8. Rescue Performance with Orbiter Refueled in Low Earth Orbit

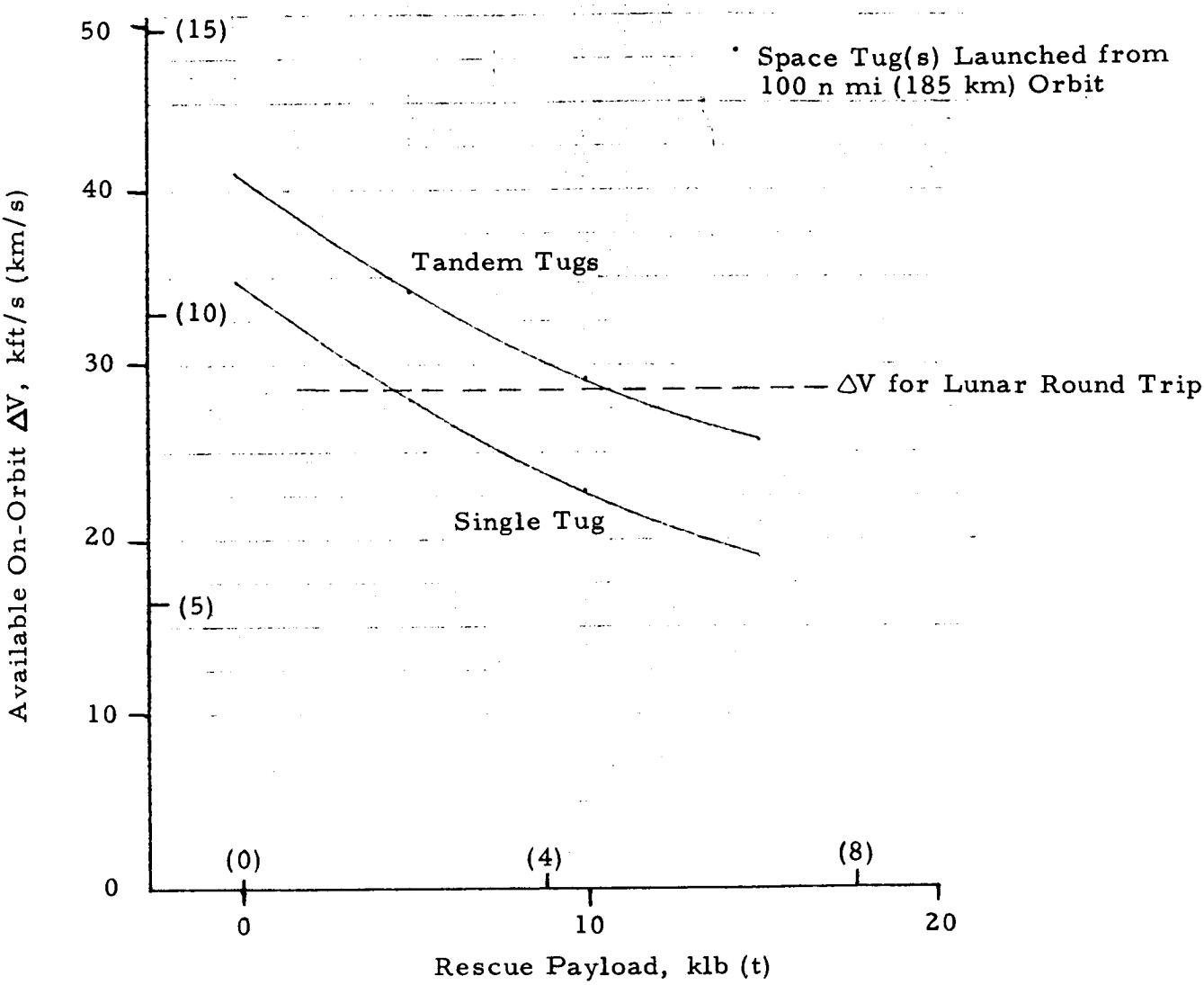

Figure J-9. Performance with Shuttle-Launched Space Tug

APPENDIX K

SYMBOLS, ABBREVIATIONS, AND DIMENSIONS

APPENDIX K

CONTENTS

APPENDIX K

K.1 SYMBOLS AND ABBREVIATIONS

AMU	Astronaut Maneuvering Unit
CIS	Chemical Interorbital Shuttle
C_D	Drag Coefficient
C_L	Lift Coefficient
EO	Earth Orbit
EOS	Earth Orbit Shuttle
ESS	Expendable Second Stage
ETR	Eastern Test Range
EVA	Extra-Vehicular Activity
IDA	Institute for Defense Analyses
L/D	Lift-Drag Ratio
LEO	Low Earth Orbit
LO	Lunar Orbit
OMS	Orbital Maneuvering System
OOS	Orbit-to-Orbit Shuttle
OPD	Orbiting Propellant Depot
P/L	Payload
REI	Reusable External Insulation
RNS	Reusable Nuclear Shuttle
SRV	Space Rescue Vehicle
TEI	Transearth Injection

TPS	Thermal Protection System
W/S	Wing Loading
WTR	Western Test Range
α	Angle of Attack
β	Bank Angle

K.2 DIMENSIONS

ft	foot
ft/s	foot per second
kft/s	kilofoot per second
°F	degree Fahrenheit
hr	hour
i	inclination
lb	pound
klb	kilopound
lb/ft^2	pound per square foot
nmi	nautical mile
g/cm^2	gram per square centimeter
kg	kilogram
°K	degree Kelvin
m	meter
m/s	meter per second
km	kilometer
km/s	kilometer per second
N	Newton
N/m^2	Newton per square meter
t	metric ton = 1000 kg